SIBYL

(Se**I**smic monitoring and vulnera**B**ilit**Y** framework for civi**L** protection)

Agreement number: ECHO/SUB/2014/695550

Deliverable DC4: **Reports on the case studies**

March 2017

Authors: Yuriy Petryna (TU-Berlin)
Sergey Tyagunov (TU-Berlin)
Stefano Parolai (GFZ)
Tobias Boxberger (GFZ)
Dino Bindi (GFZ)
Massimiliano Pittore (GFZ)
Kevin Fleming (GFZ)
Sotiria Karapetrou (AUTH)
Stavroula Fotopoulou (AUTH)
Ioannis Thomaidis (AUTH)
Evangelia Yfantidou (AUTH)
Kyriazis Pitilakis (AUTH)
Tasos Anastasiadis (AUTH)
Dimitris Pitilakis (AUTH)
Stella Karafragka (AUTH)
Iunio Iervolino (AMRA)
Eugenio Chiocciarelli (AMRA)

Contributors:

Name and Affiliation	Contribution
TU-Berlin	
Yuriy Petryna Sergey Tyagunov Alexandra Bretzke Staffan Langner (student)	Thessaloniki – Section 3 Cologne – Sections 1,3,4,5,6 L'Aquila – Sections 1,2
GFZ-Potsdam	
Stefano Parolai Tobias Boxberger Dino Bindi Massimiliano Pittore Kevin Fleming	Thessaloniki – Section 1 Cologne – Section 2 L'Aquila
AUTH	
Sotiria Karapetrou, Stavroula Fotopoulou, Ioannis Thomaidis, Evangelia Yfantidou, Kyriazis Pitilakis, Tasos Anastasiadis, Dimitris Pitilakis, Stella Karafragka	Thessaloniki – Section 2
AMRA	
Iunio Iervolino Eugenio Chiocciarelli	L'Aquila – Section 3

Table of Contents:

Introduction

Task C of the SIBYL project aimed at developing a rapid, low-cost and scientifically well-founded approach for assessing the seismic vulnerability of existing reinforced concrete (RC) buildings, both residential and public. An important part of this Task was contributed by the work carried out as part of the case studies, where the SIBYL partners conducted in-situ measurements and collected data about existing buildings for their seismic evaluation.

There were three case studies within the project, implemented at different times, namely, Thessaloniki, Greece (where the measurements were conducted in September – October 2015), Cologne, Germany (November – December 2015) and L'Aquila, Italy (May 2016). The work program of the case studies included different numbers of investigated buildings; however, all of them included ambient vibration measurements (both outside and inside the buildings) as well as visual structural surveys and in-situ inspections. The principal goal of the SIBYL work groups while undertaking these case studies was the development of the practice-oriented methodological framework for the end-users, including in-situ data collection, structural modelling and building assessment.

Seismic vulnerability analysis of existing buildings is primarily based on their structural evaluation. In accordance with Eurocode 8, Part 3 (EN 1998-3: 2005) for assessing the earthquake resistance of existing structures, the input data can be collected from a variety of sources, including available construction documentation (design drawings and specifications), contemporary building codes and standards, field investigations and in-situ or laboratory measurements and tests. Therefore, for identifying appropriate methods of analysis and corresponding confidence factors, Eurocode 8 defines three knowledge levels: KL1: Limited knowledge, KL2: Normal knowledge, KL3: Full knowledge. In addition to the three mentioned knowledge levels, we consider also a lower accuracy/higher uncertainty level, which can be designated as "very limited knowledge level" or KL0. Considering the level KL0, we assume that no construction documentation is available and the structural evaluation (as well as the vulnerability assessment) is based solely on a quick, superficial survey of the structure. This means the aggregate knowledge level KL0 is significantly less than that for knowledge level KL1 in Eurocode 8. More details can be found in Deliverable DC1: Guidelines for the building assessment procedure and short-term monitoring.

Within the framework of the SIBYL study, we mainly keep to the level KL1, KL2 and KL0. The knowledge level KL1 (limited knowledge) reflects, in our opinion, the most plausible situations in the routine practice of Civil Protection. The level KL2 (normal knowledge) corresponds to those situations when comparatively higher levels of accuracy are pursued. The level KL0 (very limited knowledge) corresponds to the reverse (but also plausible) situations, when a group of buildings or even built-up areas have to be investigated within tight deadlines, provided that a rough

vulnerability estimation is acceptable. In particular, the level KL0 directly links with the data collection approaches described in Task B of the project.

While selecting an appropriate approach for practical use, one should understand that, depending on the used input data and the selected methods of analysis, not only the level of the involved uncertainty, but also the amount of required resources may vary considerably. For example, considering the computational approaches, which while possibly allowing higher accuracy, one should keep in mind that, apart from the requirements of more detailed input data and extended time, special engineering software would also be needed, as well as suitably qualified users. On the other hand, considering simplified empirical approaches in addition to the inherently higher uncertainty, it is worth noting that very often those methods are developed for region-specific building typologies and, therefore, cannot be used universally.

We have to take into consideration the fact that the targeted end-users can meet various situations in practice (corresponding to different knowledge levels, ranging supposedly from KL0 to KL2); therefore, we offer the operational framework, which is rather flexible and affords a set of different ways (techniques) to solve the problems of vulnerability analysis under different possible conditions, balancing the required accuracy within available time frames.

The case studies represent the application of different approaches corresponding to different knowledge levels. In particular, the case study for Thessaloniki considers application of detailed numerical analysis corresponding to the normal knowledge KL2 (Section 2) situation and the simplified approach corresponding to the limited knowledge KL1 (Section 3) case; the case study in Cologne demonstrates the application of the vulnerability assessment approach for the very limited knowledge level (KL0), and the case study in L’Aquila employs the simplified approach for the limited knowledge level (KL1).

Thessaloniki

1. Ambient vibration measurements

The measurement campaign in Thessaloniki took place in the period of 28/09-01/10 2015 and included the following activities: Monitoring of the Administration and Faculty of Philosophy buildings of the Aristotle University of Thessaloniki to record ambient vibrations; measurements for creating topological models and calibrating structural models; passive 2D array measurement for shear wave profile assessment from surface wave analysis for site assessment; and SOSEWIN[1] maintenance. The two monitored buildings are shown in Figure 1.1.

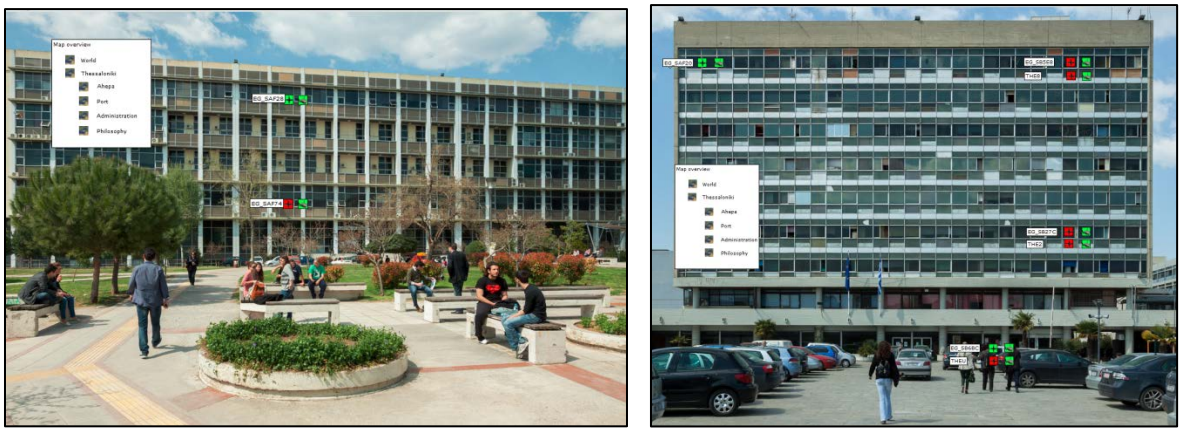

Figure 1.1: Faculty of Philosophy (left) and Administration (right) buildings.

The SIBYL work group included the partners from the Aristotle University of Thessaloniki (AUTH), Technical University of Berlin (TU-Berlin), GeoForschungsZentrum, Potsdam (GFZ) (Fig.1.2).

Figure 1.2: Administration building of the Aristotle University in Thessaloniki, selected as a test case in the SIBYL project, and the SIBYL work group.

[1] SOSEWIN – Self-Organizing Seismic Early Warning Information Network, the predecessor to the MP-WISE system (Fleming et al., 2009).

The measurements were performed using 38 CUBE digitizers connected to 4.5Hz three components geophones, shown in Figure 1.3

Figure 1.3: Equipment used for measuring seismic noise and vibrations within the selected buildings.

1.1. Philosophy building

The Philosophy building is composed of three sub-structures (called blocks hereafter) working independently, with the measurements being concentrated on the central one. This block is monitored with sensors placed at the four corners of 1st, 2nd, 3rd , and 4th floors, two sensors were installed on the roof, and two in the underground basement. The two lateral blocks were also monitored, but less densely (only the four corners of the 1st and 4th floors, and one sensor in the semi-basement). Both AUTH and TU-Berlin acquired detailed documentation of the layout arrangement, which will allow the exact location of the sensors within the building to be identified in the subsequent Sections. The ground floor (entrance) has not been monitored. The building was monitored for about 20 hours.

Figure 1.4: Location of the 2D-array measurements for the estimation of the shear-wave velocity profile (left). Installation of the instruments in the museum of the Philosophy department (right).

1.2. Administration building

This building is composed of 8 upper floors plus the ground floor and the basement. Sensors were installed at the four corners of each floor (from the ground to the 8th), with two sensors also installed in the basement. The building was monitored for about 20 hours.

Figure 1.5: Administration building (left) and an example of an installation for recording ambient vibration in the building (right).

1.3. Two-dimensional array measurements

GFZ installed the sensors in a garden between the two monitored buildings. These measurements were used to obtain a shear-wave velocity profile of the upper-most layers. The inter-station distances varied between about 2 to 73 m. The relative station locations (distance and azimuth) were found using a theodolite (Figure 1.6). The acquisition lasted for about 2 hours.

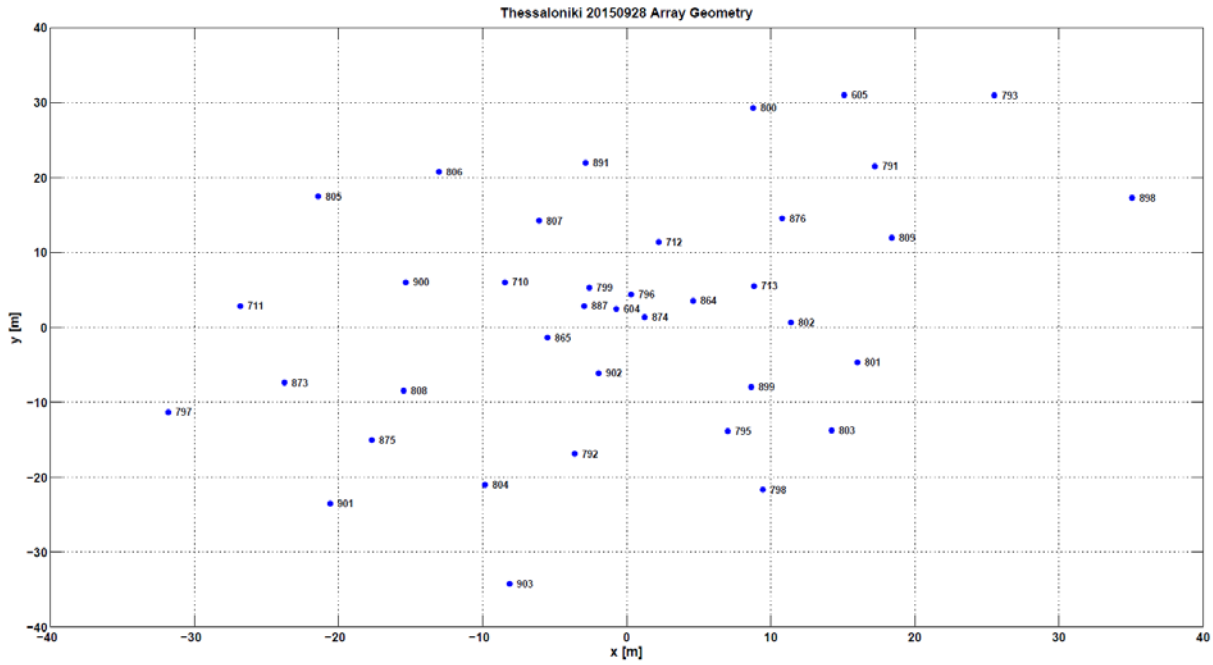

Figure 1.6: Plan of the distribution of sensors for the array measurements.

1.4. Results of the measurements

The sampling rate was set to 400 samples per second (Nyquist at 200 Hz) and the GPS synchronization was performed before and after the installation of the stations inside the building. About 20 hours of natural vibrations measurements are available for each building, and about two hours for the array. The data were stored in CUBE[2] binary format, and later converted to MiniSEED[3] and disseminated through the GFZ ftp site. The MiniSEED[4] files have the length of 1hr and the three components are split between separate files. The extensions for the three components are: .pri0 for the vertical component; .pri1 for the transverse component (i.e., along the red arrow on the geophone); .pri2 for the longitudinal component (orthogonal to the red arrow). Matlab routines to read the MiniSEED files are also provided in the ftp repository.

The available time segments for the different stations are shown in Table 1.1, where the time is measured considering the GMT meridian (Thessaloniki local time during the experiment was GMT+3). The precise layout of the installations will be later provided by TU-Berlin and AUTH. A preliminary layout is given in Table A2. The geophone has poles at 4.5*[-4.443± i 4.443] Hz and two zeros in the origin. The overall constant to go from counts to [m/s] is $28.8*2^{24}/8.192$.

[2] http://www.gfz-potsdam.de/en/section/geophysical-deep-sounding/infrastructure/geophysical-instrument-pool-potsdam-gipp/instruments/seismic-pool/recorder-dss-cube/
[3] http://ds.iris.edu/ds/nodes/dmc/data/formats/miniseed/
[4] http://ds.iris.edu/ds/nodes/dmc/data/formats/

	array	array	1st	1st	1st	1st	1st	1st	1st	1st	1st	1st	1st	1st	1st	1st	1st	1st	1st	2nd	2nd	2nd	2nd	2nd	2nd	2nd	2nd	2nd	2nd	2nd	2nd	2nd	2nd	2nd	2nd	2nd	2nd	2nd	
cube	28. Sep		29. Sep													30. Sep																		01. Okt					cube
	14	15	10	11	12	13	14	15	16	17	18	19	20	21	22	23	0	1	2	3	4	9	10	11	12	13	14	15	16	17	18	19	20	21	22	23	0	1	2	3	4	
604																																									604
605																																									605
710																																									710
711																																									711
712																																									712
713																																									713
791																																									791
792																																									792
793																																									793
795																																									795
796																																									796
797																																									797
798																																									798
799																																									799
800																																									800
801																																									801
802																																									802
803																																									803
804																																									804
805																																									805
806																																									806
807																																									807
808																																									808
809																																									809
864																																									864
865																																									865
873																																									873
874																																									874
875																																									875
876																																									876
887																																									887
891																																									891
898																																									898
899																																									899
900																																									900
901																																									901
902																																									902
903																																									903

Table 1.1: Available (green) time segments for the different installations (red: not available). Time is relative to GMT. 1st and 2nd indicate the Philosophy and Administration buildings, respectively. The CUBE number is indicated on the rows.

Administration (4 corners)

	605	864
8th	891	873
	900	901
7th	797	875
	796	803
6th	795	799
	807	604
5th	806	865
	713	876
4th	798	874
	710	791
3rd	899	712
	800	809
2nd	804	808
	887	801
1st	802	805
	902	903
ground	792	711
	898	
basement	793	

Philosophy - LEFT			Philosophy- CENTRAL		Philosophy-Rigl	
			801	797		
ROOF						
	808	710	802	807	903	805
4th	864	902	803	800	887	875
			791	798		
3rd			712	804		
			899	792		
2nd			711	865		
	604	795	873	796	874	713
1st	809	605	898	901	876	806
				799		
basement	900		891			793

Table 1.2: Locations of the CUBE units in the two monitored buildings.

1.5. Fourier analysis

In order to verify the data quality and to provide preliminary information about the modal shapes of the monitored buildings, the Fourier amplitude spectra (FAS) for the available recordings have been computed.

1.5.1 Philosophy building

Figure 1.7 shows the FAS over the analyzed frequency range, including the fundamental bending modes for the central substructure/unit/block of the Philosophy building. The pri1 component is shown in blue, the pri2 in red. The fundamental modes along the transverse and longitudinal directions are clearly depicted at 1.59 and 1.73 Hz, respectively.

An interesting feature is a second peak appearing on the pri1 direction at 1.78 Hz. This peak appears only in the stations located at specific sides of the blocks (see also Figure 1.8 for the left and right blocks). In particular, it appears on the left (external) side of the left block, the right side of the central block, and the left side (internal) of the right block. At the external side of the right block, the fundamental peak at 1.59 Hz almost disappears and the peak at 1.78 Hz becomes the first peak on the pri1 recordings.

In Figure 1.9, a zoom of the spectra in the central unit over the frequency range [2-2.5] Hz is provided. Finally, a summary of the peaks is provided in Figure 1.10 (central unit, left corners) and Figure 1.11 (central unit, right corners).

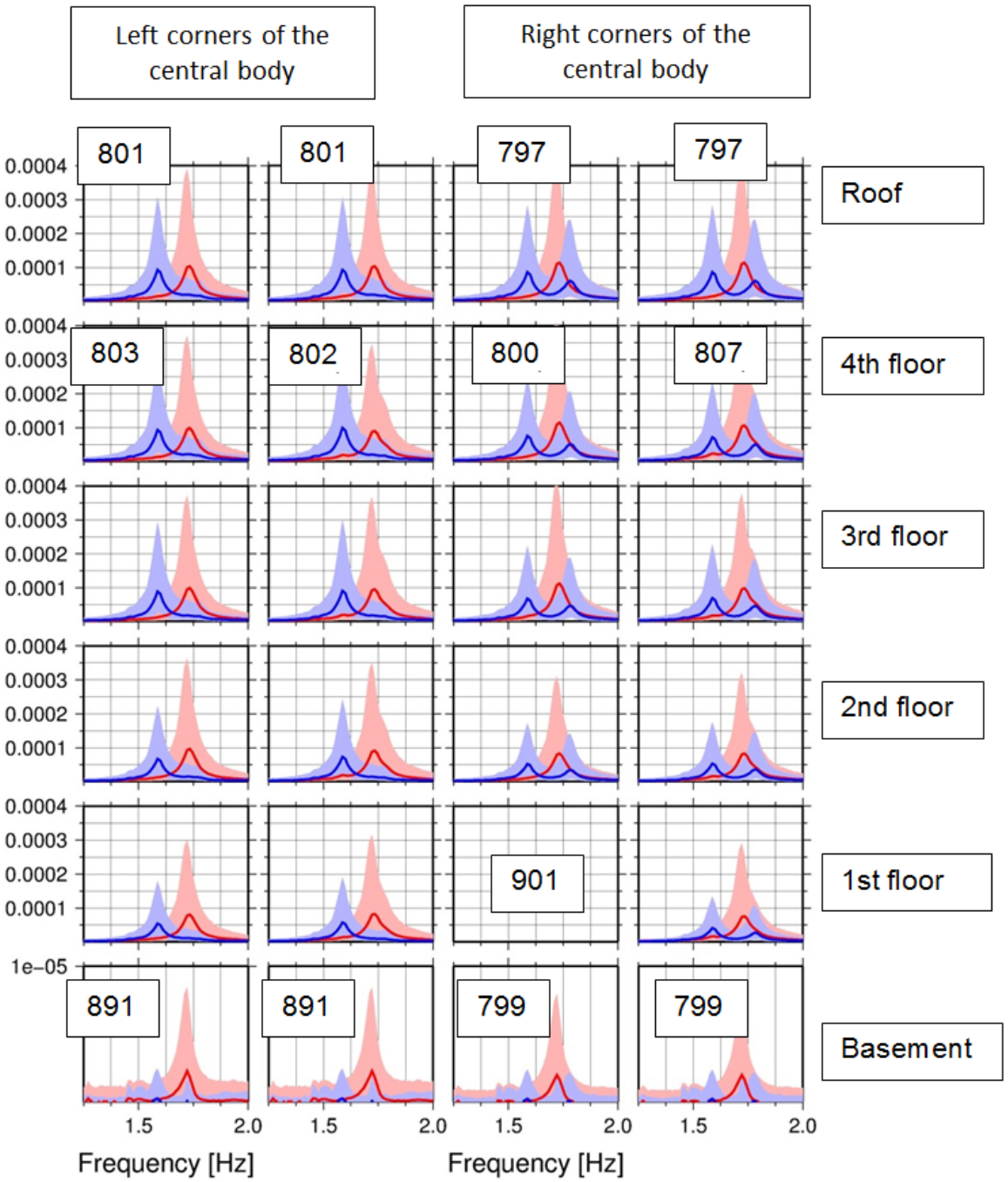

Figure 1.7: Central unit of the Philosophy building. Blue: pri1 (along the red arrow, transverse); red: pri2 (longitudinal). From bottom to top: basement, 1st, 2nd, 3rd, 4th floors, roof. Note the y-scale for the basement differs.

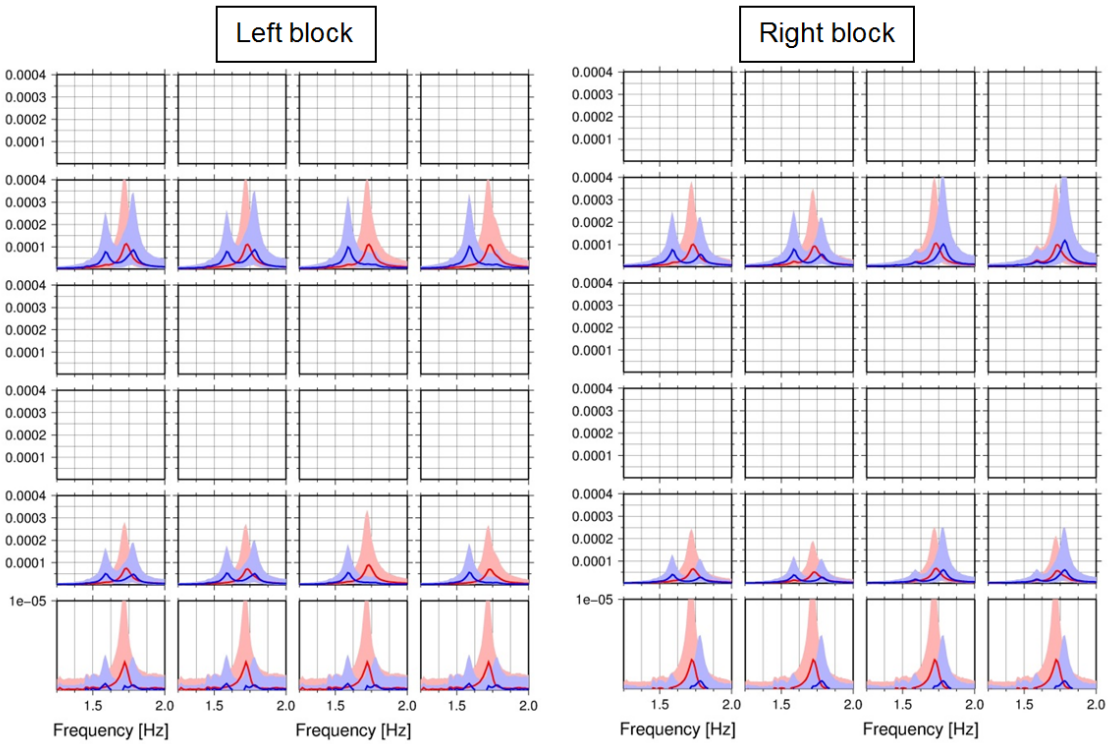

Figure 1.8: Left-block (left) and right-block (right) of the Philosophy building.

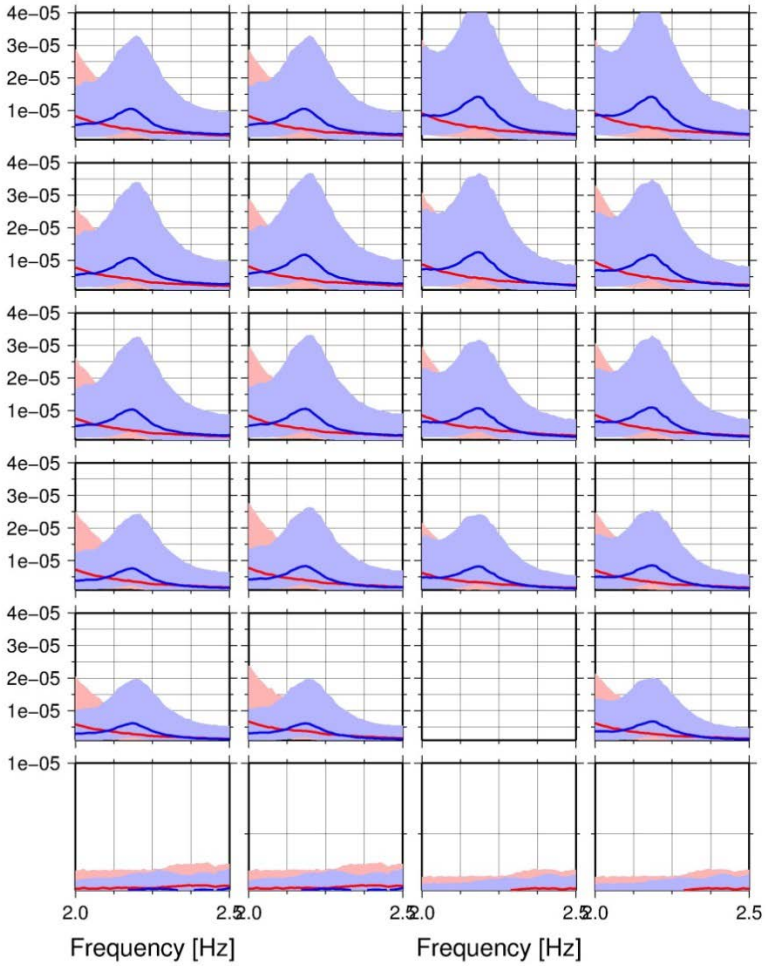

Figure 1.9: Central unit zoom over the frequency range 2-2.5 Hz.

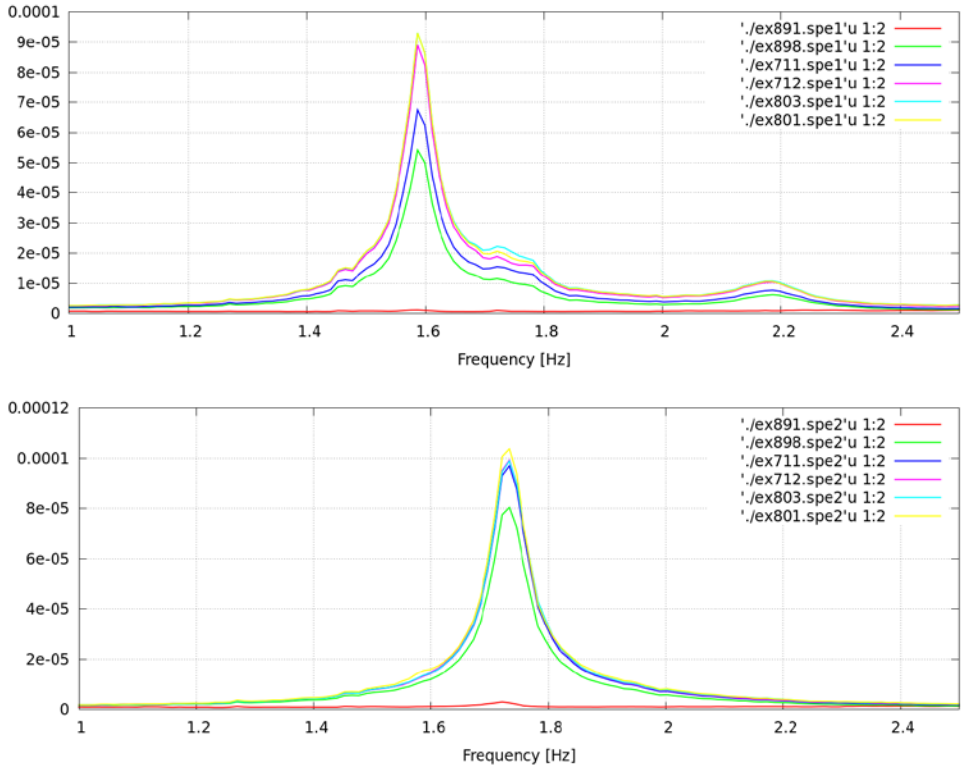

Figure 1.10: Central unit, left side: fundamental peaks for the pri1 (top) and pri2 (bottom) components.

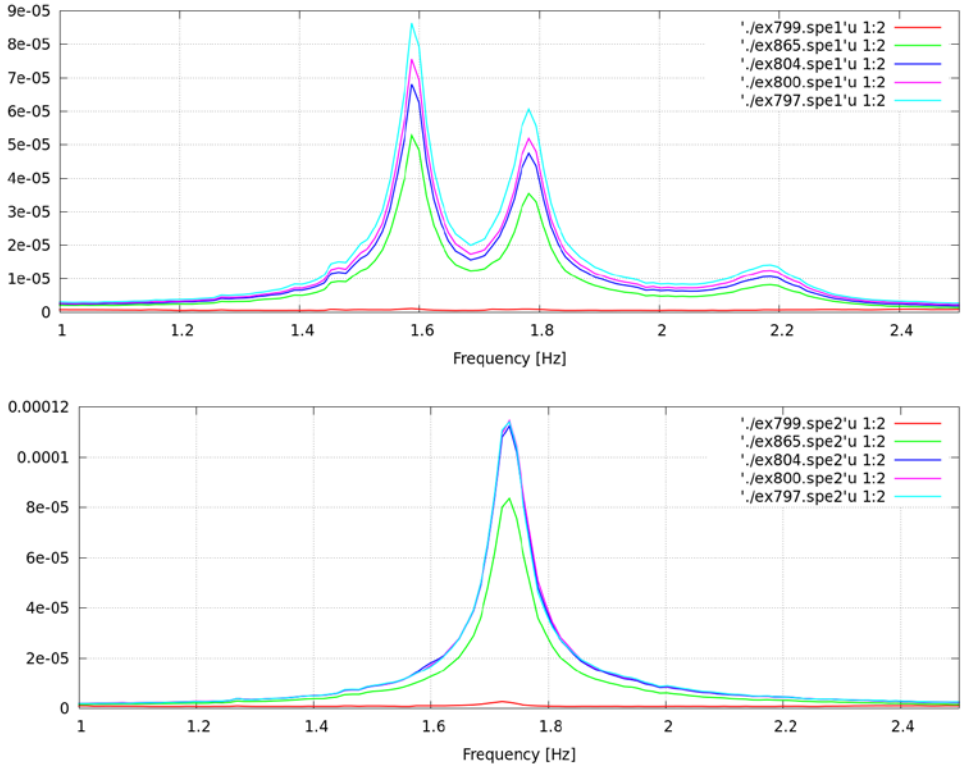

Figure 1.11: Central unit, right side: fundamental peaks for the pri1 (top) and pri2 (bottom) components.

Time-frequency analyses are performed to assess the stability over time of the spectral features. Figure 1.12 shows the spectra versus time for the .pri1 component of cubes 900 (basement), 795 (1st floor) and 710 (4th floor). The features are more evident during the day, when the overall level of noise is higher. In particular, the peak at 1.78 Hz (second peak) is less prominent during the night.

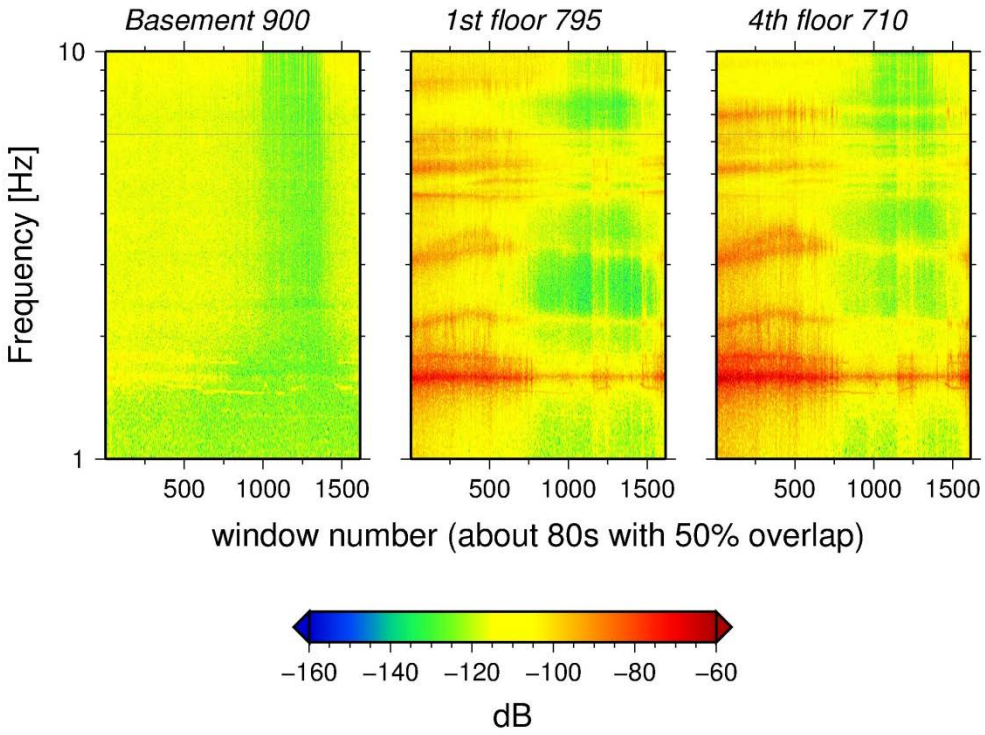

Figure 1.12: Time-frequency analysis for three stations installed in the Left-body of the Philosophy building.

1.5.2. Administration building

The Administration building is more regular and taller than the Philosophy building. Figure 1.13 shows the main peaks over the two horizontal components. The fundamental bending modes (1.172 and 1.245 Hz), the fundamental torsion (1.69 Hz), and the first higher bending modes (3.89 and 4.27 Hz) have been detected (Figure 1.14).

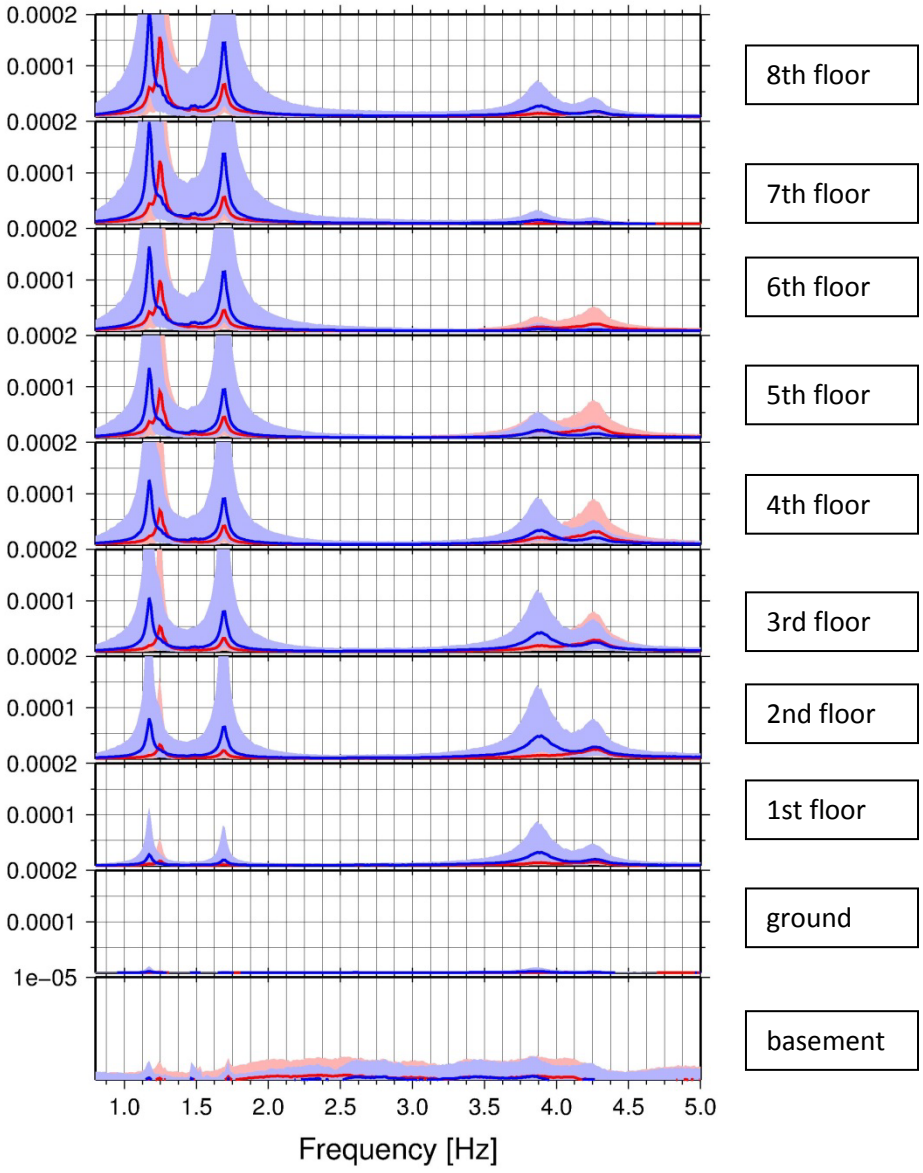

Figure 1.13: Administration building. Fundamental and first modes are detected for the pri1 (transverse, along the red arrow, in blue) and pri2 (longitudinal, in red) components.

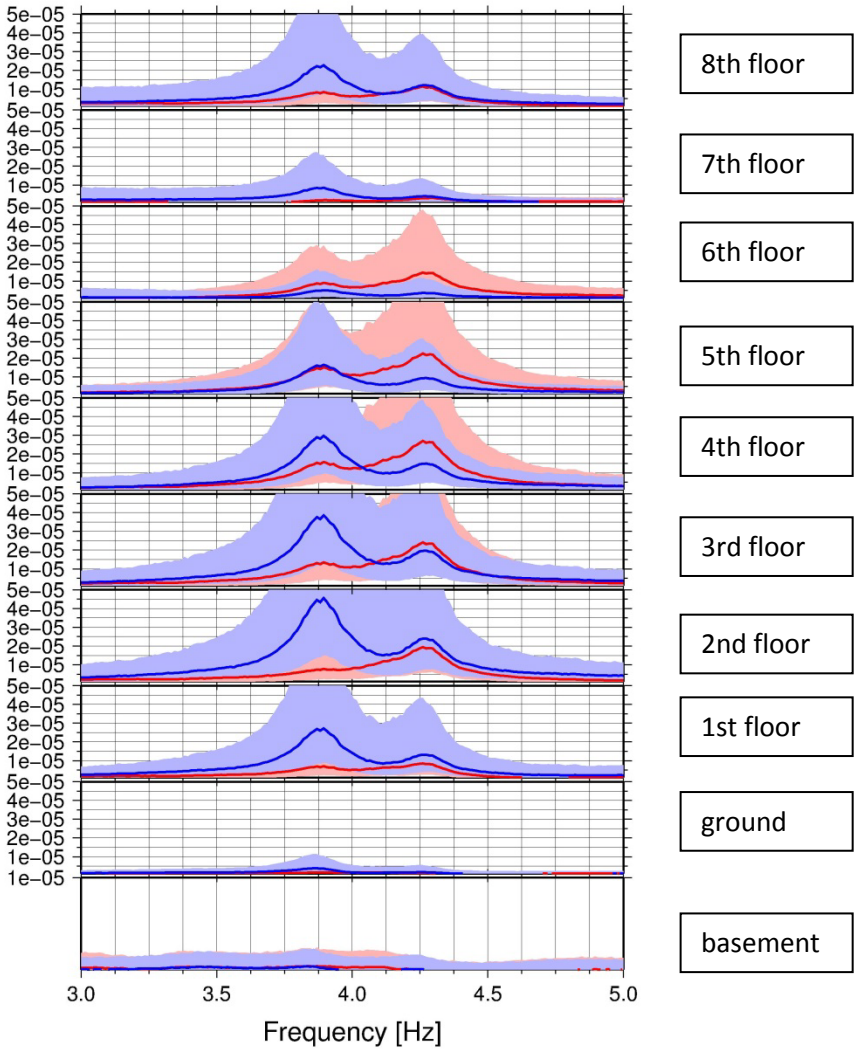

Figure 1.14: Administration building. First modes detected for the pri1 (transverse, along the red arrow, in blue) and pri2 (longitudinal, in red) components. The nodal point for the pri1 component is about the 6th floor, with a larger displacement at the 2nd floor; for pri2 component, the maximum and nodal points are at the 4th and the 7th floors, respectively.

2. Building-specific vulnerability assessment using monitoring data and finite element modelling

Risk and vulnerability of urban sites to earthquake hazard lead to an emerging need for developing operational frameworks that can be used by the various authorities (e.g. civil protection, town planners) in pre-crises situations to establish decision making procedures and risk mitigation strategies. The collection of monitoring data is a prerequisite to enhance the reliability of the safety assessment of structures.

In the context of seismic vulnerability assessment of buildings, the use of field monitoring data constitutes a significant tool for the representation of the actual structural state, reducing uncertainties associated with the building configuration properties as well as many non-physical parameters (age, maintenance, etc.), enhancing thus the reliability in the risk assessment procedure.

The present work aims at the evaluation of the seismic vulnerability of existing reinforced concrete (RC) buildings, combining through a comprehensive methodology the numerical analysis and field monitoring data. Two buildings from the Aristotle University campus in Thessaloniki are studied, namely the Administration and the Faculty of Philosophy building, which are both designed with low seismic code provisions.

The following sections describe in detail the buildings under investigation as well as the different steps of the applied methodological framework, starting from the instrumentation layouts implemented on the buildings and resulting to their nonlinear seismic response evaluation and vulnerability assessment.

2.1. Description of the Administration and the Faculty of Philosophy building and the AHEPA hospital

The Aristotle University of Thessaloniki (AUTh) is the largest university in Greece. The main campus is located in the centre of the city of Thessaloniki and comprises 10 faculties made-up of 40 schools and one single-School Faculty. The AHEPA general hospital, which is one of the largest hospitals in northern Greece, is also located in the campus of AUTh, as shown in Fig. 2.1.1 (Karapetrou et al., 2016). Most of the buildings hosting the faculties and schools were built before 1985 and are classified as low seismic code structures. The target buildings in this study are the Administration and the Faculty of Philosophy building and their location in the AUTh campus is shown in Fig. 2.1.1.

Fig. 2.1.1 Location of the Administration and Faculty of Philosophy building at the Aristotle University campus, and the AHEPA hospital.

The Administration building is a critical building, concentrating the most important administrative and economic activities of the University (Fig. 2.1.2). It was constructed in 1964 and is considered representative of structures that have been designed according to the old 1959 Greek seismic code ("Royal Decree" of 1959), where some important aspects related to the seismic damage prevention as the ductility and the dynamic features of the constructions are ignored. The design seismic PGA according to the particular code for Thessaloniki is defined at 0.06g, which is a much lower value compared to the present code (i.e. 0.16g). During the 1978 Thessaloniki earthquake (M=6.5, R=26.7km, Papazachos et al., 1979; Soufleris et al., 1982), which caused extensive damages and the collapse of one high-rise residence structure, the Administration building suffered moderate damages and was subjected to local repairs, such as filling the concrete cracks with epoxies and the reinforcement of specific beam elements with additional rebars and shotcrete concrete.

It is a nine-storey structure with a basement and presents irregularities in both elevation and plan as shown in Figs. 2.1.3 and 2.1.4. In particular, while the basement and the ground floor level of the structure cover a rectangular area of 56.60m by 21.60m and 59.50m by 25.50m respectively, the typical floor plan has a rectangular cross section of 44.80m by 10.80m. The total height of the building with respect to the foundation level is 34.20 m with the interstorey height varying along the building elevation. More specifically, the heights of the basement and ground floor are 4.60m and 4.00m, respectively, whereas the typical floor is 3.20m high. From the structural point of view, the building is characterized by a dual force resisting mechanism comprising frames as well as core walls. In the basement and

ground floor level there are frames in both the longitudinal and transverse direction, whereas the typical floor plan, which reflects the structural properties of the 1st, 2nd, 3rd, 4th, 5th, 6th, 7th and 8th floors, comprises externally frames only along the longitudinal direction. The two core walls surrounding partially the staircases and the lift shafts are located eccentrically in the floor plan closer to the right side of the building as shown in Fig. 2.1.3. The reinforced concrete walls are in general 0.15m thick, except for the wall T_7 (Fig 2.1.3) which has a thickness of 0.20m. The columns have a circular cross section with varying diameter along the structure's height, starting from 0.75m at the lowest level (basement) and 0.40m at the upper floor. At the basement level the inner and outer columns are connected by deep beams with cross section of 0.30m × 0.70m and 0.40m × 0.70m, respectively. The foundation system consists mainly of isolated footings without tie beams.

Due to the eccentricities existing between the center of mass and the center of rigidity, the building is expected to exhibit torsional effects. Furthermore, it should be noted that in the basement and ground floor levels, there are structural joints connecting the beam with the column elements and their locations are shown in Fig. 2.1.3 and 2.1.4. Finally, Fig. 2.1.5 shows the connection of the building with nearby structures which is, however, limited only to the 1st storey level.

Fig. 2.1.2. Administration building at AUTh campus.

Using the SYNER-G taxonomy (Pitilakis et al., 2014) for RC structures to describe the typology of the Administration building, it may be defined as high-rise dual system designed based on low seismic code provisions.

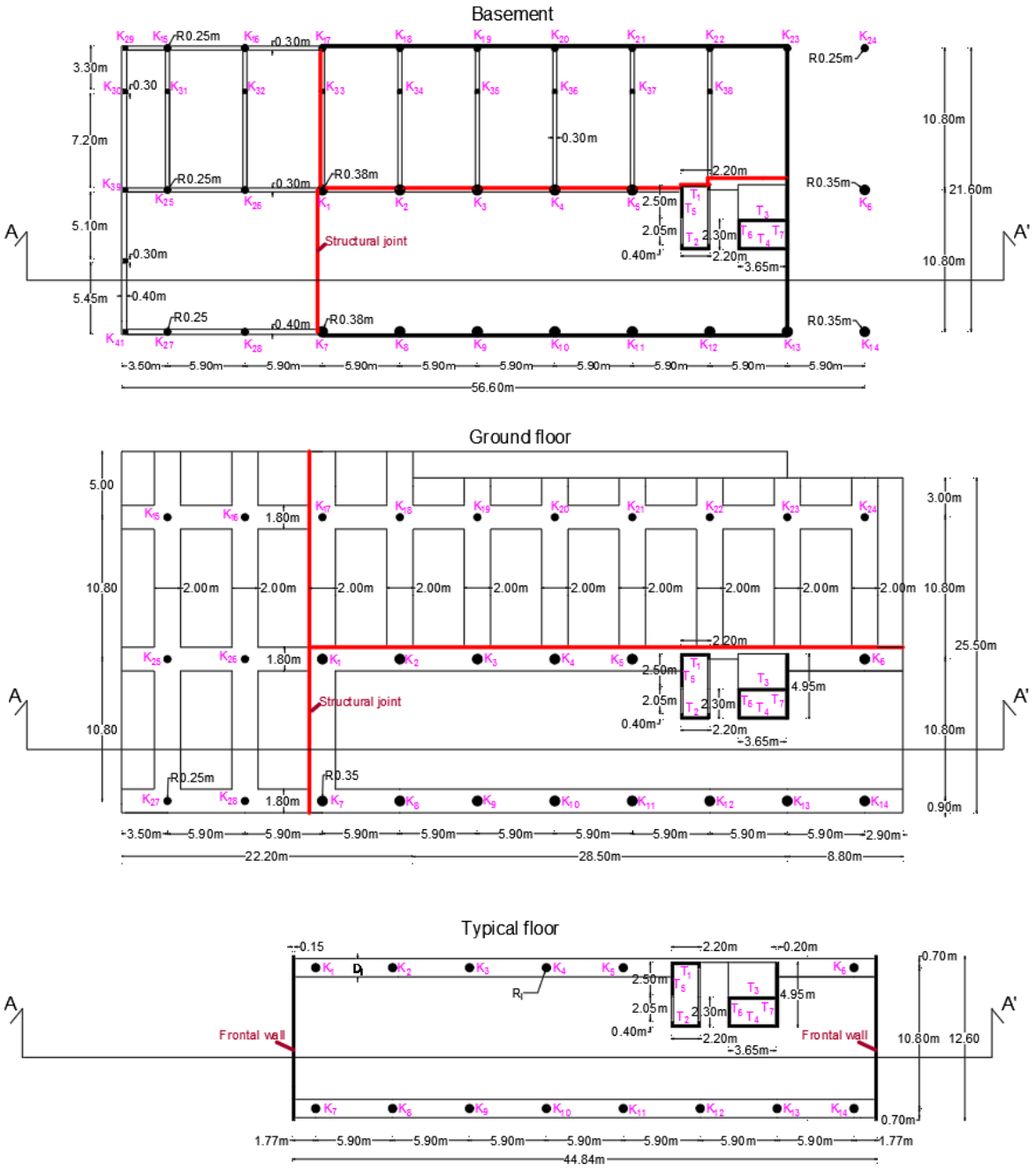

Fig. 2.1.3. Plan view of the basement, the ground floor and the typical floor of the Administration building.

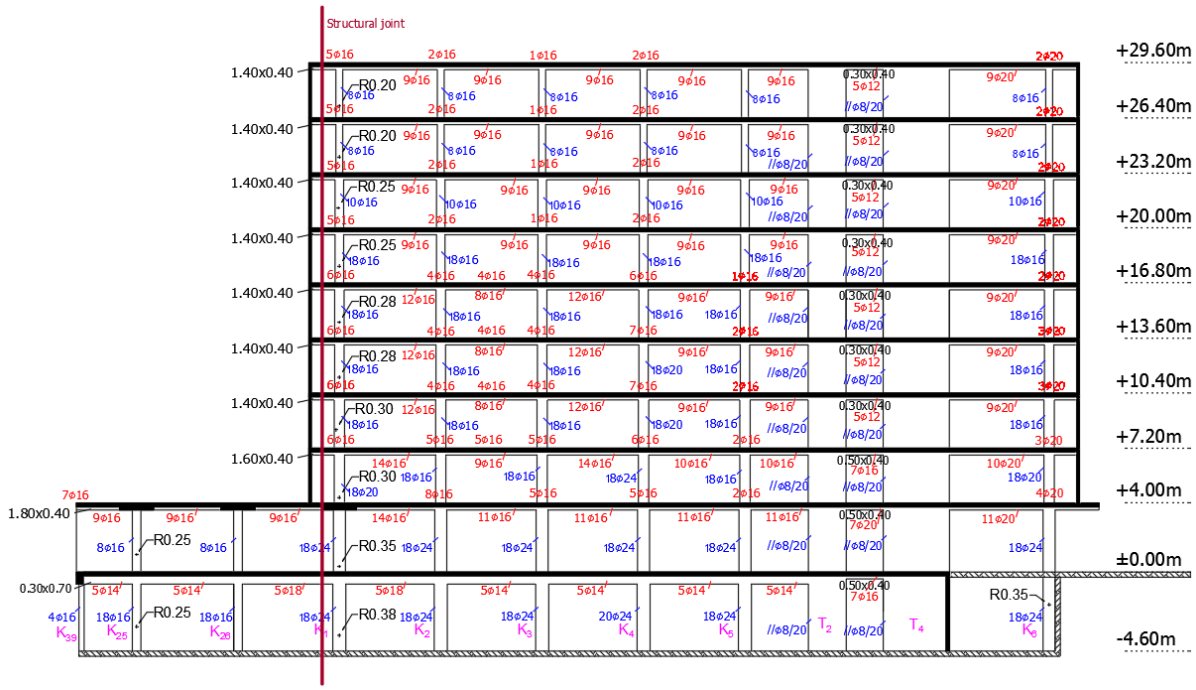

Fig. 2.1.4**.** Section A-A' along the longitudinal direction of the building as shown in Fig. 2.1.3

Fig. 2.1.5. Connection of the Administration building with nearby structures**.**

The Faculty of Philosophy building was built in 1965 and initially consisted of the basement, the semi-basement, the ground floor and three floors levels. Like the Administration building, it was also designed with low seismic code provisions (Royal Decree of 1959). In 1984, an additional floor level was constructed (last floor), for which, however, design information such as plans or structural detailing are not available. The building is characterized by its oblong plan with a length of 105m and width of 25.5m. It is divided in three parts with structural joints per 35m as shown in Fig. 2.1.6.

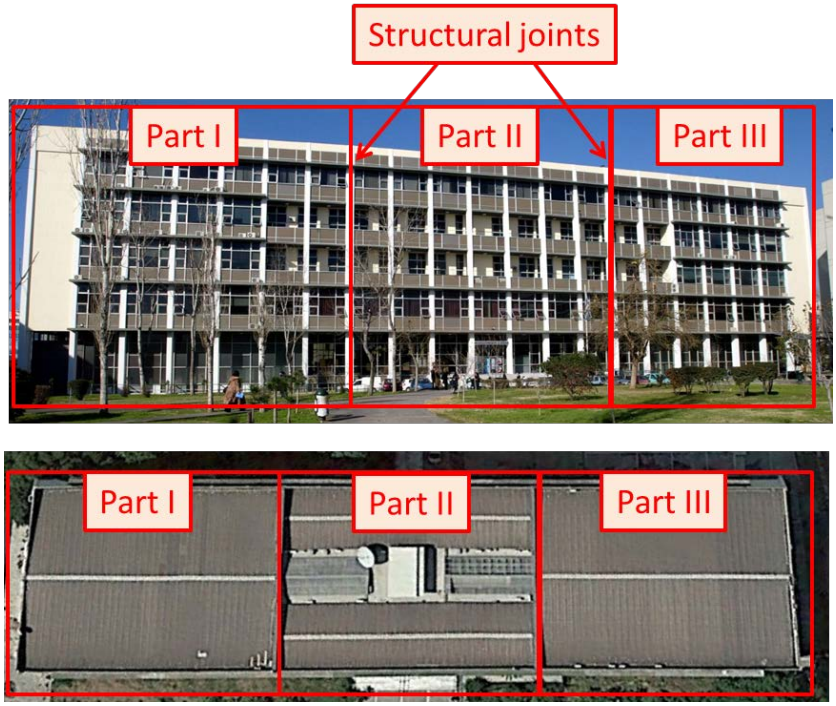

Fig. 2.1.6. Connection of the Administration building with nearby structures**.**

The building‘s force resisting mechanism comprises longitudinal and transverse reinforced concrete moment resisting frames. The columns’ cross section, as well as the beams’, decrease as the story level of the building increase. For example, inner column sections of 0.70m x 0.70m at the basement level reduce to 0.40m x 0.30m at the third floor. Since no design and construction plans are available for the later constructed last floor, in situ measurements were conducted in order to define the dimensions of structural elements and the floor height to detect the existing reinforcement and to estimate the depth of the concrete cover. More details of the in-situ experiment are provided in section 2.2 of this report.

Only the second and third floors of the building comprise external infill panels along the longitudinal direction. Peripheral concrete walls are present at the basement level while the foundation system consists of isolated and strip footings. Figs 2.1.7 and 2.1.8 present the foundation system and the typical floor plan of Part I and Part II. From the structural point of view, Part III is practically the mirror of Part I in plane and therefore the corresponding plans are not included in the figures. It is observed that

the beams are located densely along the transverse direction, forming at several positions beam to beam connections. Especially in the middle part of the building, namely Part II, the presence of beam-to-beam connections in combination with staircases and elevator shafts constitute a complex structural system. The total height of the building with respect to the foundation level is 28.65m and the sketch of Fig. 2.1.9 shows the floor levels and the interstorey heights of the different parts.

Based on the SYNER-G taxonomy the Faculty of Philosophy building may be considered typical of mid-rise moment resisting frame buildings whose design is based on low seismic code provisions.

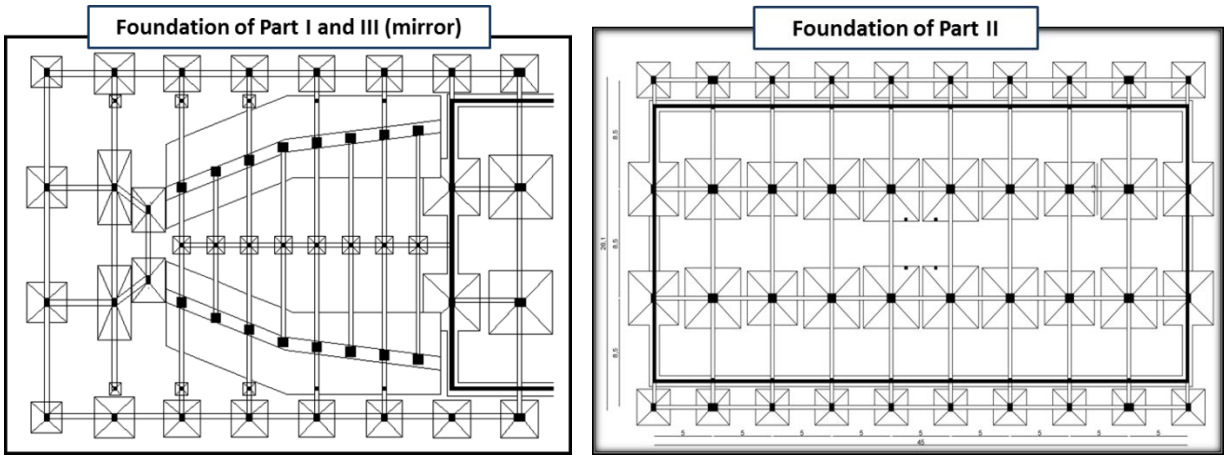

Fig. 2.1.7 Foundation system of the different parts of the Faculty of Philosophy building.

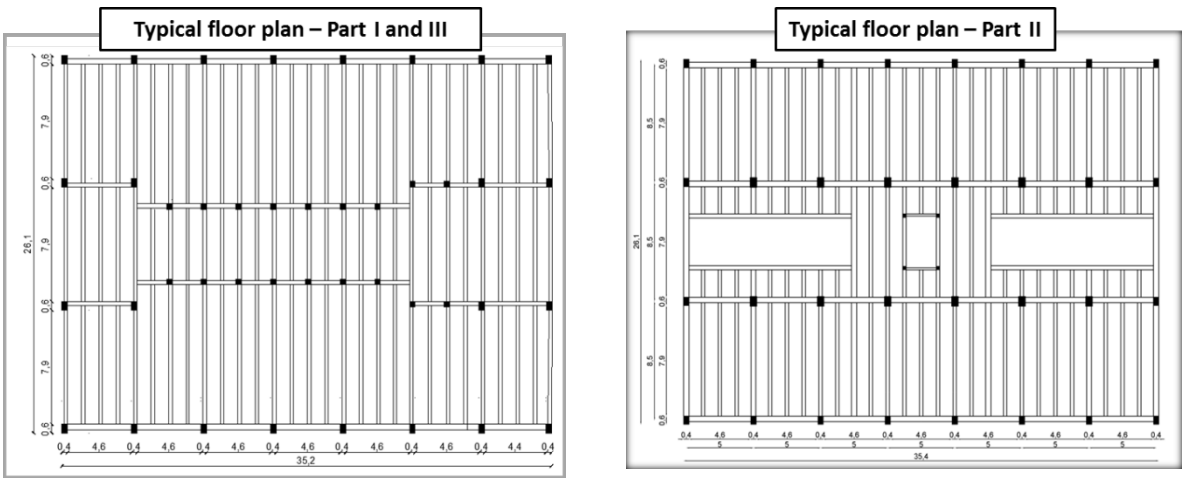

Fig. 2.1.8 Typical floor plans of the different parts of the Faculty of Philosophy building.

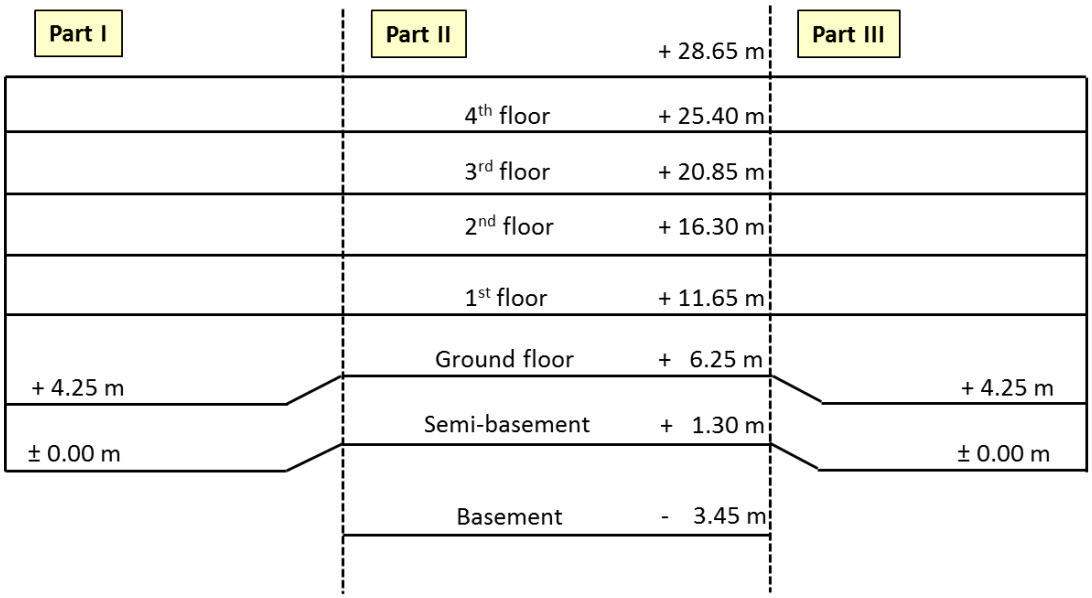

Fig. 2.1.9 Floors levels and interstorey heights of the different parts of the Faculty of Philosophy building.

In the fall of 2015, ambient noise measurements were performed at the campus to assess the soil conditions and site effect characteristics namely the soil characterization in terms of resonant frequency, amplification factor and shear wave velocities with depth close to the two buildings under study. The results showed that the foundation subsoil conditions of the two buildings and below the first 8-9m thick surface layer (composed mainly by artificial landfills), is characterized by quite stiff soils with Vs velocities greater than 400-500m/sec. Based on these results the foundation soil at the two buildings can be characterized as soil type B according to EC8 soil classification. The seismic bedrock (Vs>1000m/s) is found below 35m depth. Detailed description of the experiment campaign and the analysis results may be found in Deliverable DC2: “Guidelines for undertaking site-effect surveys”.

2.2. Building-specific vulnerability assessment using monitoring data

The methodological framework has been described in detail in SIBYL Deliverable DC1 “Guidelines for the building assessment procedure and short-term monitoring”. The schematic flowchart shown in Fig. 2.2.1 describes the different steps of the applied procedure. Ambient noise measurements are used to derive the experimental modal model of the building and identify its modal properties based on operational modal analysis (OMA). The modal identification results are used to update and better constrain the initial finite element model of the building, which is based on the design and construction documentation plans. Model updating aims at the “correction” or “update” of the initial finite element model based on data processing, obtained from measurements conducted on the test structure (Mottershead and Friswell, 1993). The main purpose of calibrating the modal model is to modify iteratively updating parameters to result in structural models that better reflect the measured data than the initial ones. One of the key issues during the updating process is the selection of

the appropriate updating parameter. In general, if not serious geometrical modifications are identified, structural features such as material or mass properties are likely to be selected as updating parameters in order to increase the correlation between the observed dynamic response of the structure and the predicted from the numerical modal model (Scodeggio et al., 2012). Other parameters, such as soil-foundation-structure interaction or the foundation conditions, which influence the modal properties, may contribute in the updating process, however, they might include high uncertainty levels and additional tests are required for their determination (e.g. non-destructive tests).

In the present methodology, a manual updating scheme is proposed to be applied considering only a limited number of parameters, so called control parameters, which allows a good observation of the process in order to gain complete insight into the effects of the sensitivity parameters on the structural behavior. The updating procedure consists of an eigenvalue sensitivity analysis of the elastic numerical modal models in order to identify the most sensitive parameters influencing the structural modes of interest, which are used in the manual updating process to define the optimal analytical models that reflect the experimental results. The selection of the best updated finite element (FE) model of the building is made by evaluating an appropriate response correlation function between experimental and numerical results (e.g., Modal Assurance Criterion, Allemang and Brown, 1982). Finally, three-dimensional nonlinear incremental dynamic analyses (IDA, Vamvatsikos and Cornell, 2002) of the nonlinear updated models are performed in order to estimate the failure mechanism of the structure and derive the building-specific fragility functions.

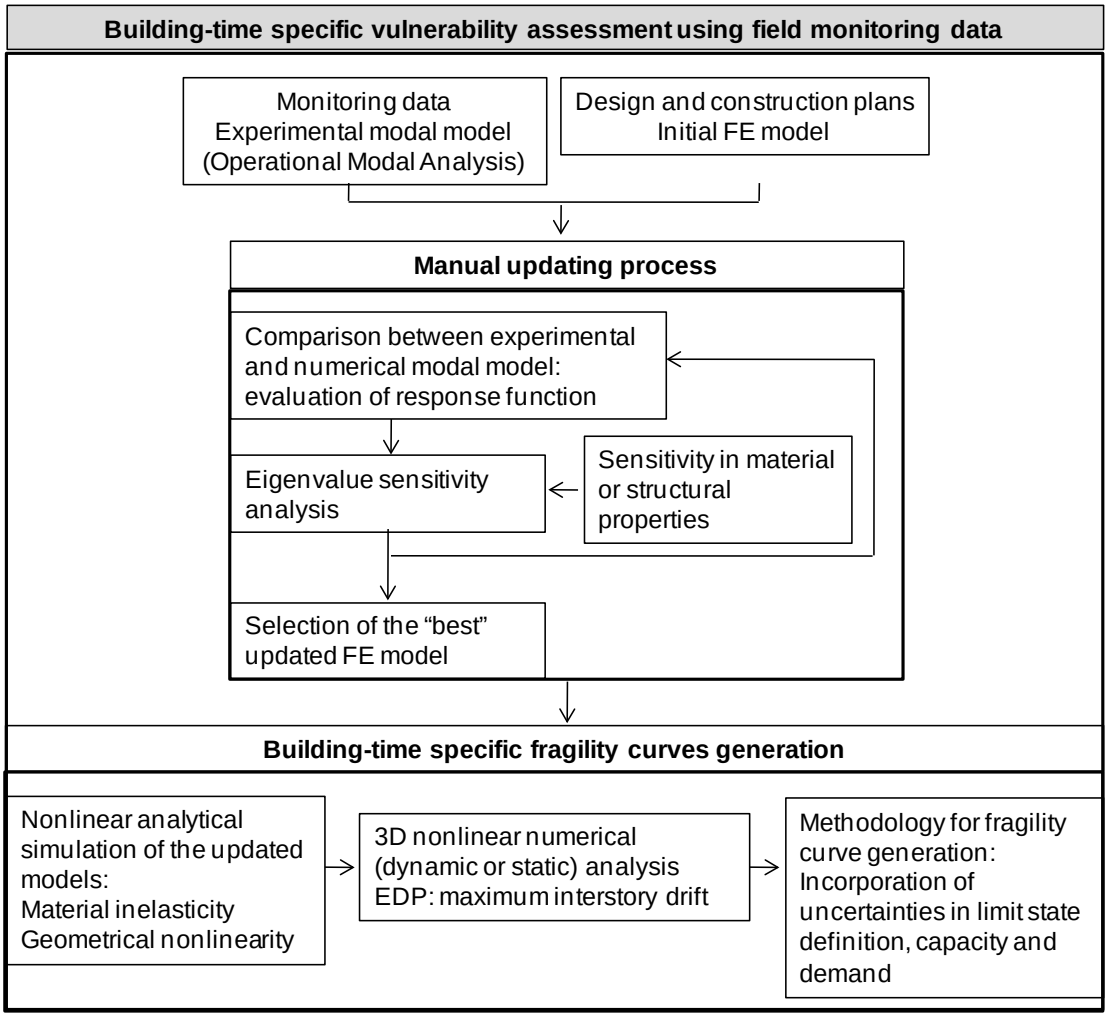

Fig.2. 2.1. Methodological framework for the derivation of building – specific fragility curves of RC buildings.

2.2.1. Administration building - AUTh

2.2.1.1. Seismic instrumentation

A permanent accelerometric array, the so called SOSEWIN network, has operated in the Administration building since April 2015. The permanent network is installed for long-term building monitoring. It is composed by sensing units where the building motion is measured in real time through MEMS sensors. It is mainly intended to monitor the building's response to earthquakes. Furthermore, the earthquake recordings from the permanent instrumentation array are used to develop an operational framework for Early Earthquake Warning (EEW) and rapid post-earthquake damage assessment. The SOSEWIN network constitutes of 4 triaxial accelerometers (MEMS ADXL203 chip). In particular, one sensor has been installed in the basement (CA00), one in the second floor (CA21) and two in the eighth floor (CA81, CA82). Several earthquake events have already been recorded and the

instrumentation array continues to transfer data streams to the Seiscomp3 server installed at the SDGEE-AUTH premises.

In addition to the permanent network, a temporary instrumentation array was also implemented at the end of September 2015 under the responsibility of the Soil Dynamics and Geotechnical Earthquake Engineering of the Aristotle University of Thessaloniki (SDGEE-AUTH) and in close cooperation with the Technische Universität Berlin (TU-Berlin) and the Helmholtz Centre Potsdam, German Centre for Geosciences (GFZ). Ambient noise measurements are used for the dynamic characterization of the building deploying a denser network of stations equipped with velocimeters, which have a better amplitude resolution and a lower internal noise than the MEMS. The instrumentation layout included 38 CUBE digitizers connected to 4.5Hz components geophones. GPS antennas guaranteed the time synchronizations among all instruments. The sensors recorded along the two orthogonal horizontal and along the vertical directions (three components). The two horizontal components are oriented along the longitudinal and transversal direction of the building. Ambient noise was recorded simultaneously for about 20 hours in all stations with a sampling rate of 400Hz. In order to capture the translational and torsional modes of the building, 4 sensors were installed at the corners of each floor close to the vertical structural elements (i.e. reinforced concrete columns) (Fig. 2.2.2). Table 2.2.1 summarizes the serial codes and locations of the employed instruments for the ambient noise experiment whereas Figs. 2.2.3 and 2.2.4 illustrate the location of the sensors of the permanent and the temporary network inside the building.

Fig. 2.2.2 Installation of the temporary network. Sensors located close to the RC columns.

Table 2.2.1 **Serial number and position of all the stations used in the ambient noise experiment.**

Station code	New code	Floor
793/172	**ABa**	Basement
898/157	**ABb**	
792/182	**AGa**	Ground floor
902/161	**AGd**	
711/185	**AGb**	
903/174	**AGc**	
802/168	**A1a**	1st
887/170	**A1d**	
805/173	**A1b**	
801/183	**A1c**	
804/164	**A2a**	2nd
800/181	**A2d**	
808/179	**A2b**	
809/165	**A2c**	
899/171	**A3a**	3rd
710/190	**A3d**	
712/163	**A3b**	
791/160	**A3c**	

Station code	New code	Floor
798/178	**A4a**	4th
713/169	**A4d**	
874/154	**A4b**	
876/167	**A4c**	
806/166	**A5a**	5th
807/196	**A5d**	
865/177	**A5b**	
604/189	**A5c**	
795/158	**A6a**	6th
796/192	**A6d**	
799/155	**A6b**	
803/175	**A6c**	
797/156	**A7a**	7th
900/176	**A7d**	
875/187	**A7b**	
901/162	**A7c**	
891/194	**A8a**	8th
605/159	**A8d**	
873/184	**A8b**	
864/191	**A8c**	

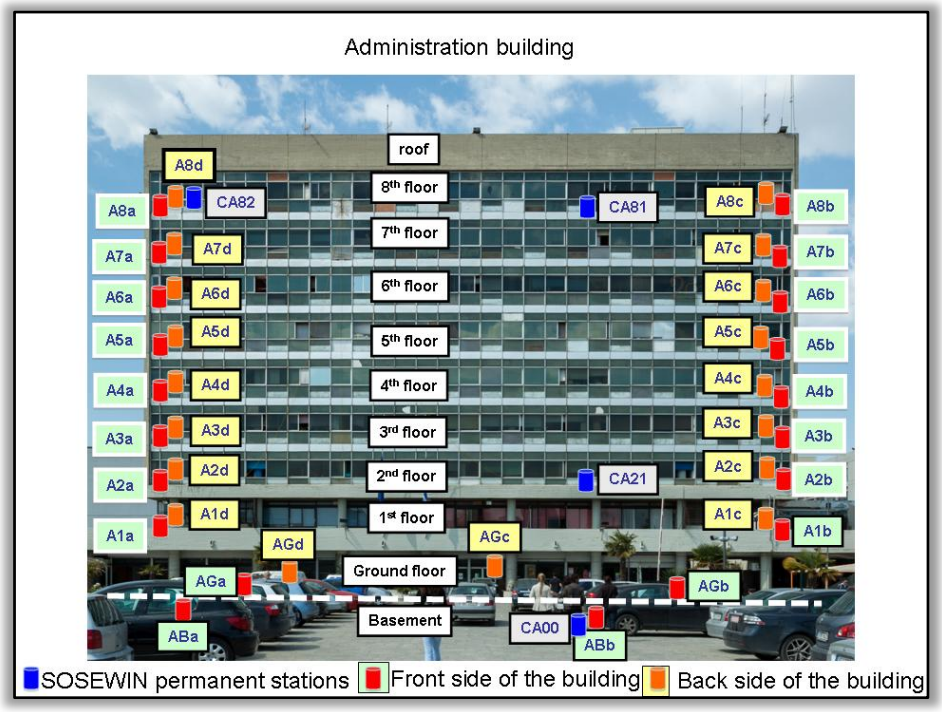

Fig. 2.2.3 Instrumentation arrays deployed inside the administration building (permanent and temporary networks).

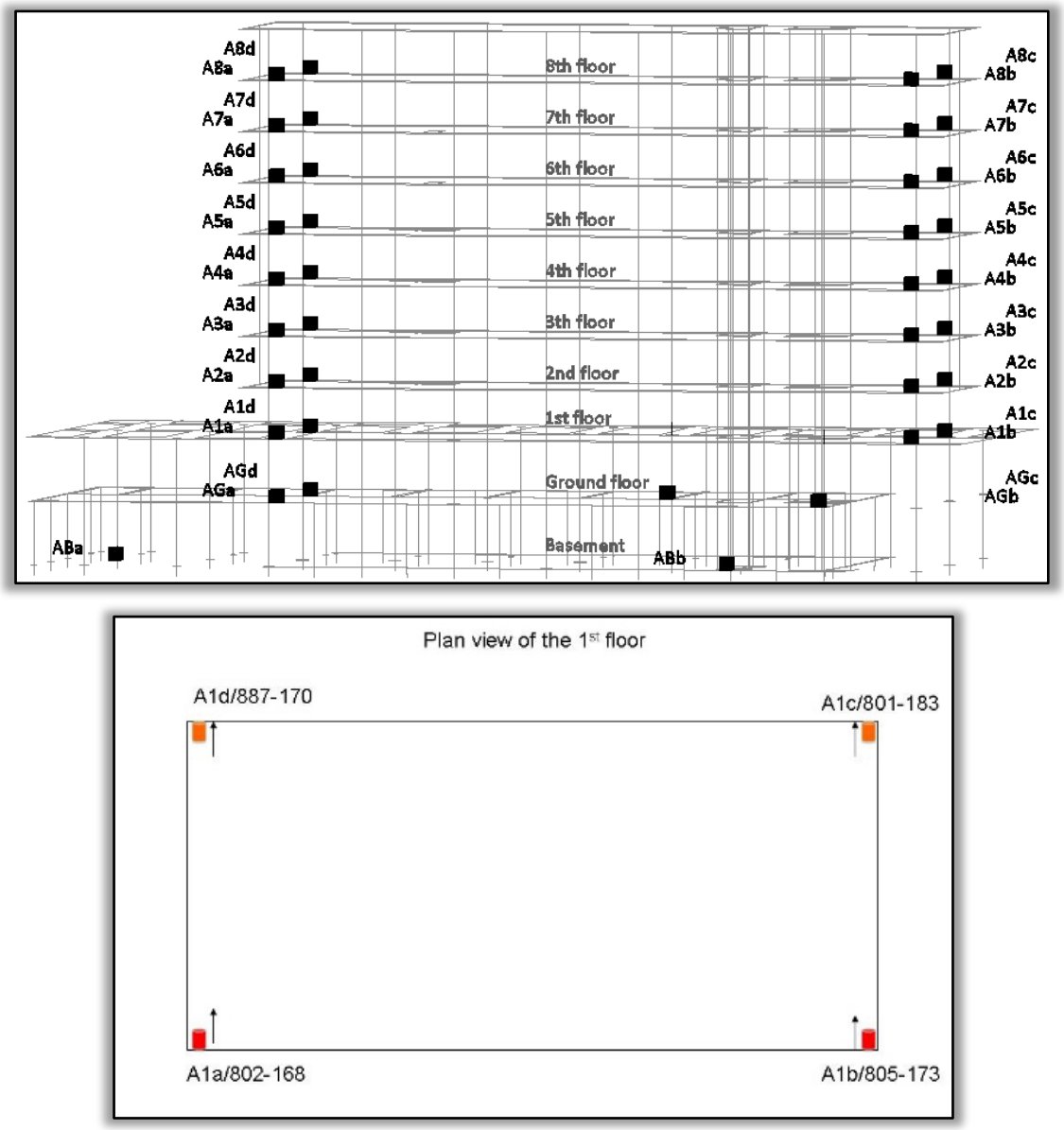

Fig. 2.2.4 Instrumentation arrays deployed inside the administration building (3D and plan view of the temporary network).

2.2.1.2. Operational modal analysis using ambient noise measurements

To evaluate the dynamic characteristics of the Administration building, namely the natural frequencies and mode shapes, system identification and Operational Modal Analysis (OMA) were performed using MACEC 3.2 software (Reynders et al., 2011). In MACEC 3.2, the OMA procedure is divided in three distinct steps: (1) the collection of the data and preprocessing, (2) system identification and (3) the determination of the modal parameters from the identified system model. Operational modal analysis is performed considering only the horizontal components of the measurements.

The geometrical characteristics of the models introduced and analyzed in MACEC 3.2 are illustrated in Fig. 2.2.5. The grid of the model is built so that the defined

nodes correspond to the nodes that have been actually measured. In order to investigate the variation of the modal parameters of the structure, from the 20-hours of measurements, the data of four smaller one-hour recording sets were analyzed, covering different time periods during the day- and night time (i.e. 3:00-4:00, 10:00-11:00, 15:00-16:00, 20:00-21:00, GMT-time). Each time window used for OMA has duration of 1800sec (30min) as tests on the stability of the results showed that 30 minutes is enough to get reliable results. Before the identification, the data were decimated by a factor of 10 and filtered with a low-pass anti-anti-aliasing filter with a cut-off frequency of 20Hz and re-sampled at 40Hz, reducing thus the number of data, and avoiding unnecessary computational burden in the modal analysis where the frequencies of interest are less than 20Hz.

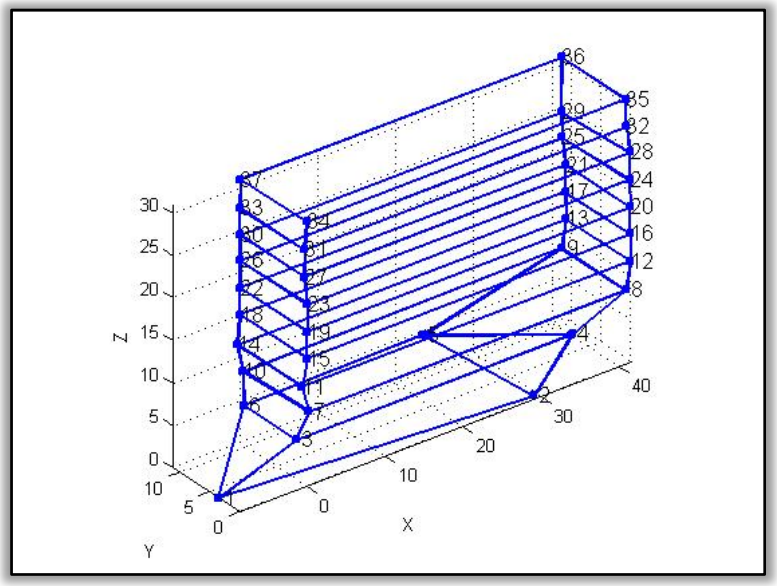

Fig. 2.2.5 Visualization of the building's geometry in MACEC 3.2.

In order to verify and enhance the modal identification results, analyses have been conducted using both non-parametric and parametric identification techniques. More specifically, the methods that have been applied in MACEC 3.2 are the following:

- Nonparametric power spectral density PSD+ estimation using the correlogram method in frequency domain.
- Reference-based covariance-driven stochastic subspace identification in the time domain.

In the non-parametric methods, system identification is based on the calculation of the Positive Power Spectral Density (PSD+) matrix at discrete frequency lines. For the PSD+ estimation of the measured outputs collected from all channels, the correlogram method was applied. In the correlogram approach, the auto and cross-PSDs of one or two quasi-stationary ergodic sequences is estimated as the Laplace transform of the auto or cross correlation functions, respectively

(Reynders, 2012). In Fig. 2.2.5, an illustrative cross-correlation PSD is shown. Modal analysis of the identified non-parametric models has been conducted based on the Frequency Domain Decomposition (FDD) method. In the FDD method, the singular values are obtained from the decomposition of the PSD matrix and the modal parameters are estimated by picking the peaks of the first singular value.

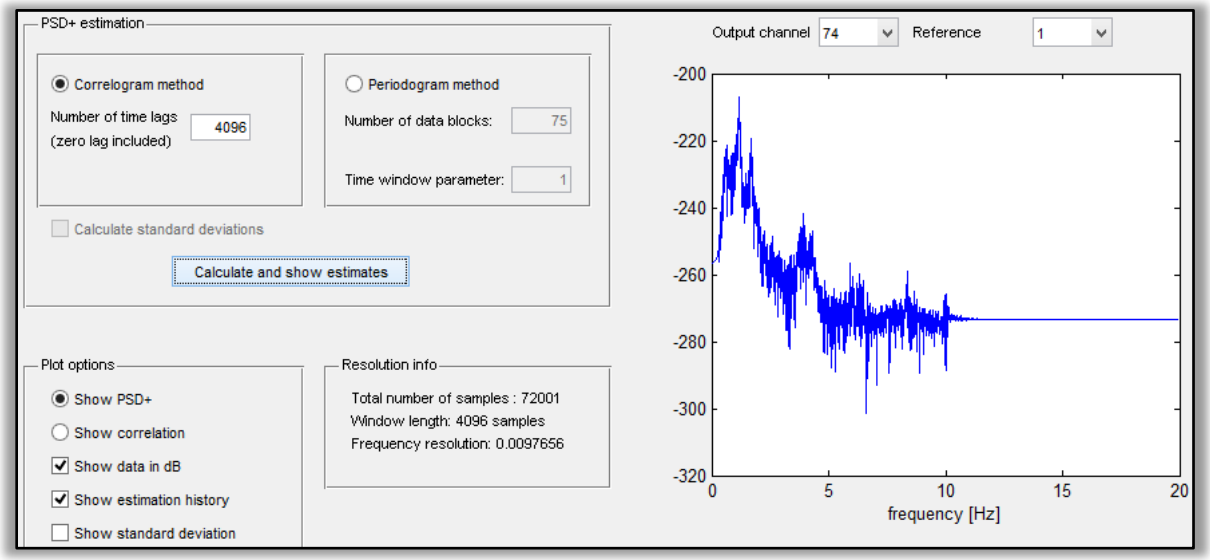

Fig. 2.2.5 An indicative cross-correlation PSDs+ used for the FDD analysis in MACEC 3.2.

Modal identification based on parametric methods was conducted by applying the reference-based covariance-driven stochastic subspace method. The number of block rows in the Toeplitz matrix was selected as 2x(expected system order)/number of outputs). After the QR and singular value decomposition step of the SSI algorithm, the real order was estimated based on the singular values (Fig. 2.2.6). For noiseless data, the system order equals the number of nonzero singular values, while for noisy data, the noise causes some singular values to be different of zero. Due to the fact that the noise is present in the recorded ambient vibration data, the identified system contains both system and noise dynamics. A common approach in modal analysis is then to over-specify the model (Peeters et al., 1999) such that the true system modes (physical modes) are separated from the noise modes (mathematical modes) (Reynders et al., 2011). In general, the selection of the model order for the construction of the stabilization diagrams for the SSI method depends on the number of modes of interest as well as the number of sensors. For the construction of the stabilization diagram, a model order range from 2 to 200 in steps of 2 was selected. The aim is to use the stabilization diagrams to detect the columns of stable modes that satisfy the defined stabilization criteria and continuously select a representative mode from each column.

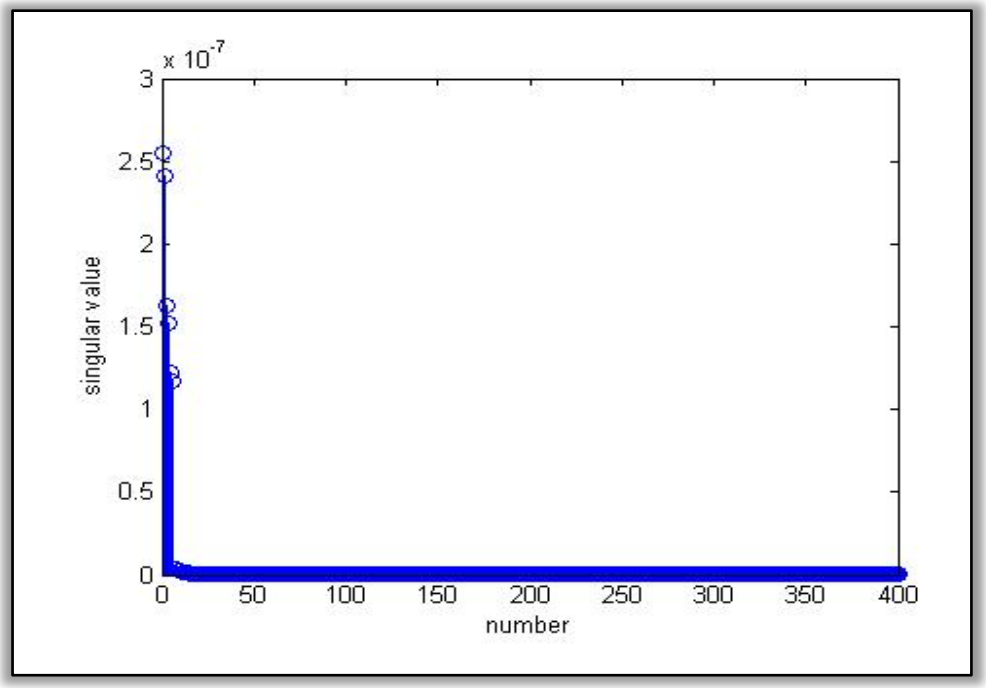

Fig. 2.2.6 Singular values of covariance-driven SSI method in decreasing order of magnitude.

The results of the nonparametric and parametric analyses for the Administration building are presented in Fig. 2.2.7. Fig. 2.2.8 shows some representative eigenfrequency and mode shape results of the identified modes, corresponding to the SSI analysis results for the recording time window of 10:00-11:00 am (GMT time). The building is exhibiting coupled sway and torsional modes in the frequency range of interest, which are expected in case of geometric and structural irregularities or eccentricities between the center of mass and center of rigidity. The highly coupled obtained mode shapes reveal the complex vibrational characteristics of the building, especially for the first two identified frequencies. Although coupled, the predominant motion of the first mode is mainly along the transverse direction, whereas the second one along the longitudinal direction.

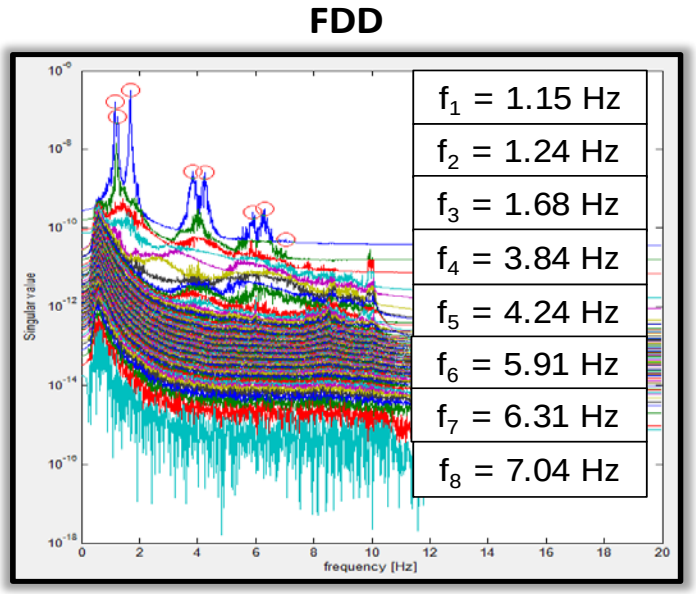

(a)

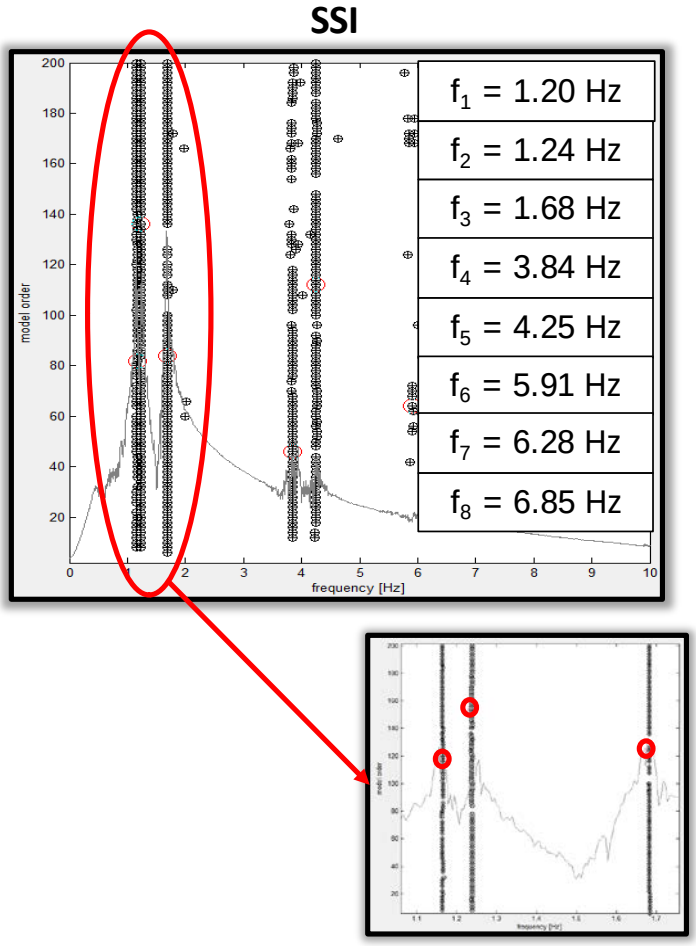

(b)

Fig. 2.2.7 Identification results through OMA for the Administration building based on (a) FDD and (b) SSI methods.

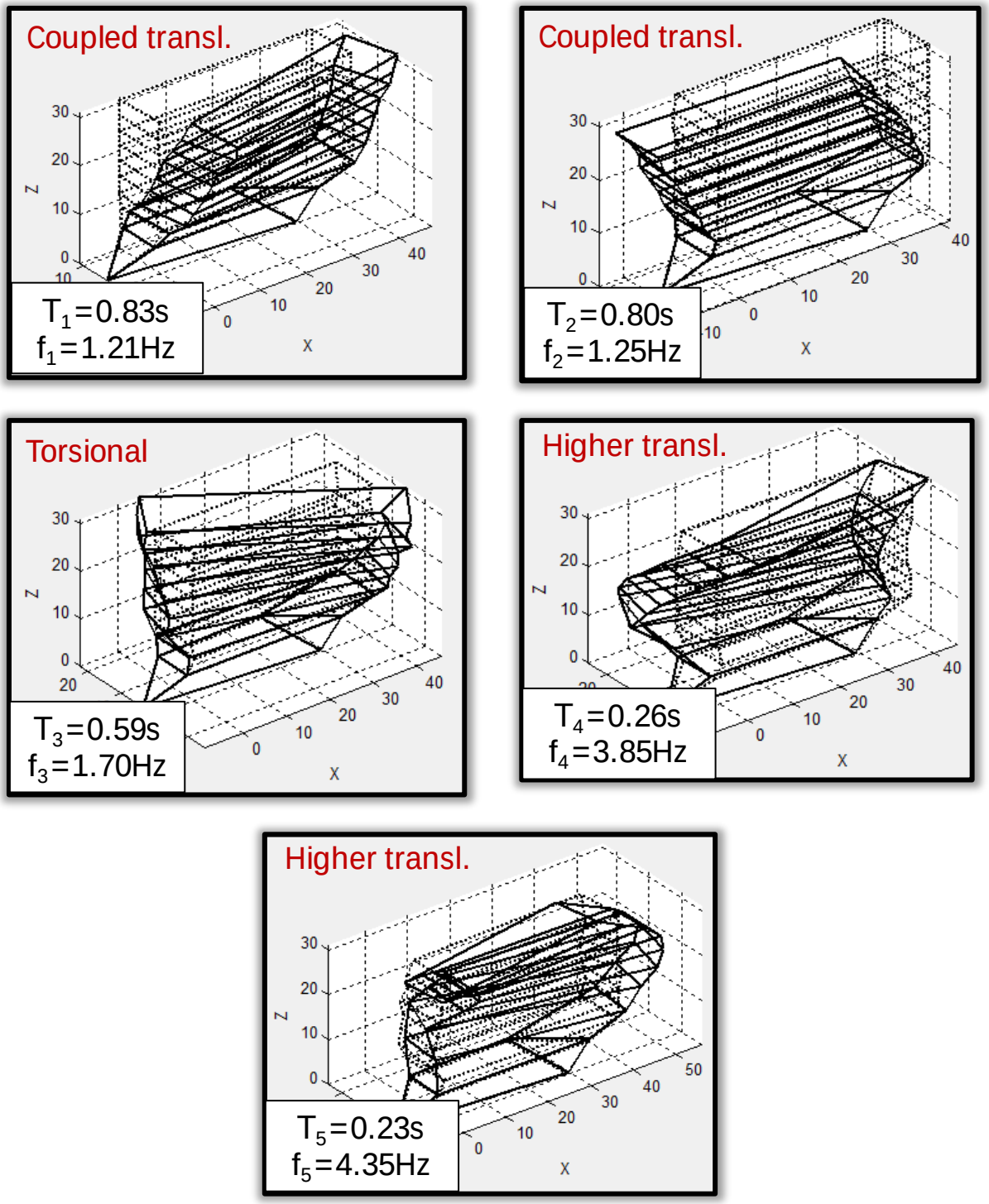

Fig. 2.2.8 Eigenperiods/Eigenfrequencies and mode shapes for the first five identified modes for the Administration building (T: period, f: frequency).

Table 2.2.2 shows the variation in the eigenfrequency values for the different time windows. The resonant frequencies are practically the same for the three first modes, whereas only slight variations (of the order of 1-3%).are observed for the higher modes of interest (i.e., 4th and 5th modes).

Table 2.2.2 Variation of the fundamental frequencies of the Administration building during the recorded timeframes (GMT time).

	Time window of recorded data			
Frequencies (Hz)	Recording 3:00-4:00 a.m.	Recording 10:00-11:00 a.m.	Recording 15:00-16:00 p.m.	Recording 20:00-21:00 p.m.
f_1	1.20	1.21	1.20	1.20
f_2	1.25	1.25	1.25	1.25
f_3	1.70	1.70	1.69	1.70
f_4	3.91	3.85	3.88	3.91
f_5	4.29	4.35	4.26	4.27

2.2.1.3. Elastic numerical simulation and modal analysis of the structural model

The finite element modeling of the Administration building is based on the available design and construction plans. In order to evaluate the elastic structural performance of the building, the numerical modeling was conducted using two finite element codes, SAP2000 (Computers and Structures, Inc) and SeismoStruct (SeismoSoft, v.7). The aim was to simulate a 'reliable' structural model in SAP2000 by using a detailed modeling approach for the concrete walls and the floor diaphragms through shell elements. Based on the static and modal analyses of the detailed model in SAP2000, a more 'simplified' structural model was generated in SeismoStruct using beam-column elements for the wall and constraints for the diaphragm modeling respectively in order to perform the series of dynamic analyses required for the vulnerability assessment of the building. The frame elements in both codes were simulated as linear elastic beam-column elements. The support conditions of the structure at the bottom of the basement were considered as fixed base. In order to take into account the existence of the basement, the translational degrees of freedom at the ground floor level were restrained. Finally link elements were utilized for the structural joint modeling at the basement and ground floor level (Fig. 2.1.3). Link elements were also used to model the connection of the building with the nearby structures at the 1st storey level as shown in Fig. 2.1.5.

The total mass of the structure is estimated equal to 7219 tn taking into account the self-weight of the structural elements as well as the dead and live load acting on each floor level. Based on the available data, the strength class of concrete and reinforcement steel are considered as B300 (C25/30) and StIIIb (S400) respectively. Fig 2.2.9 illustrates the structural models in SAP2000 and SeismoStruct whereas Fig. 2.2.10 shows the comparison results of the modal analysis performed using the two finite elements codes. The results show that the structural model consisting only of beam column elements approaches adequately the dynamic behavior of the detailed analytical model in terms of eigenperiods and mode shapes. The first and second modes are coupled translational modes mainly along the transverse and longitudinal direction respectively whereas the third mode is a rotational mode.

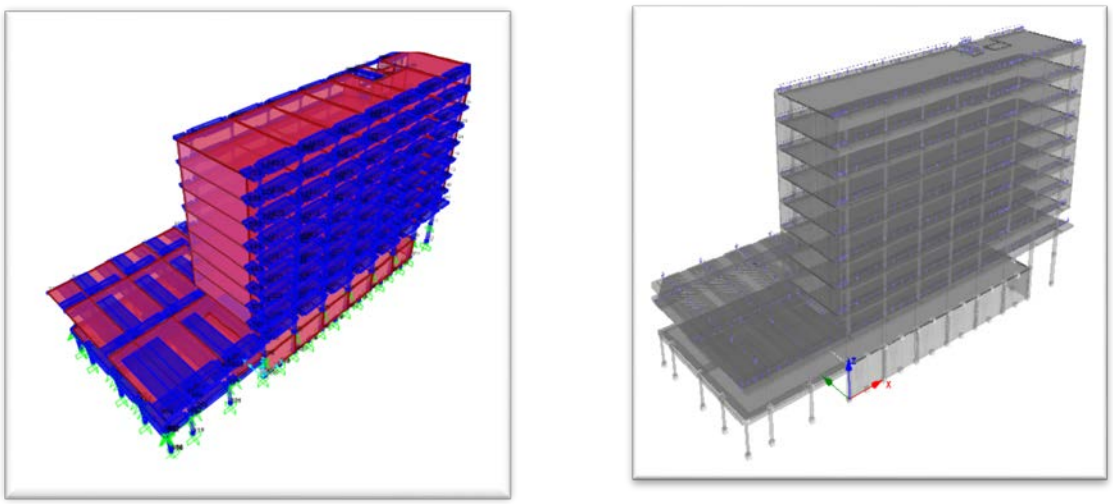

Fig. 2.2.9 Numerical simulation of the Administration building in SAP2000 using shell elements (left) and in SeismoStruct using beam-column elements (right).

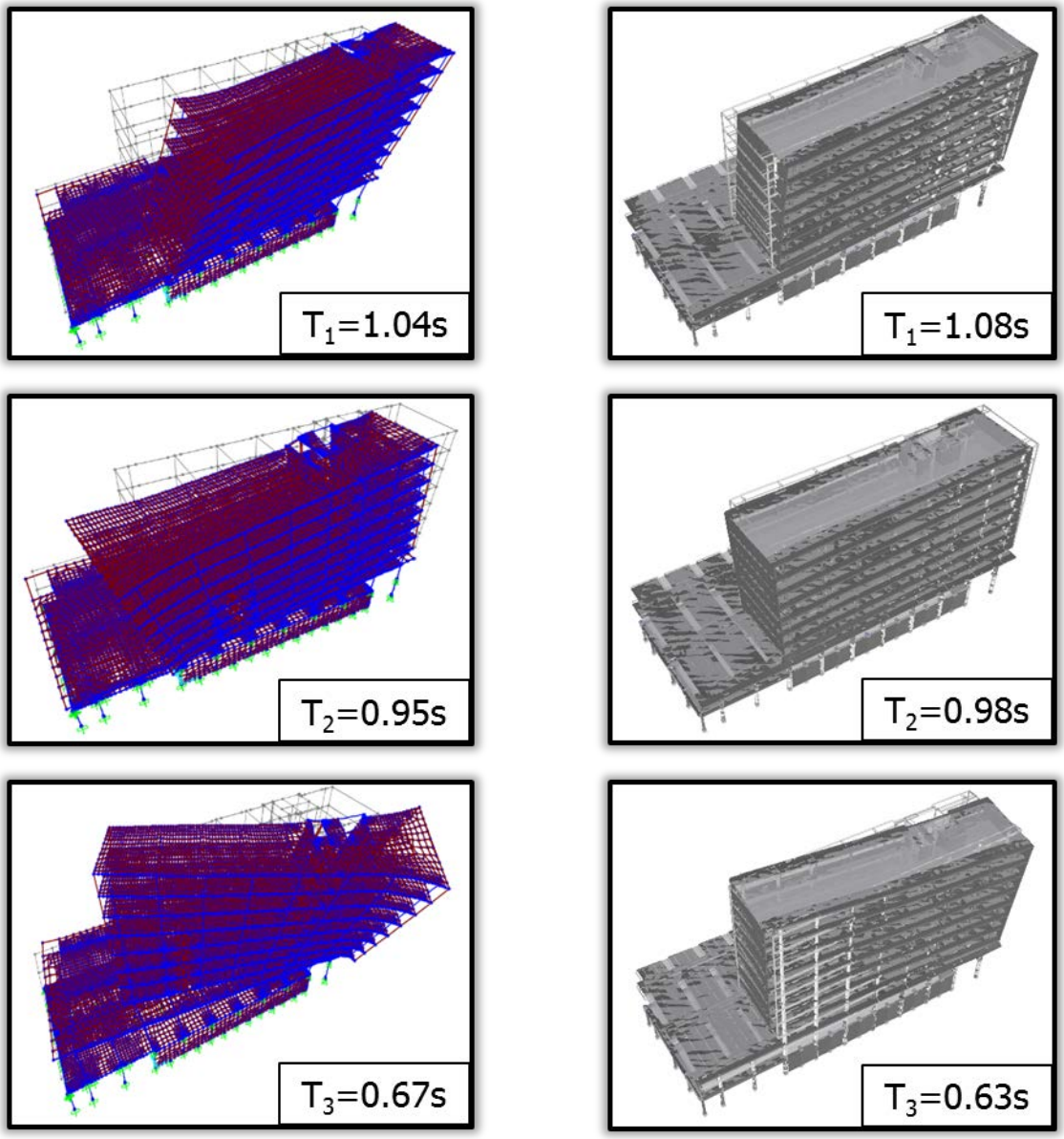

Fig. 2.2.10 Comparison of the eigenperiods and mode shapes of the detailed structural model in SAP2000 (left) and for the more simplified model SeismoStruct (right). (T: period)

2.2.1.4. Comparison between the analytical and the experimental modal analysis results. Finite element model updating.

The main purpose of this task is to modify iteratively updating parameters to result in a structural model of the Administration building that will better reflect the measured data than the initial one which was built based on the design and construction plans. One of the key issues during this process is the selection of the appropriate updating parameter. In general, if not serious geometrical modifications are identified, as in the present case, structural features, such as material or mass properties, are likely to be selected as updating parameters in order to calibrate the numerical modal model, i.e. increase the correlation between the observed dynamic response of the structure and the predicted from the numerical modal model (Scodeggio et al., 2012). In this particular case as updating parameter the stiffness parameter of the link elements K_0 is selected since no data are available for this property and therefore its definition includes high uncertainty levels. More specifically six stiffness parameter values that correspond to the translational and rotational degrees of freedom are investigated.

The updating is performed not only to improve the frequencies of the considered modes of the initial numerical model presented in Fig. 2.2.10 but also to calibrate the numerical mode shapes in order to fit the experimental data. A manual updating scheme is applied generating a suite of numerical modal models considering different values of the stiffness parameter K_0. Modal analyses are performed for all the derived numerical models. One among them was judged as being superior compared to the initial model considered at the beginning of the updating process; this is characterized as the 'best' model representing the observed dynamic response based on the noise measurements.

The selection of the 'best' model is made based on the evaluation of the Modal Assurance Criterion (MAC, Allemang and Brown 1982) defined as:

$$MAC_{ij} = \frac{\left(\varphi_j^T \varphi_{Ei}\right)}{\left(\varphi_j^T \varphi_i\right)\left(\varphi_{Ei}^T \varphi_{Ei}\right)} \tag{2.1}$$

where φ_j the eigenvector *j* from numerical model and φ_{Ei} the eigenvector *i* from field monitoring test.

The computation of the MAC values and the correlation of the responses between the experimental and numerical modal model are made at the measured nodes for which actual recorded noise data are available. A good correlation between the two tested modes was considered to be achieved for MAC values greater than 0.8. The updating scenario that was found to represent most accurately the experimental results for the modes under investigation considers the following stiffness parameter values: $K_0=10^4$ kN/m for the translational and $K_0=10^6$ kNm/rad for the rotational degrees of freedom.

Fig. 2.2.11 shows the comparison of the between the updated numerical and experimental modal models of the Administration building in terms of resonance

periods and mode shapes presenting also the resulting MAC values for the three first modes. The eigenfrequencies and mode shapes of the updated finite element model are compared to the initial ones as well as to the experimental results. It is seen that the updated model correlates well with the experimental results for all the modes under investigation (MAC>0.8).

Initial FEM T (sec)/f (Hz)	Mode shape of updated FEM T (sec)/f (Hz)	Mode shape of experimental model T (sec)/f (Hz)	MAC
Coupled translational along the transverse direction T_1=1.08sec / f_1=0.93Hz	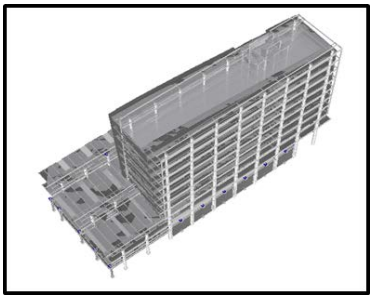	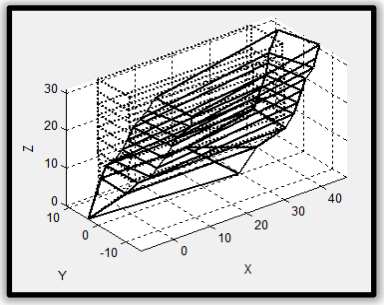	0.89
	T_1=1.09sec / f_1=0.92Hz	T_1=0.83sec / f_1=1.21Hz	
Coupled translational along the longitudinal direction T_2=0.96sec / f_2=1.04Hz	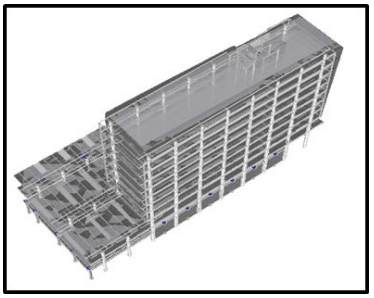	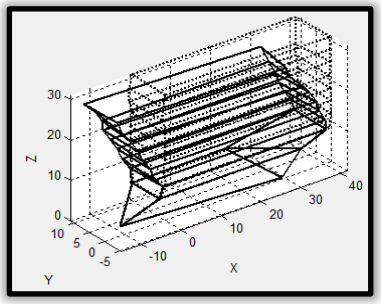	0.90
	T_2=0.96sec / f_1=1.04Hz	T_1=0.80sec / f_1=1.25Hz	
Torsional T_2=0.63sec / f_2=1.59Hz	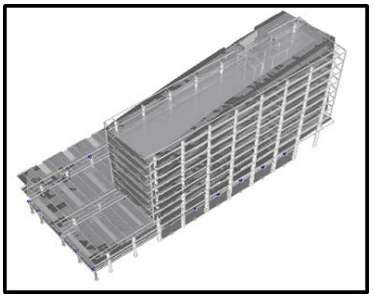	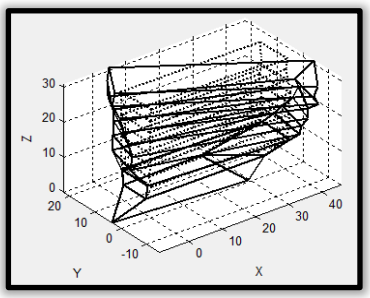	0.87
	T_3=0.59sec / f_3=1.69Hz	T_3=0.59sec / f_3=1.69Hz	

Fig. 2.2.11 Comparison of the updated finite element model of the Administration building and the experimental results (T: period, f: frequency).

2.2.1.5. Nonlinear finite element modeling

The nonlinear numerical modeling of the updated structure is conducted using SeismoStruct. Inelastic force-based formulations are employed for the simulation of the nonlinear three-dimensional, with six degrees of freedom, beam-column elements. The applied formulations allow both geometric and material nonlinearities to be captured. Distributed material plasticity along the element length is considered based on the fiber approach to represent the cross-sectional behavior. Each fiber is associated with a uniaxial stress-strain relationship; the sectional stress-strain state of the beam column elements is obtained through the integration of the nonlinear uniaxial stress-strain response of the individual fibers in which the section is subdivided. Figures 2.2.12 shows the constitutive stress-strain relationships used in SeismoStruct for the definition of steel and concrete material inelasticity. The concrete model of Mander et al. (1988) is used to define the behavior of the concrete fibers while for the steel reinforcement the bilinear steel model with kinematic strain hardening was implemented. Tables 2.2.3 and 2.2.4 summarize the material properties of the defined constitutive laws.

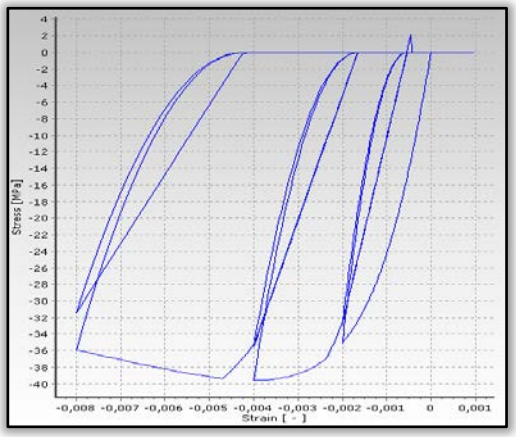

Concrete model by Mander et al. (1988)

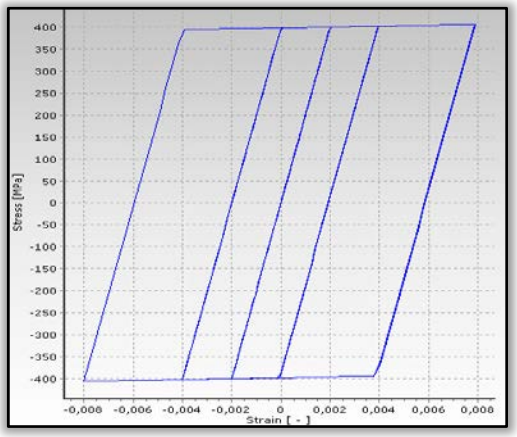

Steel bilinear model

Fig. 2.2.12 Constitutive stress-strain relationships of concrete and steel reinforcement material adopted in SeismoStruct for the nonlinear modelling of the Administration building.

Table 2.2.3 Properties of the defined concrete material model.

Modulus od Elasticity (GPa)	Mean compressive strength (MPa)	Mean tensile strength (MPa)	Strain at peak stress
31	31	24	0.002

Table 2.2.4 Properties of the defined steel material model.

Modulus od Elasticity (GPa)	Yield strength (MPa)	Strain hardening parameter	Fracture / buckling strain
200	400	0.005	0.1

2.2.1.6. Nonlinear static analysis

The seismic performance of the updated model of the Administration building is first assessed by means of nonlinear static procedure (pushover analysis) using the SeismoStruct software. The pushover procedure allows tracing the sequence of yielding and failure on the member and structure level, as well as the progress of the overall capacity curve of the structure. Although pushover analysis provides crucial information on response parameters that cannot be obtained with conventional elastic methods (either static or dynamic), it is not exempt from some limitations such as the inability to account for the characteristics of earthquake records and the variation in applied seismic demand with increasing structural degradation as well as the poor representation of the deformed shape of structures that do not respond predominantly in the first mode (e.g. Krawinkler and Seneviratna, 1998; Fajfar 2000).

Pushover curves are derived for both longitudinal and transverse direction of the building. The nonlinear model is displaced to a predefined roof displacement and the resulting internal deformations and forces are determined. The load distribution along the height of the building in both directions is defined according to Eurocode 8 based on the inertial forces developed at each story level for the design earthquake. Figure 2.2.13 shows the implemented load patterns along the building height in the longitudinal and transverse direction.

Figure 2.2.14 shows the derived pushover curves in both directions of the building for two control points K6 and K10 which correspond to the nodes of the corresponding columns as shown in Figure 2.1.3 the at the top floor level (8^{th} floor). K6 is located between concrete wall T7 and the left frontal wall whereas K10 is located on the opposite side of the core walls approximately in the middle of the two frontal walls (Figure 2.1.3). The specific control points have been selected as they are expected to provide the smallest and largest displacements respectively. The results of Figure 2.2.14 show that the maximum displacement of the two control points along the longitudinal direction of the building are very close (20.8 cm for K6 and 21.9 cm for K10). On the other hand, the maximum displacement of K6 along the transverse direction is much smaller in comparison to K10. This is an additional evidence of the torsional effects the building experiences and thus the columns placed close to the core walls present significantly smaller transversal displacements.

2.2.1.7. Selection of the input motion

To perform the nonlinear dynamic analysis of the building, a target spectrum for stiff soil conditions ($V_{s,30}$=410 m/s, Deliverable DC2) corresponding to the normal seismic design scenario (i.e., T_m=475 years) and a suite of acceleration time histories are needed, representative of this scenario.

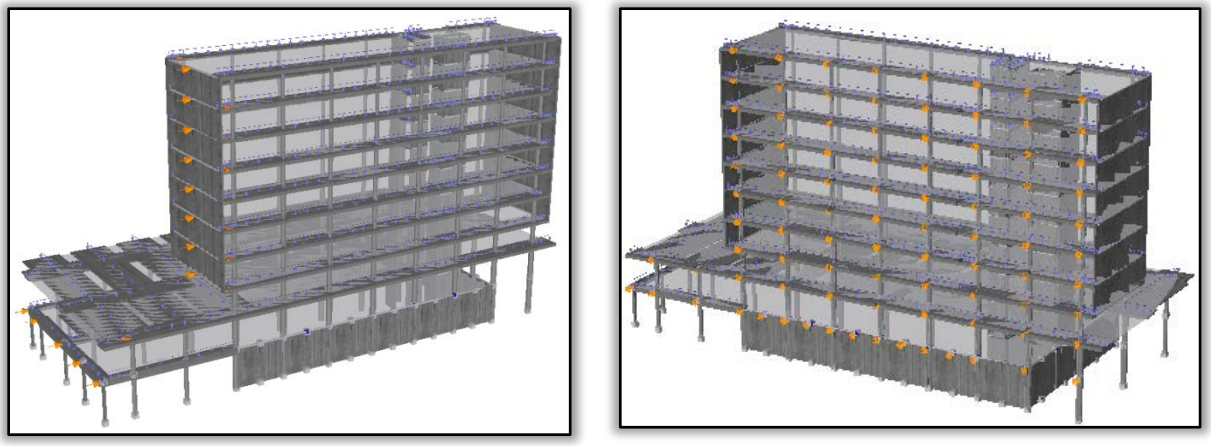

(a) (b)

Fig. 2.2.13 Load distribution along the height of the Administration building for the pushover analysis in (a) longitudinal and (b) transverse direction.

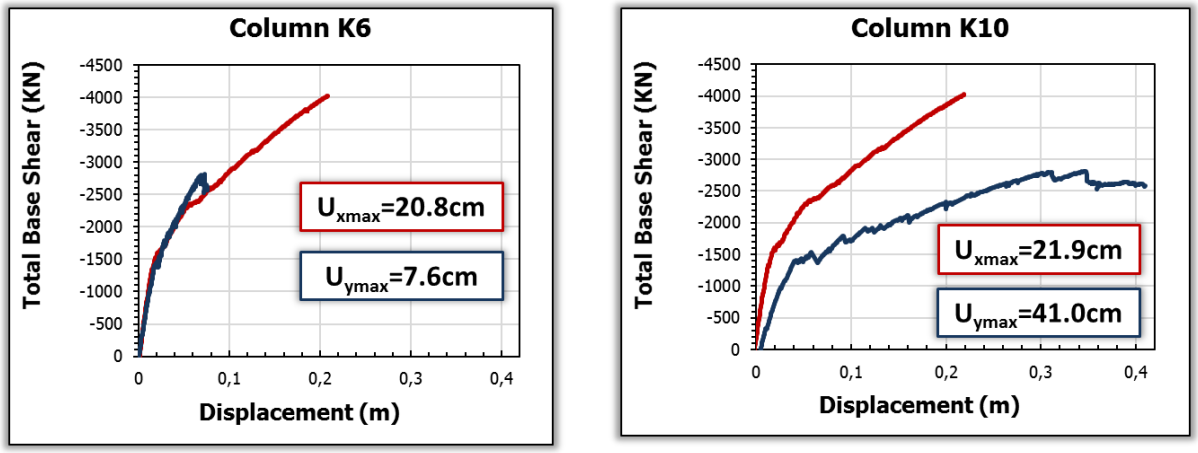

Fig. 2.2.14 Pushover curves of the Administration building in the longitudinal (x) and transverse (y) direction for the two adopted control points K6 and K10.

The target spectrum is defined based on the disaggregation of the probabilistic seismic hazard analysis (PSHA) results for the Aristotle University area (SRM-LIFE project, coordinator Prof. K. Pitilakis). This study has shown that the most significant contribution to seismic hazard is associated with the Anthemountas fault system (i.e. a normal fault) regardless of the return period. In particular, for the 475 years scenario, it was shown that the fault yields the maximum annual exceedance probability for a certain PGA value with a moment magnitude M_w of 5.675 and an epicentral distance R_{epi} of 11.67 km. The R_{jb} distance (i.e. the closest distance to the surface projection of the rupture zone) and the rupture distance R_{rup} (i.e. the closest distance to rupture zone) are estimated as 5 km and 10 km respectively.

Figure 2.2.15 shows a comparative plot of the 5% damped median acceleration spectra when using the ground motion prediction equations (GMPEs) of Akkar and

Bommer (2010), Akkar et al. (2014), Cauzzi et al. (2015) and Danciu and Tselentis (2007). Cauzzi et al. (2015) is a global model, Akkar and Bommer (2010) and Akkar et al. (2014) are pan-European models while Danciu and Tselentis (2007) is a local model based on existing Greek strong-motion data. A normal rupture mechanism was considered in all models consistently with the seismotectonic setting.

The comparison indicates good agreement between the Akkar and Bommer (2010) and Akkar et al. (2014) spectra although Akkar et al. (2014) spectrum is slightly more amplified in the resonance frequency and more constrained in the short-period range. The spectral ordinates of Cauzzi et al. (2015) model are lower with respect the Akkar and Bommer (2010) and Akkar et al. (2014) models. Danciu and Tselentis (2007) model shows great variation with respect to the former ones. The differences between the models could be attributed, among other reasons (e.g. the different databases used, the different functional form adopted, the different parameterization of local site conditions), to the different distance metrics used. In particular, in Akkar and Bommer (2010) and Akkar et al. (2014) models the R_{jb} distance has been used (although Akkar et al. (2014) models also allows the use of epicentral and hypocentral distances) while Cauzzi et al (2015) and Danciu and Tselentis (2007) use the R_{rup} and R_{epi} distances respectively.

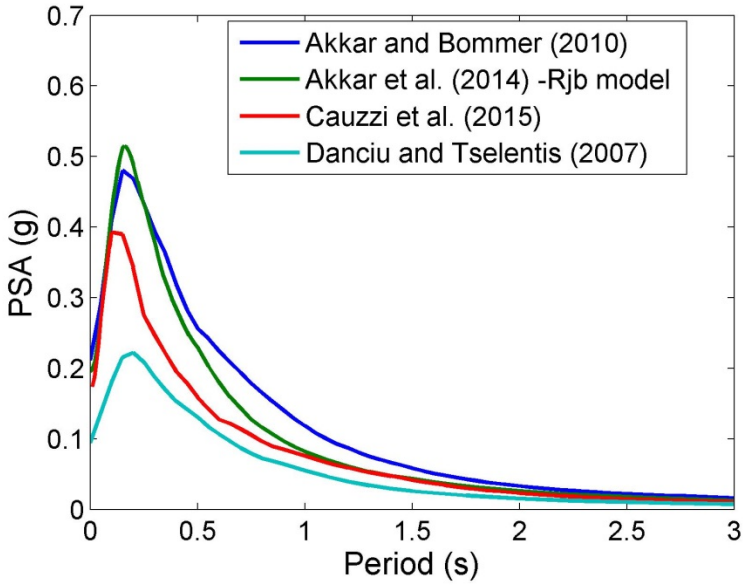

Fig. 2.2.15. Comparison of the 5% damped median acceleration spectra of Akkar and Bommer (2010), Akkar et al. (2014), Cauzzi et al. (2015) and Danciu andTselentis (2007)

In addition to magnitude and distance, both hazard scenarios should include an error term ε (which measures the number of standard deviations of logarithmic residuals accounted for in GMPE) that will be responsible for an appreciable proportion of spectral ordinates and the contribution from ε will grow with the return period (Bommer and Acavedo, 2004). Thus, the median spectral values plus 0.5 standard deviations was considered. This is also in line with the earthquake scenarios selected

in Akkar et al. (2014) to generically represent the moderate seismicity (median + 0.5σ for an M_w 6 event) regions in Europe.

Figure 2.2.16a to d shows the spectral ordinates (including the corresponding ε term) when using the ground motion prediction equations of Akkar et al. (2014), Akkar and Bommer (2010), Cauzzi et al. (2015) and Danciu and Tselentis (2007) respectively in comparison with the SHARE uniform hazard spectrum for soil class B of EC8 (using period dependent amplification factors to account soil conditions other than rock), the EC8 elastic response spectrum for PGA=0.16g (for the city of Thessaloniki) and soil class B (stiff soil), and the corresponding elastic spectrum provided by Pitilakis et al. (2013).

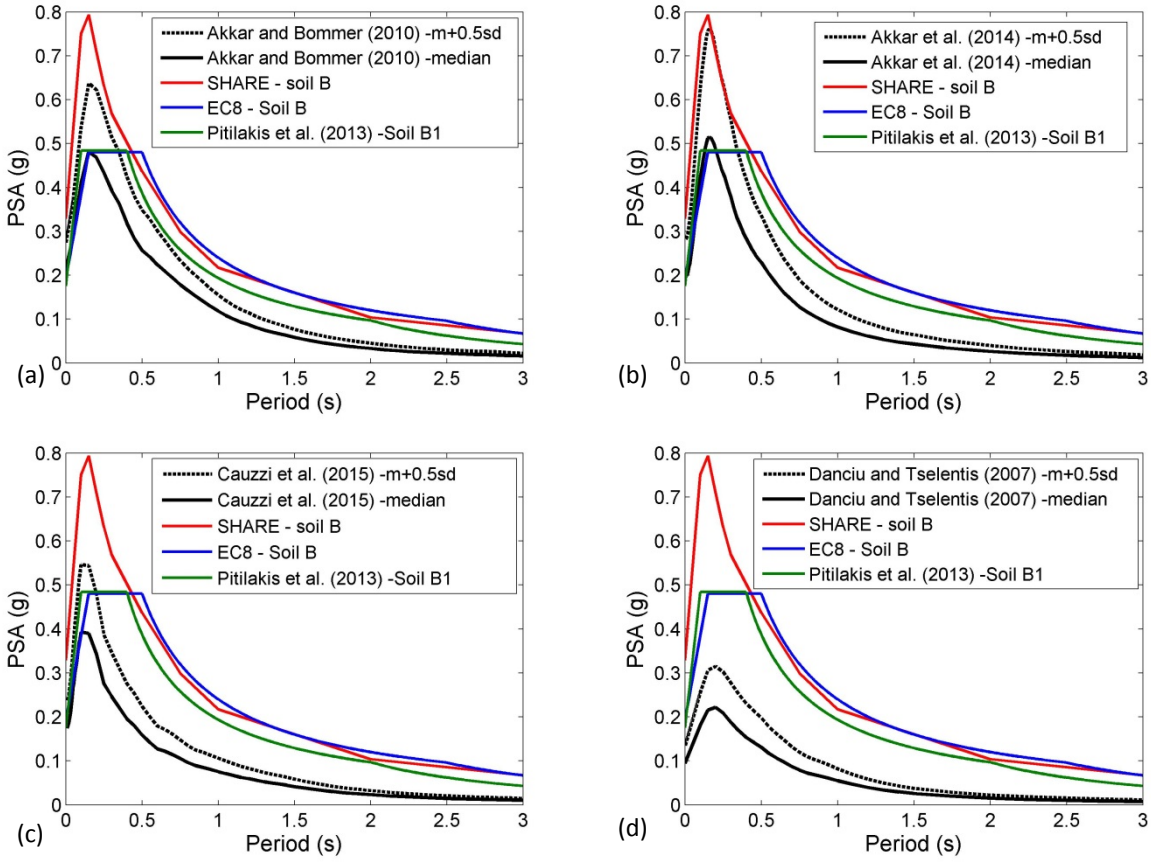

Fig. 2.2.16. Comparison of the 5% damped median and the median plus 0.5 standard deviation acceleration spectra of Akkar and Bommer (2010) with the SHARE uniform hazard spectrum for the study area, the EC8 elastic response spectrum and the Pitilakis et al. (2013) spectrum

The median spectra plus the corresponding standard deviations provided by Akkar et al. (2014) is selected as the target as it is shown to better describe the hazard in the study area.

A representative set of 10 accelerograms was selected obtained from the European Strong-Motion Database (Table 2.2.5). They are all referring to stiff soils (soil type B according to EC8) with moment magnitude (Mw) and epicentral distance that range

between 5.5<Mw<6.5 and 0<R<45km respectively. The primary selection criterion is the average acceleration spectra of the set to be of minimal ε (Baker and Cornell, 2005) at the period range of 0.00<T<2.00sec with respect to the corresponding 5% damped median plus 0.5 standard deviations Akkar et al. (2014) spectrum. The optimization procedure is performed by making use of the REXEL software (Iervolino et al., 2010) that allows obtaining combinations of accelerograms, which on average are compatible to the reference spectrum. Figure 2.2.17 depicts the mean elastic response spectrum of the records in comparison with the corresponding median plus 0.5 standard deviations Akkar et al. (2014) spectrum. As shown in the figure, a good match between the two spectra is achieved.

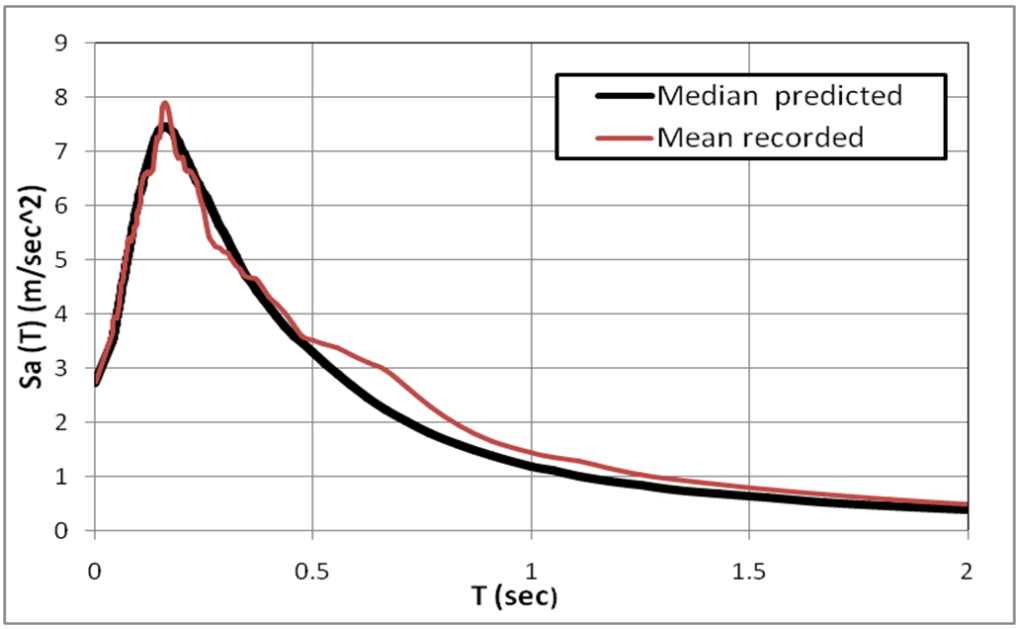

Fig. 2.2.17. Mean elastic response spectrum of the input motions in comparison with the corresponding reference spectrum proposed by Akkar et al. (2014) plus 0.5 standard deviation.

Table 2.2.5 List of records used for the dynamic analyses

Earthquake name	Station ID	Date	Mw	R [km]	PGA_X [m/s2]	PGA_Y [m/s2]	Waveform ID
Umbria Marche	ST60	14.10.1997	6	11	5.1383	4.5383	000594
Harbiye	ST568	22.01.1997	5.7	19	1.3093	1.4518	001761
Firuzabad	ST3297	20.06.1994	5.9	7	9.8239	10.444	007162
Ano Liosia	ST1100	07.09.1999	6	16	2.6014	3.012	001313
Kefallinia (aftershock)	ST1303	23.03.1983	6.2	9	1.7881	2.3029	002015
Montenegro (aftershock)	ST76	24.05.1979	6.2	21	1.6273	1.3034	000231
Kefallinia island	ST1303	23.01.1992	5.6	14	1.2493	2.2233	006040
Kalamata	ST163	13.09.1986	5.9	11	2.3537	2.6703	000414
Ano Liosia	ST1258	07.09.1999	6	14	2.3842	2.1588	001714
Umbria Marche (aftershock)	ST86	14.10.1997	5.6	20	0.9604	1.3159	000640

2.2.1.8. Incremental dynamic analysis

The incremental dynamic analysis (IDA) procedure (Vamvatsikos and Cornell, 2002) is used to determine the seismic performance and assess the seismic vulnerability of the initial and updated finite element model of the Administration building. Within this study the damage measure is expressed in terms of maximum interstorey drift ratio. More specifically, the maximum peak SRSS drift, maxISD (i.e. the maximum over all stories of the peak of the square-root-sum-of-squares of each storey's drift) in the two principal directions is selected (Wen and Song, 2002). The seismic intensity is described using peak ground acceleration (PGA) recorded on soil type B according to EC8 (CEN, 2004). PGA is selected as intensity measure due to the fact that the derived curves should be able to be incorporated in an operational tool for Early Earthquake Warning and rapid post-event damage assessment that will be used by the civil protection authority. In this context, PGA is considered appropriate due to its simple computation in real-time and its efficient use by the authorities.

IDA is conducted for the structural model of the Administration building by applying the 10 progressively scaled records (in both longitudinal and transverse direction) of Table 2.2.5. In particular, a tracing algorithm is applied for each record with an initial step of 0.1g, a step increment of 0.1g and a first elastic run at 0.05g. For certain records it was necessary to reduce the step size of the algorithm to increase the accuracy close to the flatline of the IDA curve. The minimum number of converging runs is allowed to vary from 8 to 10 per record depending on the characteristics of the structure and the records itself.

It should be noted at this point that for the IDA the connection of the building to the nearby structures (Fig. 2.1.5) is taken into account only for analyses cases that consider low seismic intensity for which the structure‘s behavior is limited in the linear elastic branch. The limit intensity level where the interaction between the structures is expected to be weak was defined at 0.1g. Beyond that level the structures are expected to experience strong nonlinearities with progressive increase of the PGA and therefore no connection was considered, as their interaction may be completely different affecting consequently their seismic response and vulnerability. The fiber based approach that has been adopted for the nonlinear modeling of the structures simulates sidesway collapse associated with strength and stiffness degradation along the total length of beams and columns. The analysis model does not directly capture column shear failure as the columns in this study are expected to yield first in flexure rather than experiencing direct shear failure, as in the case of squat non-ductile RC columns. Figure 2.2.18 represents the failure modes of the particular building. It is seen that collapse modes are related to column flexural failures in the lower storeys which are defined for each seismic record based on the intensity of the input ground motion that results in structural collapse, identified in the analysis by excessive interstorey drifts. Damage at the core walls is expected to be limited and located mainly at the lower storey levels where the concentration of seismic load is higher. Furthermore, the torsional effects induced due to the eccentric location of the core

walls in plan, lead to extensive damage distribution of the elements at the left side of the building, which is located far from the core walls. Finally partial collapse of the first floor is observed which can be attributed to the absence of frontal walls at this storey level causing significant stiffness irregularity in elevation and thus high inelastic deformation demands.

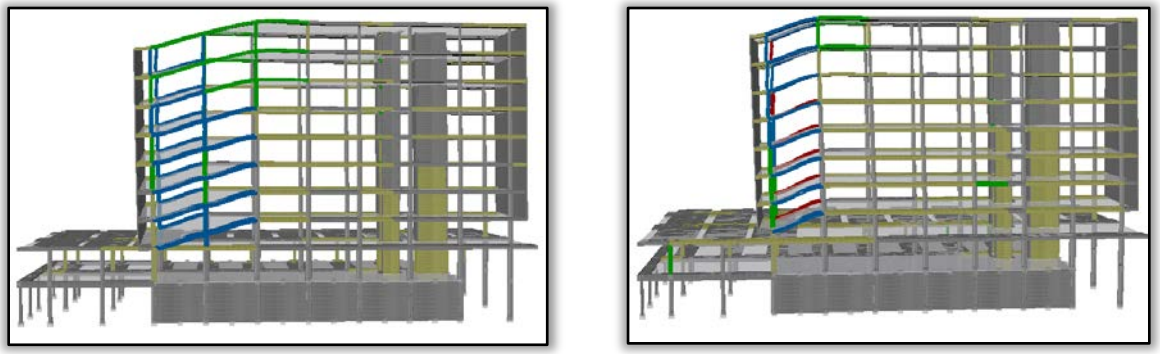

Fig. 2.2.18 Typical failure mode of the Administration building

By interpolating the derived pairs of PGA and maxISD for each record 10 continuous IDA curves are derived. For the purpose of the present study, two limit states are defined in terms of interstorey drift ratio, representing the immediate occupancy (IO, the building does not need any reparations or retrofitting after the earthquake), and collapse or near collapse prevention (CP, the building needs to be demolished), performance levels. The first limit state, namely the Immediate Occupancy corresponds to the yielding point where the elastic branch gives place to the post-elastic branch. The second limit state is assigned at a point where the IDA curve is softening towards the flat line, but at low enough values of maxISD so that we still trust the structural model (Vamvatsikos and Cornell, 2004). Thus different IO and CP limit state values are chosen on the IDA curves for the same structure depending on the individual record. The medians of the defined IO and CP limit values in terms of SRSS maxISD are used to define the IO and CP limit states and are found to be equal to 0.2% and 1.9% respectively. The assignments of the IO and CP limit state points on the IDA curves corresponding to the each record are shown in Figure 2.2.19 while Table 2.6 summarizes the defined limit maxISD values for each record. The dispersion that is observed may be attributed on one hand to the record-to-record variability in terms of frequency content and duration and on the other hand to the fact that PGA is used as intensity measure as in this case the seismic response and vulnerability depends on the input ground motion sets (Kwon and Elnashai, 2007).

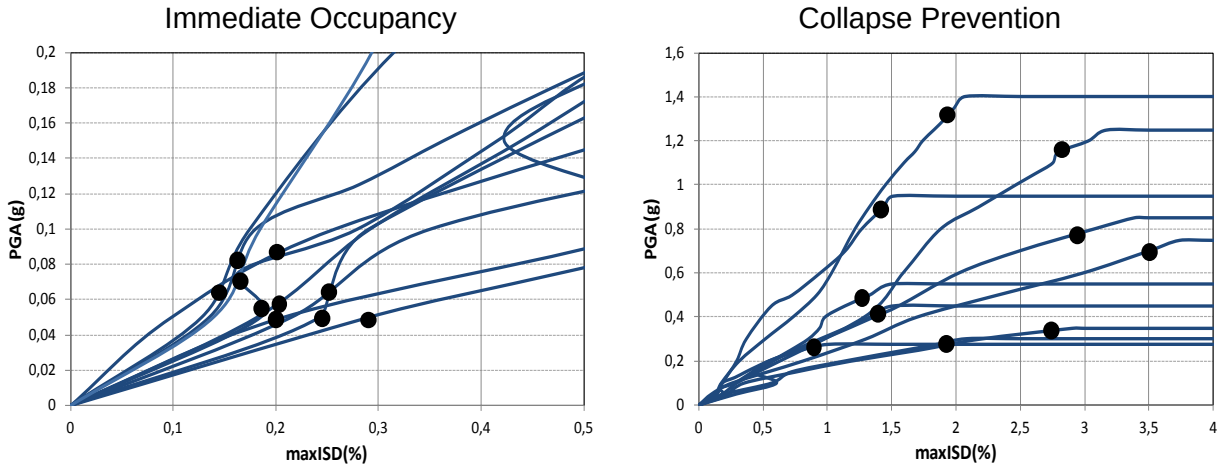

Fig.2.2.19 Assignments of the Immediate Occupancy (IO) and Collapse Prevention (CP) limit damage state points on the IDA curves for the Administration building.

Table 2.2.6 Summary of limit maxISD values for each record

Seismic record	Damage measure SRSS max Interstorey drift (%)	
	IO	CP
Umbria Marche	0.2	3.5
Harbiye	0.28	1.32
Firuzabad	0.14	1.9
Ano Liosia	0.18	2.9
Kefallinia (aftershock)	0.18	1.4
Montenegro (aftershock)	0.18	0.82
Kefallinia island	0.22	2.8
Kalamata	0.2	1.9
Ano Liosia	0.21	1.34
Umbria Marche (aftershock)	0.24	2.4

2.2.1.9. Derivation of fragility curves

The results of the IDA (PGA-maxISD) are used to derive the fragility curves for the Administration building, expressed as a two-parameter lognormal distribution function. Equation 2.2 represents the cumulative probability of exceeding a damage state *DS* conditioned on a measure of the seismic intensity *IM*:

$$P\left[DS \mid IM\right] = \Phi\left(\frac{\ln\left(IM\right) - \ln\left(\overline{IM}\right)}{\beta}\right) \qquad (2.2)$$

Where, Φ is the standard normal cumulative distribution function, IM is the intensity measure of the earthquake expressed in terms of PGA (in units of g), $\overline{IM}$ and β are the median values (in units of g) and log-standards deviations respectively of the building fragilities and DS is the damage state. The median values of PGA corresponding to the prescribed performance levels are determined based on a regression analysis of the nonlinear IDA results (PGA-maxISD pairs). More

specifically a linear regression fit of the logarithms of the PGA – maxISD which minimizes the regression residuals is adopted in the analysis cases. Figure 2.2.20 presents the PGA – maxISD relationships for the updated structural model of the Administration building.

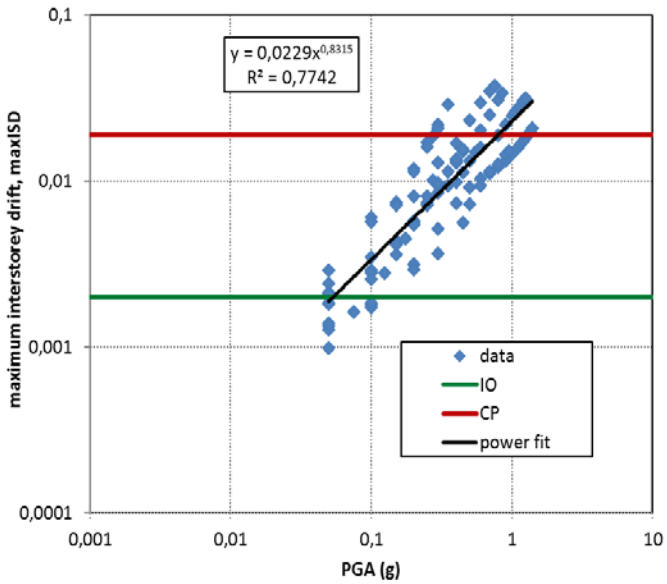

Fig.2.2.20 PGA – maxISD relationships for updated finite element model of the Administration building.

Three primary sources of uncertainty are generally taken into account for the estimation of the total variability associated to each damage state for conventionally derived fragility curves, namely the variability associated to each damage state, the capacity of the structure and the seismic demand. Demand uncertainties are associated to the effects of ground motion record-to-record variability on building response. Capacity uncertainty reflects the variability of structural properties, the lack of information in some cases, as well as the fact that the modelling procedures are not perfect. Damage state definition uncertainties are due to the fact that the thresholds of the damage indices or parameters used to define damage states are not known (Selva et al., 2013). In the present study the uncertainty associated with the demand is taken into consideration by calculating the dispersion of the logarithms of PGA – maxISD simulated data with respect to the regression fit. The log-standard deviation value in the capacity is assumed to be 0.3 for the low code structures following the HAZUS prescriptions (NIBS, 2004). Uncertainties in how well the nonlinear simulation model represents the behaviour of the real building as well as the highly nonlinear structural behaviour near collapse are incorporated in the collapse assessment and are reflected in the fragility curves through the consideration of the capacity uncertainty. As far as the uncertainty in the definition of the damage states is concerned, the damage limit values are defined on the IDA curves and since they are considered building-specific, the additional uncertainty related to the definition of the damage states is taken into consideration through the dispersion of the defined limit values of IO and CP damage states. In particular, the

corresponding β is estimated 0.19 and 0.4 for the IO and CP damage states respectively. Under the assumption that the log-standard deviation components are statistically independent, the total log-standard deviation is estimated as the root of the sum of the squares of the component dispersions. The herein computed log-standard deviation β values of the curves are equal to 0.56 and 0.66 for the IO and CP damage states respectively.

Figure 2.2.21 presents the building-specific fragility functions derived for the updated structural model of the Administration building while Table 2.2.7 summarizes the corresponding fragility parameters. For an example intensity level equal to 0.4g it is observed that the probability of the structure to experience slight damage is 100% which is expected as the IDA results showed already that the building develops relatively fast inelastic deformations due to its structural characteristics (structural eccentricities in plan and elevation). On the other hand the probability for the building to collapse under the considered intensity level is estimated approximately equal to 15%.

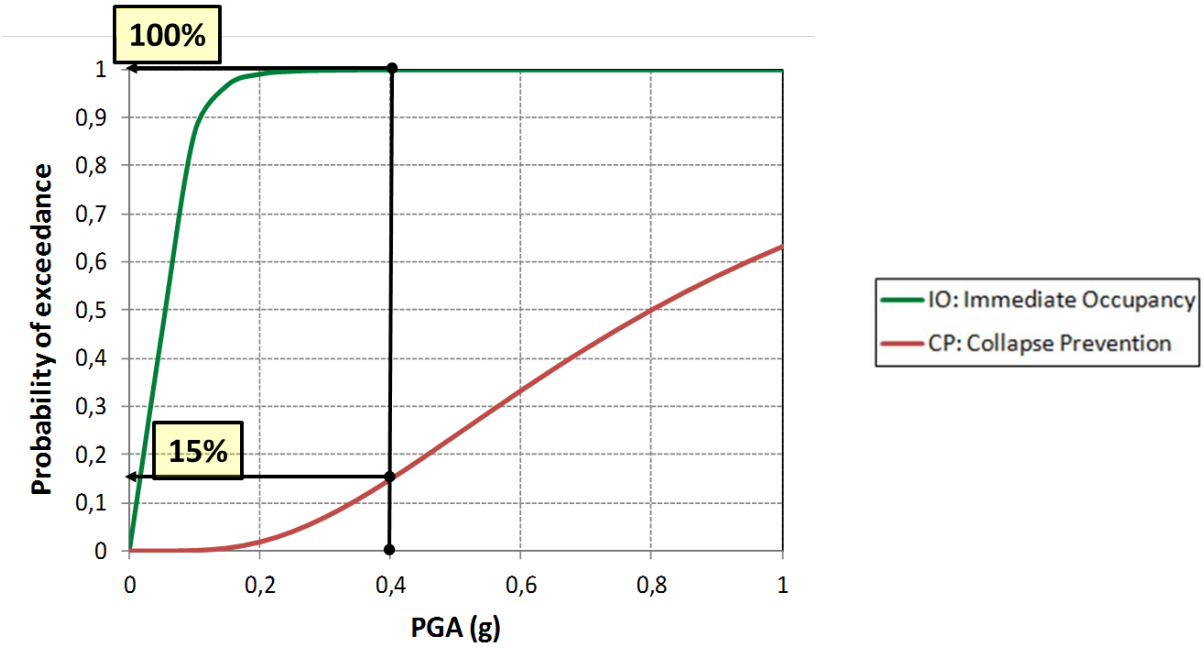

Fig.2.2.21 PGA – maxISD relationships for updated finite element model of the Administration building.

Table 2.2.7 Parameters of the derived fragility curves for the updated finite element model of the Administration building.

Damage state	Median (g)	Dispersion β
Immediate Occupancy (IO)	0.05	0.56
Collapse Prevention (CP)	0.80	0.66

2.2.1.10. Comparison of the building-specific derived fragility curves with generic curves from the literature

The derived fragility curves of the Administration building are compared with conventional curves from the literature (Pitilakis et al., 2014) that are derived for representative models of the following typologies: high-rise, bare (1) moment resisting frame and (2) dual buildings, both typologies designed according to low seismic code provisions. These two typology cases have been selected as the Administration building due to the existence of the core walls cannot be defined as a frame building, but on the other hand its seismic behaviour does also not correspond to a standard dual system where the concrete walls play a decisive role in taking on most of the seismic load.

The building-specific curves are compared with the generic curves proposed by Kappos et al. 2003 (Figure 2.2.22), Kappos et al. 2006 (Figure 2.2.23) and Tsionis et al. 2011 (Figure 2.2.24), which reflect the vulnerability of the most common typologies in Greece that have been designed according to low seismic code provisions. It is noted that most of the work presented in Kappos et al. (2003) was carried out by the same authors within the framework of RISK-UE project (Mouroux et al., 2004); The difference between the results (given in terms of fragility function) of Kappos et al. (2003) and Kappos et al. (2006), are probably due to slight geometric differences adopted for the studied RC building typologies.

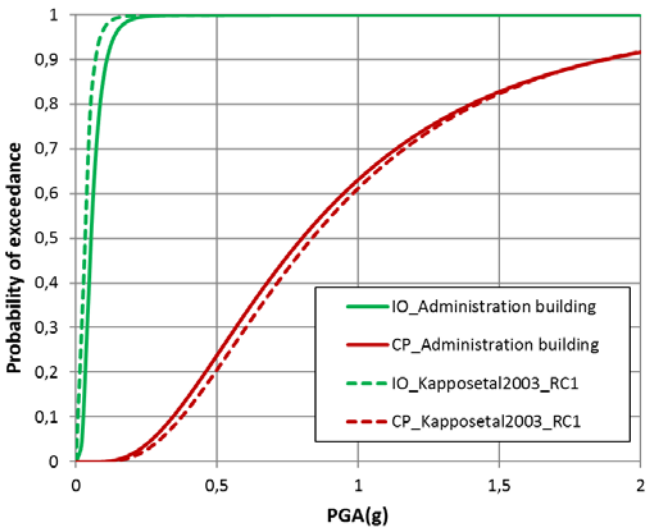

Fig.2.2.22 Comparative plot of the building-specific fragility curves derived for the Administration building with the corresponding fragility curves provided by Kappos et al. (2003). RC1: high-rise, bare, low-code designed moment resisting frame.

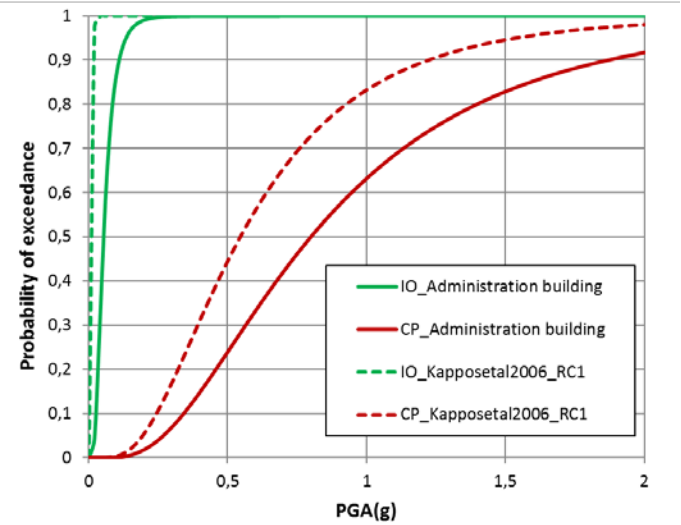

Fig.2.2.23 Comparative plot of the building-specific fragility curves derived for the Administration building with the corresponding fragility curves provided by Kappos et al. (2006). RC1: high-rise, bare, low-code designed moment resisting frame.

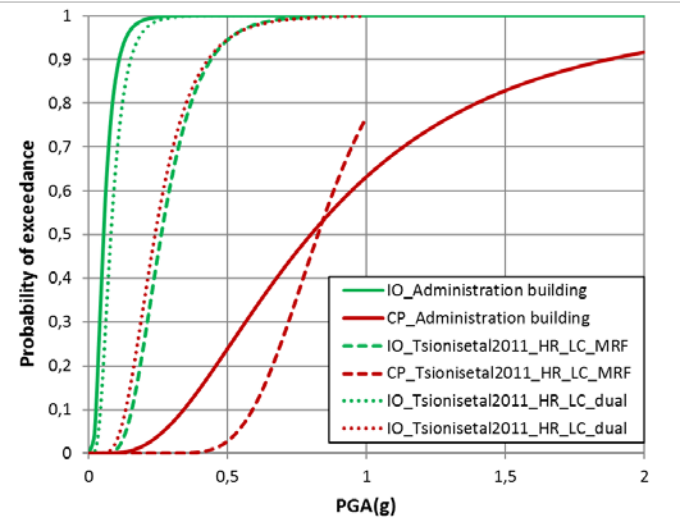

Fig.2.2.24 Comparative plot of the building-specific fragility curves derived for the Administration building with the corresponding fragility curves provided by Tsionis et al. (2011). HR-LC-MRF: high-rise, bare, low-code designed moment resisting frame; HR-LC-dual: high-rise, bare, low-code designed dual system.

The comparison of the building-specific with the generic curves by Kappos et al. (2003) and Kappos et al. (2006) shows that the vulnerability of the Administration building would be better described adopting conventional generic curves that correspond to a moment resisting frame structure. On the other hand, based on the study of Tsionis et al. (2011), the Immediate Occupancy damage state of the Administration building would be best described by adopting the generic curves corresponding to a dual system whereas for the Collapse Prevention damage state, fragility curves referring to a frame building would be more appropriate.

The scatter observed between the generic curves themselves, which represent the same structural typologies, reveal the high aleatory and epistemic uncertainties associated with the different fragility curves found in the literature and depend on different parameters, such as the modeling assumptions and analysis method used for their derivation (Pitilakis et al. 2014;. Pitilakis, 2015). Moreover, it should be noted that generally such generic curves are extracted considering either single degrees of freedom systems or simplified two-dimensional structures in order to be used at a seismic risk assessment framework at regional or urban scale. Therefore, although the conventional generic curves are considered appropriate for assessing fragility and losses in a regional/urban scale, their use may lead to inaccurate fragility and loss estimates in the case of individual building assessment. This issue constitutes a crucial component in the framework of decision making process and risk mitigation strategies (e.g. seismic safety and rehabilitation costs) on a building-specific scale, as the use of generalized curves may lead to inaccurate fragility and loss estimates as observed also in this particular study.

Regarding SIBYL the results of this comprehensive analysis should offer a perfect validation example to check the accuracy and the efficiency of the simplified model developed by TU-Berlin.

2.2.2. Faculty of Philosophy building

2.2.2.1. Seismic instrumentation and in situ measurements

The permanent accelerometric SOSEWIN network, operates in the Faculty of Philosophy building also since April 2015. The SOSEWIN network constitutes of 2 triaxial accelerometers (MEMS ADXL203 chip). Two sensors have been installed, one in the first floor (PN11) and one in the 4th floor (PN41) of the building as shown in Fig. 2.2.25. Several earthquake events have already been recorded and the instrumentation array continues to transfer data streams to the Seiscomp3 server installed at SDGEE-AUTH premises.

In addition to the permanent also a temporary instrumentation array recording ambient noise was implemented at the end of September 2015 under the responsibility of the Soil Dynamics and Geotechnical Earthquake Engineering of the Aristotle University of Thessaloniki (SDGEE-AUTH) and in close cooperation with the Technische Universität Berlin (TU-Berlin) and the Helmholtz Centre Potsdam, German Centre for Geosciences (GFZ). The ambient noise measurements are used to derive the dynamic properties of the building. The same sensors that were used for the Administration building were also deployed for the Faculty of Philosophy. The instrumentation layout included 38 sensors which recorded along the two orthogonal horizontal and along the vertical directions (three components). The two horizontal components are oriented along the longitudinal and transversal direction of the building. Ambient noise was recorded simultaneously for about 20 hours in all stations with a sampling rate of 400Hz. The instrumentation layout is shown in Fig.

2.2.26. In particular, two sensors were installed at the basement, two at the semi-basement, twelve at the first floor, four at the second and third floor respectively, twelve at the fourth floor, two at the roof and one sensor was installed outside the building as a reference free field station. The sensors were installed at each floor level close to the columns far and close to the structural joints. Indicative photos of the installations are shown in Fig. 2.2.27.

Fig. 2.2.25 SOSEWIN network installed at the Faculty of Philosophy building for the long term structural monitoring.

In addition to the permanent also a temporary instrumentation array recording ambient noise was implemented at the end of September 2015 under the responsibility of the Soil Dynamics and Geotechnical Earthquake Engineering of the Aristotle University of Thessaloniki (SDGEE-AUTH) and in close cooperation with the Technische Universität Berlin (TU-Berlin) and the Helmholtz Centre Potsdam, German Centre for Geosciences (GFZ). The ambient noise measurements are used to derive the dynamic properties of the building, i.e., the resonant frequencies and mode shapes of the building. The same sensors that were used for the Administration building were also deployed for the Faculty of Philosophy. The instrumentation layout included 38 sensors which recorded along the two orthogonal horizontal and along the vertical directions (three components). The two horizontal components are oriented along the longitudinal and transversal direction of the building. Ambient noise was recorded simultaneously for about 20 hours in all stations with a sampling rate of 400Hz. The instrumentation layout is shown in Fig. 2.2.26. In particular, two sensors were installed at the basement, two at the semi-basement, twelve at the first floor, four at the second and third floor respectively, twelve at the fourth floor, two at the roof and one sensor was installed outside the

building as a reference free field station. The sensors were installed at each floor level close to the columns far and close to the structural joints. Indicative photos of the installations are shown in Fig. 2.2.27.

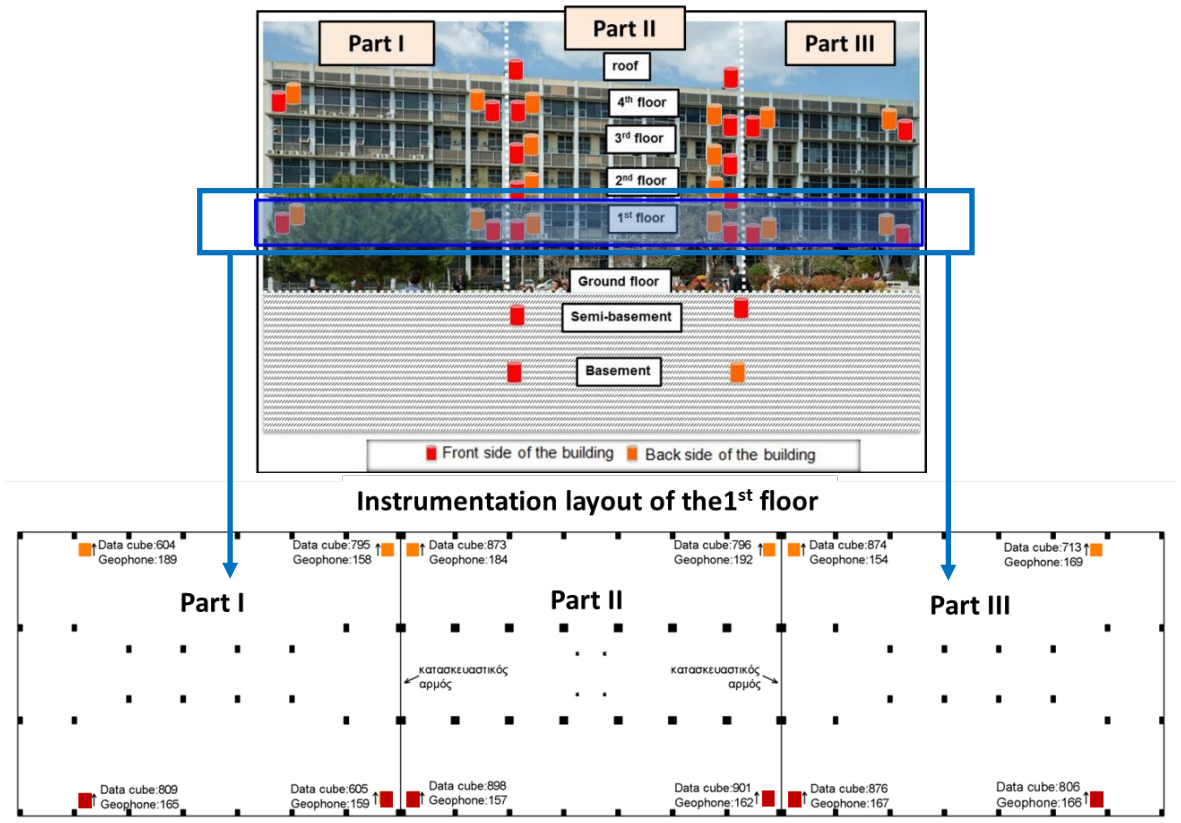

Fig. 2.2.26 Installation of the temporary network at the Faculty of Philosophy building. Sensors located close to the RC columns.

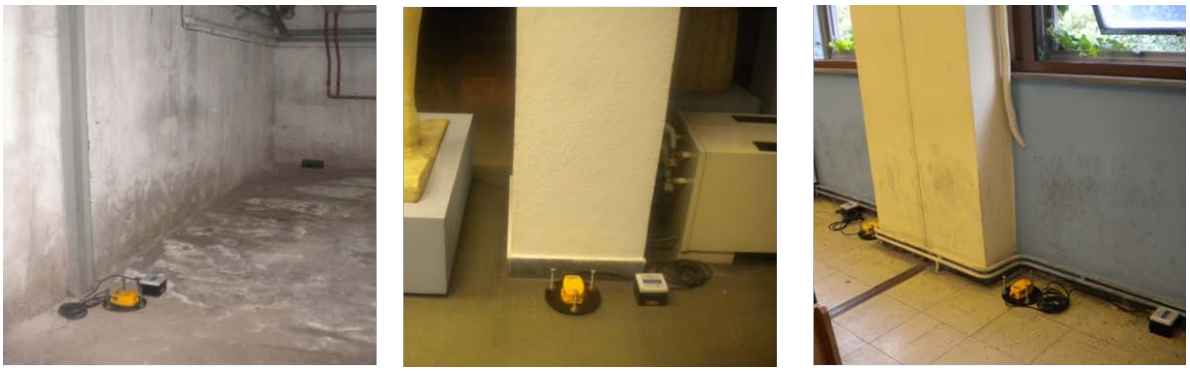

Fig. 2.2.27 Indicative photos of the sensors used for the temporary instrumentation of the Faculty of Philosophy building.

In addition to the ambient noise experiment, in-situ testing was conducted in order to define the structural properties of the fourth floor, which was constructed approximately twenty years after the first construction of the building and no design or construction data were available. In particular, the testing included the measurement of the dimensions of structural elements and of the floor height, the

detection of the existing reinforcement and the estimation of the concrete cover depth. During these measurements, it was observed that the dimensions of several column sections at different floor levels were not in accordance with the provided design plans. Fig. 2.2.28 shows indicatively the measured dimensions of the columns at the ground floor in comparison to the column dimensions provided by the design plans while Fig. 2.2.29 shows the measured dimensions of the column sections at the fourth floor.

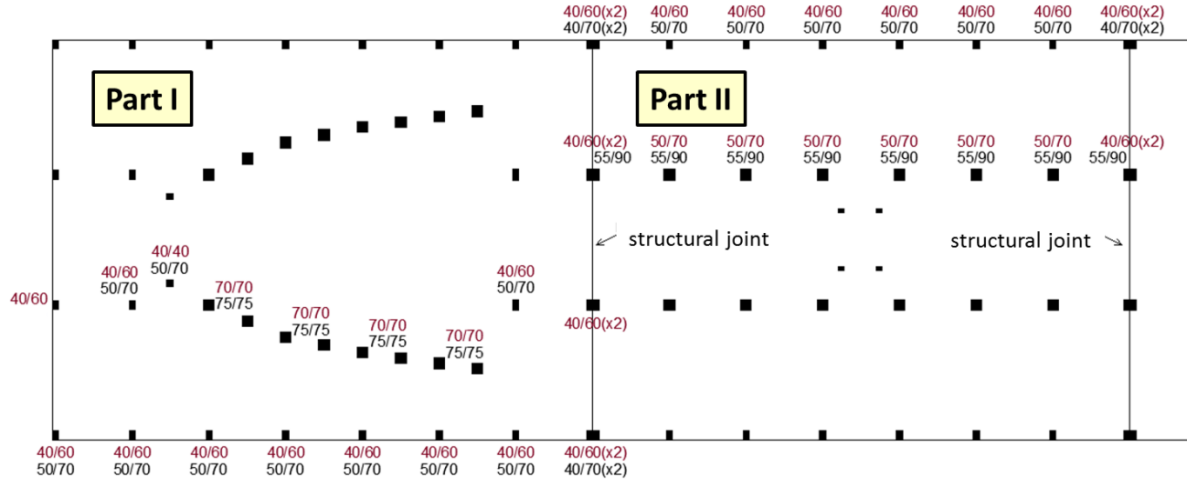

Fig. 2.2.28 Comparison between the measured (in black) and the provided from the design plans (in red) column section dimension at the ground floor of the building.

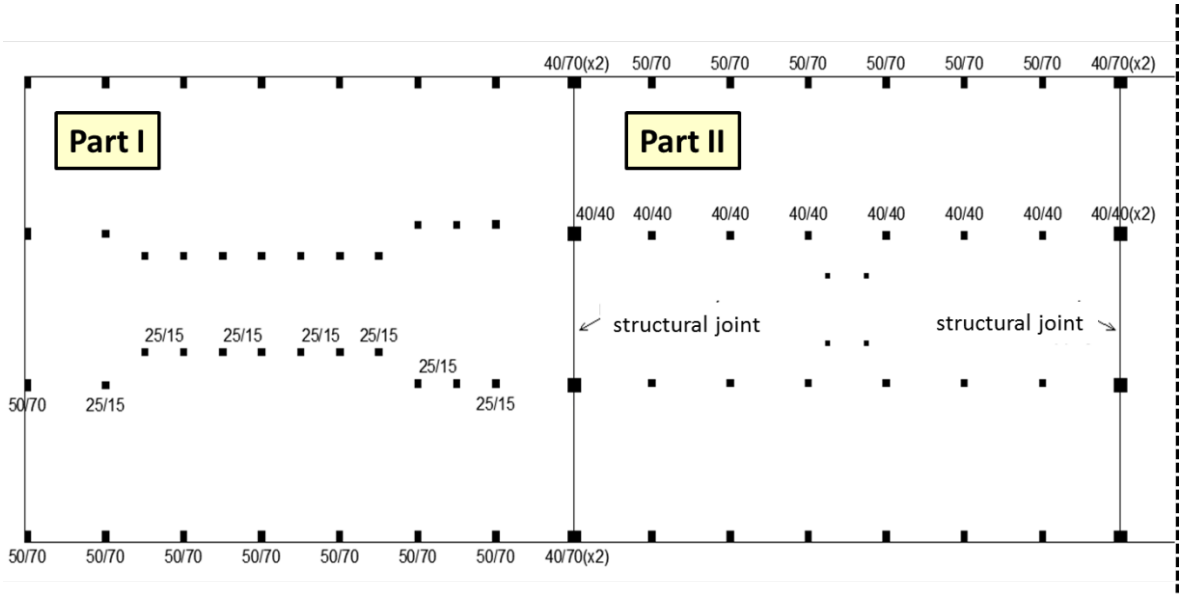

Fig. 2.2.29 Measured column section dimensions at the fourth floor of the building.

2.2.2.2. Operational modal analysis

To evaluate the dynamic characteristics of the Faculty of Philosophy building, namely the natural frequencies and mode shapes, system identification and Operational Modal Analysis (OMA) were performed using MACEC 3.2 software (Reynders et al., 2011). The geometrical characteristics of the model introduced and analyzed in MACEC 3.2 are illustrated in Fig. 2.2.30. The grid of the model is built so that the defined nodes correspond to the nodes that have been actually measured. In order to investigate the variation of the modal parameters of the structure, from the 20-hour measurements the data of four smaller one-hour recording sets were analyzed, covering different time periods during the day- and night time (i.e. 3:00-4:00, 10:00-11:00, 15:00-16:00, 20:00-21:00, GMT-time). Each time window used for OMA has duration of 1800sec (30min) as tests for stability of the results showed that 30 minutes are enough to get reliable results. Before identification, the data were decimated with a factor of 10 and filtered with a low-pass anti-anti-aliasing filter with a cut-off frequency of 20Hz and re-sampled at 40Hz reducing thus the number of data avoiding unnecessary computational burden in the modal analysis where the frequency of interest are smaller than 20Hz.

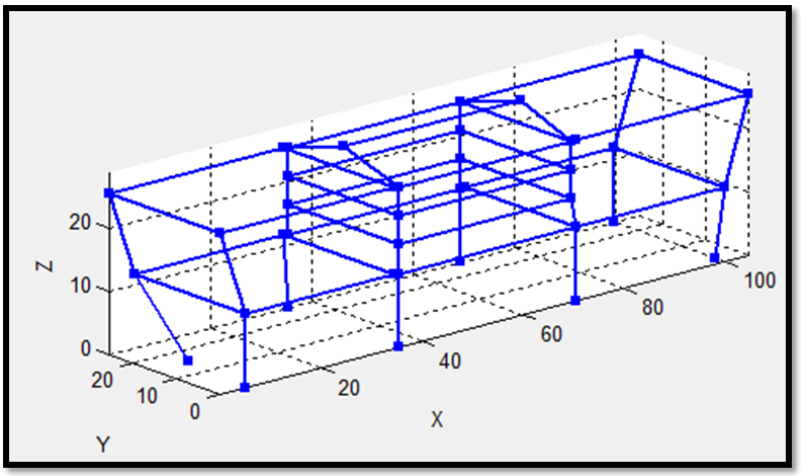

Fig. 2.2.30 Visualization of the building's geometry in MACEC 3.2

In order to verify and enhance the modal identification results, analyses have been conducted using both non-parametric and parametric identification techniques which are described in more detail in section 2.2.1.2 where the OMA procedure is described for the Administration building.

The results of the nonparametric and parametric analyses for the Faculty of Philosophy building are presented in Fig. 2.2.31.

Fig. 2.2.32 shows representative eigenfrequency and mode shape results of the identified modes, corresponding to the SSI analysis results for the recording time window of 10:00-11:00 am (GMT time). The building is exhibiting coupled sway and torsional modes in the frequency range of interest. Although coupled, the predominant motion of the first mode is mainly along the transverse direction whereas the second one along the longitudinal direction.

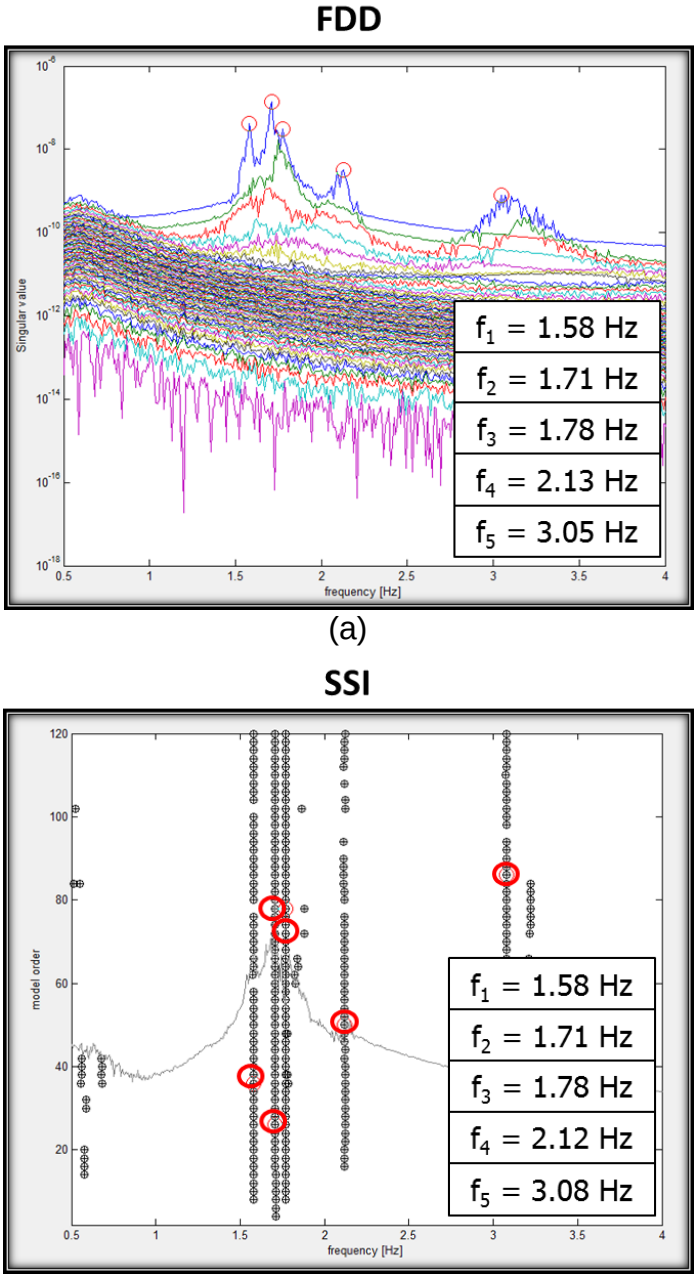

Fig. 2.2.31 Identification results through OMA for the Faculty of Philosophy building based on (a) FDD and (b) SSI methods.

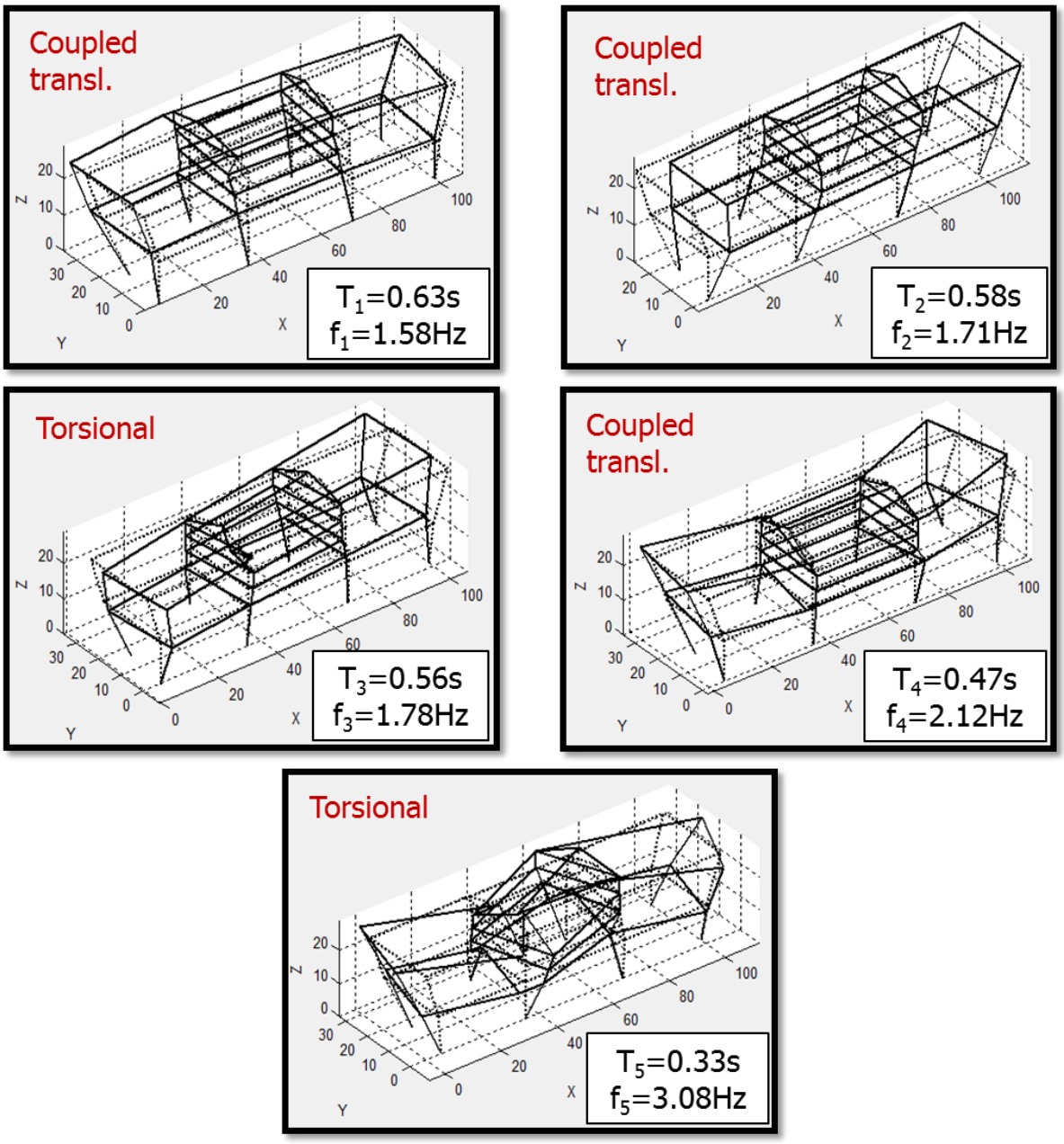

Fig. 2.2.32 Eigenperiods/Eigenfrequencies and mode shapes for the first five identified modes for the Faculty of Philosophy building (T: period, f: frequency).

Table 2.2.8 shows the variation of the eigenfrequency values for the different time windows. The resonant frequencies are practically the same for the three first modes whereas only slight variations are observed for the higher modes of interest (i.e. 4th and 5th modes) in the order of 6-8%.

Table 2.2.8 Variation of the fundamental frequencies of the Faculty of Philosophy building during the recorded timeframe (GMT time).

	Time window of recorded data			
Frequencies (Hz)	Recording 3:00-4:00 a.m.	Recording 10:00-11:00 a.m.	Recording 15:00-16:00 p.m.	Recording 20:00-21:00 p.m.
f_1	1.58	1.58	1.58	1.60
f_2	1.75	1.71	1.71	1.75
f_3	1.78	1.78	1.78	1.78
f_4	2.14	2.13	2.28	2.14
f_5	3.32	3.05	3.30	3.32

2.2.2.3. Elastic numerical simulation and modal analysis of the structural model

The finite element modeling of the Faculty of Philosophy building is based on the available design and construction plans. In order to evaluate the elastic structural performance of the building, the numerical modeling was initially conducted in SAP2000 (Computers and Structures, Inc). The frame elements were simulated as linear elastic beam-column elements. The support conditions of the structure at bottom of the basement were considered as fixed base. In order to take into account the existence of the basement, the translational degrees of freedom at the ground floor level were restrained. For the linear modeling of the masonry infills the equivalent beam- column model is adopted to take into account the in plane stiffness of the infill panel. Finally gap link elements (compression only elements) were utilized for the structural joint modeling separating the different parts of the building (Fig. 2.1.6).

The total mass of the structure is estimated equal to 9360 tn taking into account the self-weight of the structural elements as well as the dead and live load acting on each floor level. Based on the available data, the strength class of concrete and reinforcement steel are considered as B225 (C16/20) and StIIIb (S420) respectively while the infill strength $f_{m\theta}$ is taken equal to 3MPa. Fig 2.2.33 illustrates the structural model generated in SAP2000.

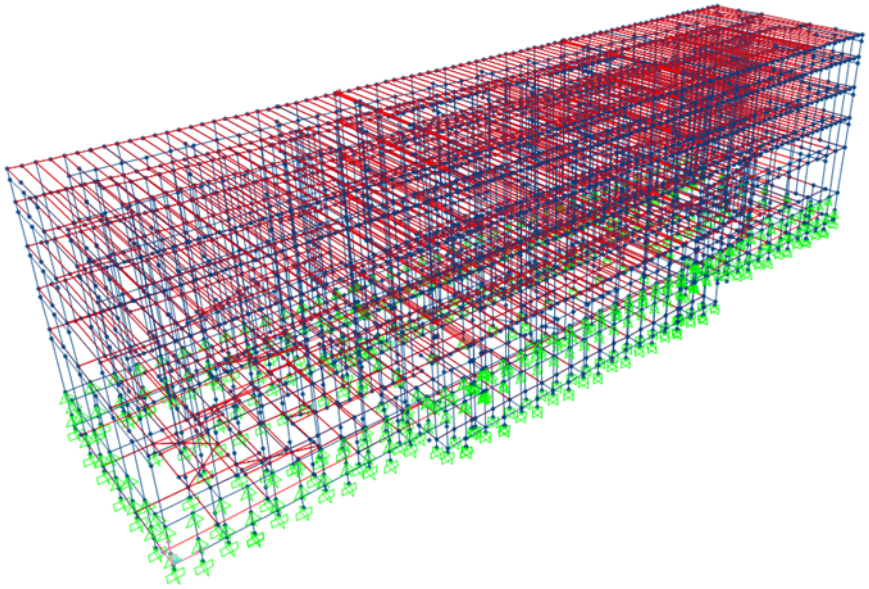

Fig. 2.2.33 Elastic finite element model of the Faculty of Philosophy building in SAP2000.

2.2.2.4. Comparison between the analytical and the experimental modal analysis results. Finite element model updating.

The main purpose of this task is to modify iteratively updating parameters to result in a structural model of the Faculty of Philosophy building that will better reflect the measured data than the initial one which was built based on the design and construction plans. We chose as the updating parameter the stiffness of the structural joint separating the different parts of the building, since no data are available for this property and therefore its definition includes high uncertainty levels. More specifically six stiffness parameter values that correspond to the translational and rotational degrees of freedom are investigated.

The updating is performed not only to improve the frequencies of the considered modes of the initial numerical model presented in Fig. 2.2.33 but also to calibrate the numerical mode shapes in order to fit the experimental data. A manual updating scheme is applied generating a suite of numerical modal models considering different values of the stiffness parameter K_0. Modal analyses are performed for all the derived numerical models. One among them was judged as the best approximation compared to the initial model considered at the beginning of the updating process; this one is characterized as the ‘best’ model representing the observed dynamic response based on the noise measurements.

The selection of the ‘best’ model is made based on the evaluation of the Modal Assurance Criterion MAC defined in section 2.2.1.4.

The computation of the MAC values and the correlation of the responses between the experimental and numerical modal model are made at the measured nodes for which actual recorded noise data are available. A good correlation between the two tested modes was considered to be achieved for MAC values greater than 0.8. The

updating scenario that was found to represent most accurately the experimental results for the modes under investigation considers the stiffness parameter values for the translational and rotational degrees of freedom as shown in Fig. 2.2.34.

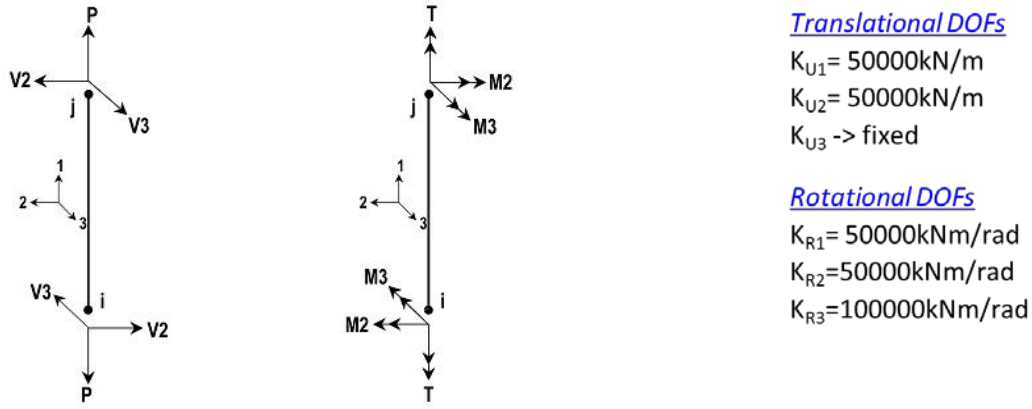

Fig. 2.2.34 Stiffness properties of the gap link elements adopted through the updating procedure.

Fig. 2.2.35 shows the comparison of the modal parameters between the updated numerical and experimental modal models of the Faculty of Philosophy building in terms of resonance periods and mode shapes presenting also the resulting MAC values for the three first modes. The eigenfrequencies and mode shapes of the updated finite element model are compared to the initial ones as well as to the experimental results. It is seen that the updated model correlates well with the experimental results only for the first and second modes under investigation (MAC>0.8) whereas for the third mode it was not possible to capture a higher MAC value and probably another sensitivity parameter related not only to the stiffness parameters of the structural joint but also to the stiffness and mass properties of the different parts would be more appropriate.

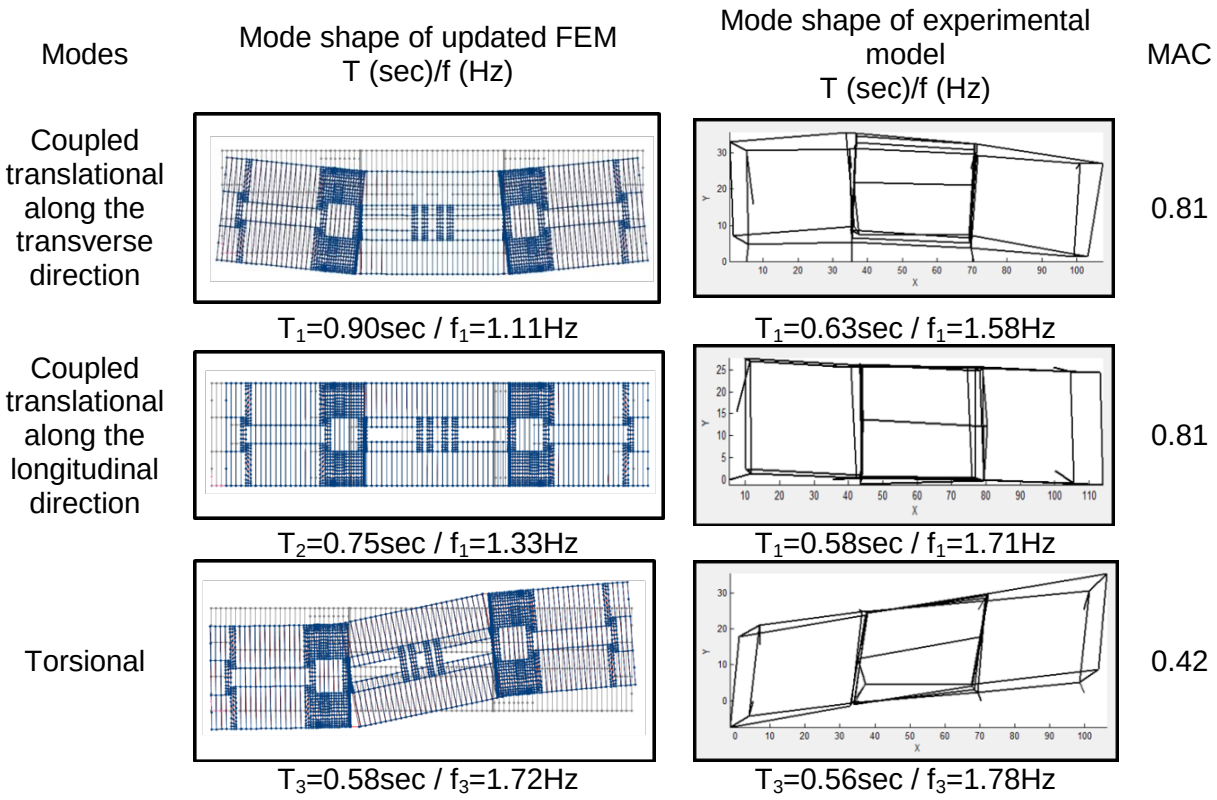

Fig. 2.2.35 Comparison of the updated finite element model of the Faculty of Philosophy building and the experimental results (T: period, f: frequency).

2.2.2.5. Nonlinear finite element modeling

The initial aim was to follow the steps of the methodology applied for the Administration building and conduct the nonlinear finite element modeling of the Faculty of Philosophy building also in SeismoStruct in order to utilize the fiber based approach for the nonlinear simulation of the RC elements. However the size of the model and the extreme high number of beam-column elements shown in Fig. 2.2.36 did not allow performing with the academic version of the software not even the modal analysis of the elastic model. Therefore it was decided to proceed with the nonlinear simulation of the structure in SAP2000 (Fig. 2.2.37) utilizing the hinge model for the representation of the nonlinear beam-column elements. Although the static analysis considering only gravity loads was performed successfully, the pushover analysis could not be completed due to convergence problems attributed most probably to numerical issues caused by the large number of nonlinear beam elements that exist at each floor level of the building.

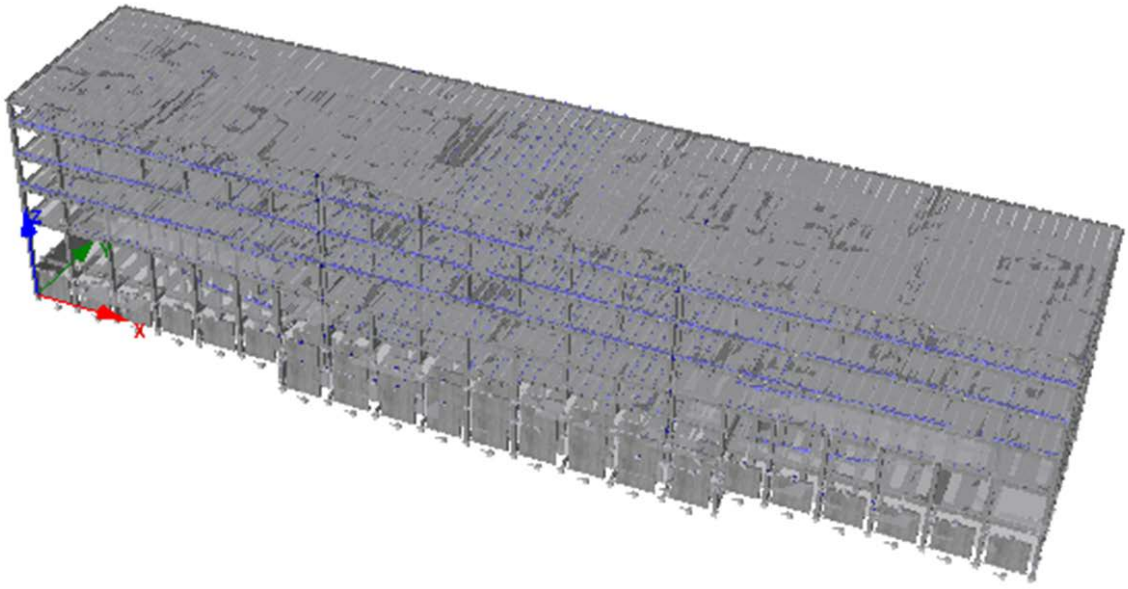

Fig. 2.2.36 Finite element model of the Faculty of Philosophy building in SeismoStruct.

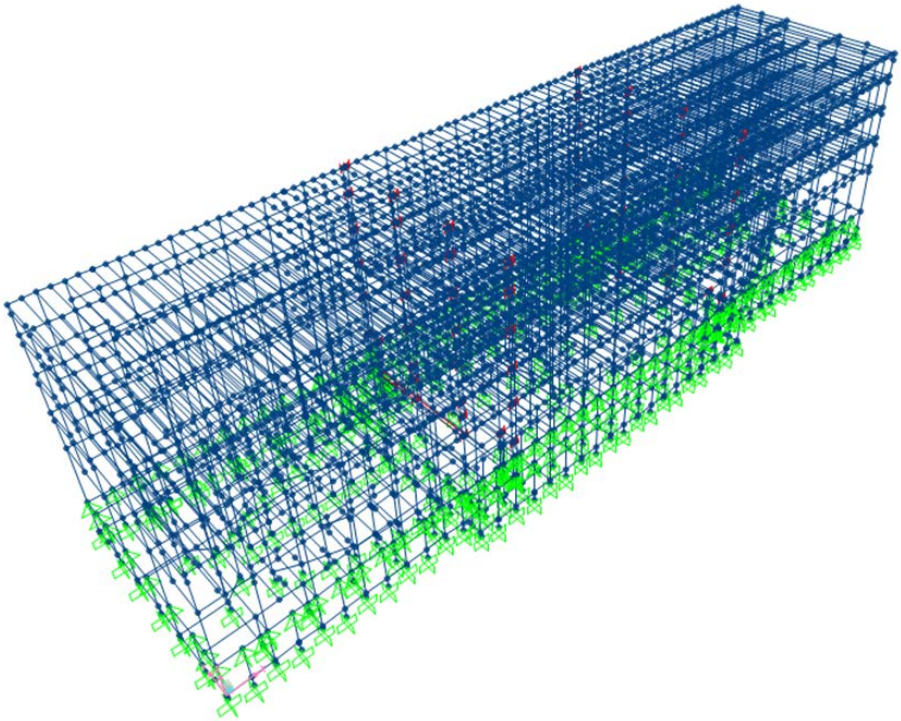

Fig. 2.2.37 Finite element model of the Faculty of Philosophy building in SAP2000.

In order to reduce the size of the numerical model, it was attempted to perform the analysis only for Part II of the building. As shown in Fig. 2.2.38, the middle part was simulated both in SAP2000 and SeismoStruct. However considering only the middle part it is not possible to represent the actual dynamic characteristics of the complete building realistically as shown in Fig. 2.2.39. In the figure the modal parameters of the

numerical model when considering only Part II are compared with the experimental results and it is seen that the building becomes much more flexible with the torsional mode activating higher percent of the total mass of the building. This can be attributed to the fact that the stiffness in the transverse direction is not captured properly since the external structural parts are omitted in the simulation procedure.

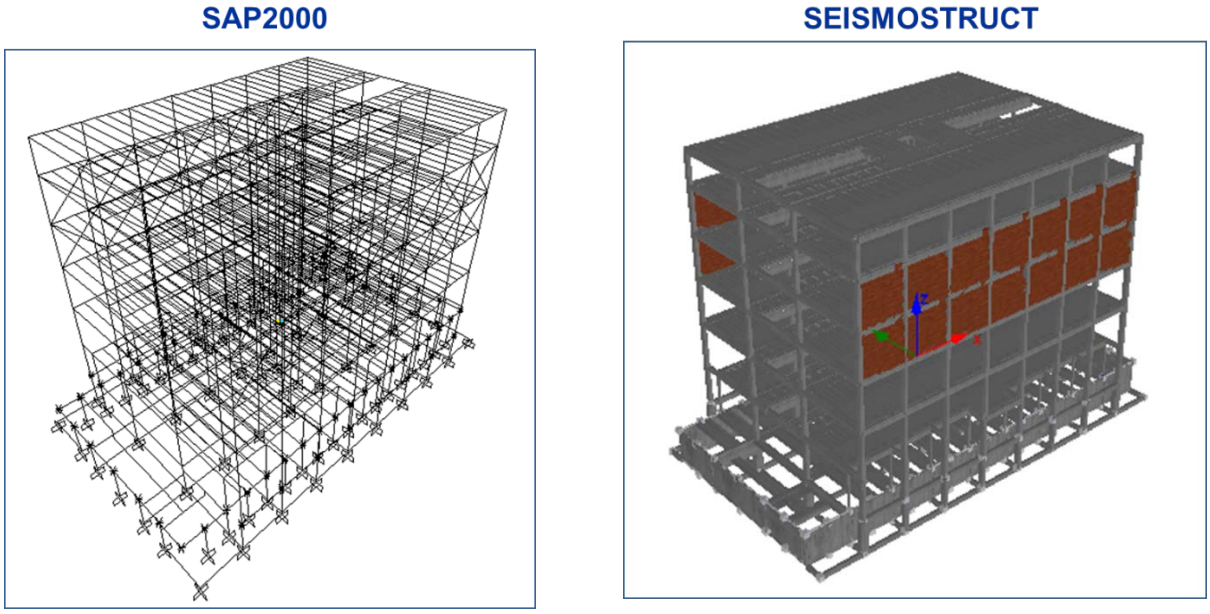

Fig. 2.2.38 Numerical simulation of only Part II of the Faculty of Philosophy building in SAP2000 and SeismoStruct.

Modal analysis of elastic numerical building		
1st mode	2nd mode	3rd mode
T_1=1.85sec	T_2=1.48sec	T_3=1.41sec
Translational along the transverse direction	Torsional	Translational along the longitudinal direction
T_1=0.83sec	T_2=0.58sec	T_3=0.56sec
Translational along the transverse direction	Translational along the longitudinal direction	Torsional

Ambient noise data

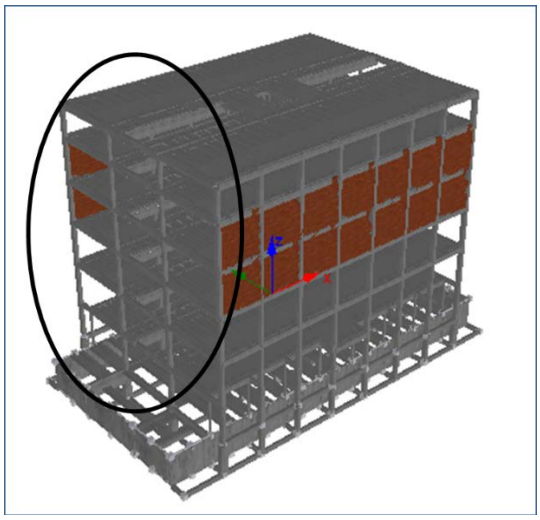

Fig. 2.2.39 Comparison of the modal parameters of the numerical model of the Faculty of Philosophy building with the experimental results when considering only Part II.

Thus, further investigation is planned to be carried out in order to succeed in generating a smaller numerical model that will represent realistically the actual dynamic behavior of the complete building that will be used to derive the building-specific fragility functions of the Faculty of Philosophy building.

2.3. Conclusions

Ambient noise measurements have been employed to assess the real present seismic vulnerability of two buildings at the campus of Aristotle University in Thessaloniki, namely the Administration and the Faculty of Philosophy building. The monitoring data were used to derive the experimental modal model of the buildings and to identify their modal properties based on system identification and OMA respectively.

The modal identification results were used to update and better constrain the initial finite element models of the two structures under study, which were based on the design and construction documentation plans provided by the Technical Service of the University. For both cases a sensitivity parameter related to the structural joint properties was adopted for the updating procedure, namely the stiffness parameter of the joint. In general a good correlation with the experimental results was achieved for both buildings.

For the updated model of the Administration building nonlinear static pushover analysis as well as three-dimensional incremental dynamic analyses were performed to evaluate its seismic performance and to assess its vulnerability. The fragility functions were derived for the immediate occupancy (IO) and the collapse prevention (CP) limit states in terms of PGA. The comparison of the derived building-specific fragility curves with curves adopted from the literature showed that the use of conventional generic curves, although appropriate for assessing vulnerability and losses in a regional/urban scale, may lead to inaccurate fragility and loss estimates in the case of individual building assessment, which constitute crucial components in the framework of decision making and risk mitigation strategies (e.g. seismic safety and rehabilitation costs).

For the updated model of the Faculty of Philosophy building, unfortunately, it was not possible within the available timeframe of the project to complete the vulnerability assessment procedure due to difficulties in the nonlinear modeling and analysis of the structure. Several nonlinear models were generated in different finite element codes however numerical issues associated with the large amount of the inelastic structural elements did not allow to perform any nonlinear analysis. Further investigation is already in progress aiming at limiting the model in order to reduce the data size but representing at the same time realistically the structural and dynamic behavior of the building.

3. Structural survey and simplified building assessment

In accordance with Eurocode 8, depending on the amount and quality of available information required for building assessment, three knowledge levels can be identified: KL1: Limited knowledge, KL2: Normal knowledge, KL3: Full knowledge. The factors determining the appropriate knowledge level (KL) are (EN 1998-3: 2005):

i) *geometry:* the geometrical properties of the structural system, and of such nonstructural elements (e.g. masonry infill panels) as may affect structural response.
ii) *details:* these include the amount and detailing of reinforcement in reinforced concrete, connections between steel members, the connection of floor diaphragms to lateral resisting structure, the bond and mortar jointing of masonry and the nature of any reinforcing elements in masonry,
iii) *materials:* the mechanical properties of the constituent materials.

Considering the achieved knowledge level, the corresponding method for seismic analysis of the structures (either linear or non-linear, static or dynamic) can be used.

In the previous section the approach corresponding to the higher knowledge levels (KL2 or even KL3) was considered, which required both detailed input and special software for the computational analysis. Here we consider practical application of the developed simplified integral structural modelling (SISM) approach corresponding to the limited knowledge level KL1.

As mentioned in the previous sections, two buildings of the Aristotle University of Thessaloniki (AUTH), namely the Administration building (AB) and the building of the Faculty of Philosophy (FB), were selected for the investigation in the framework of SIBYL. The buildings are located in the main campus of the university close to each other (Fig.3.1).

Figure 3.1: Faculty of Philosophy (FB) building and Administration building (AB)

3.1. Philosophical Faculty Building (FB)

According to the original design documents provided by AUTH, the building of the Philosophical Faculty (FB) was designed and constructed in the sixties of the past century. The main façade, the plan of the ground floor as well as the longitudinal cross-section of the building are shown in Fig.3.2.

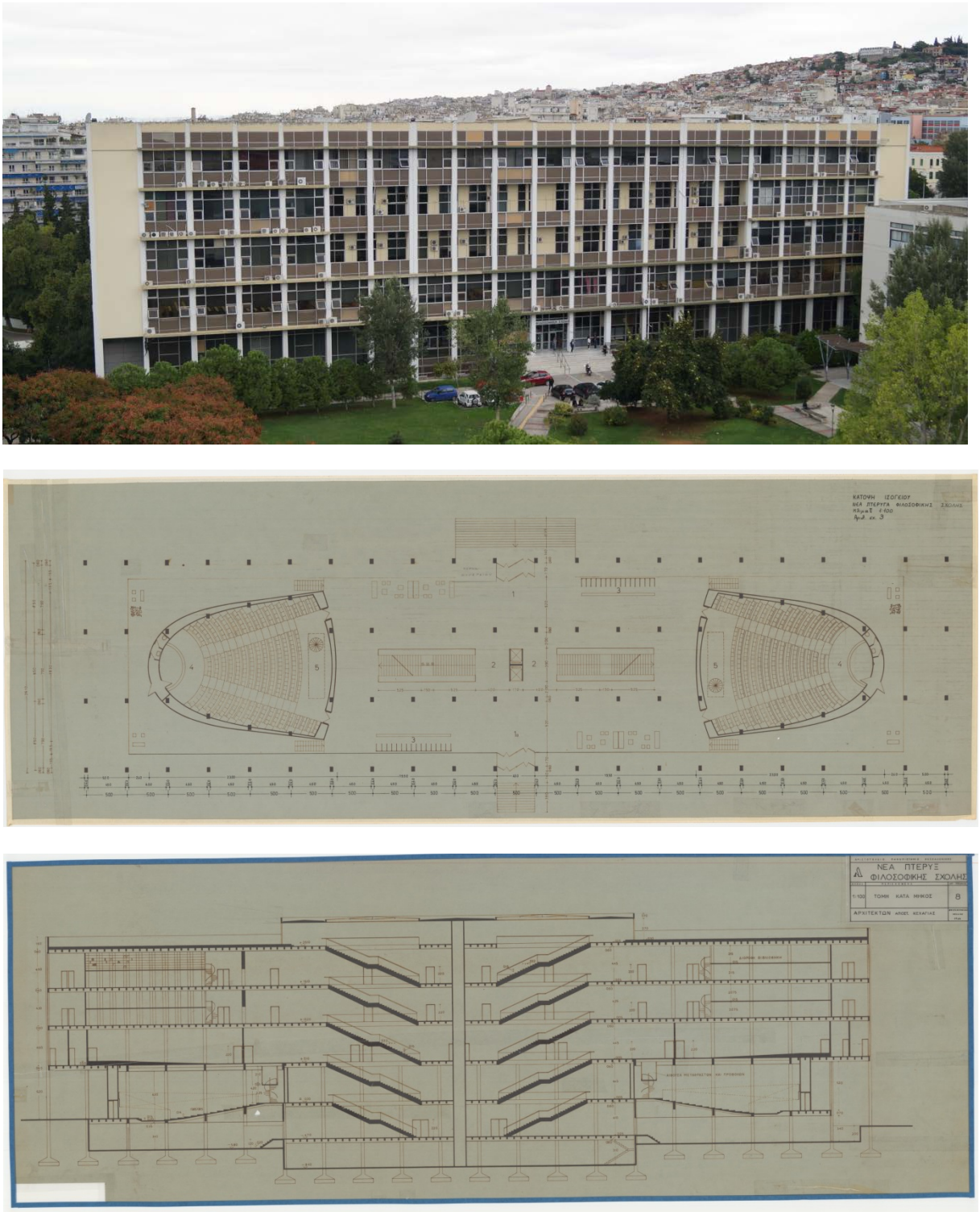

Figure 3.2: Main façade (a), plan of the ground floor (b) and longitudinal cross-section (c) of the building of the Faculty of Philosophy (FB)

The bearing structural system of the building is represented by reinforced concrete frames consisting of columns and beams. The building consists of three units separated by two separation joints. In comparison with the original drawings, in the current state the building has one extra floor; furthermore, in the course of the in-situ measurements considerable changes in the cross-sectional dimensions of structural elements were identified. One may, obviously, conclude that all these modifications were implemented during the process of the building exploitation (more details can be found in Section 2 of the case study).

Considering the complex structure of the building, in particular, irregular spatial distribution of supporting columns in the wing units of the building, for the simplified structural analysis we focus on the central part of the building. Keeping this purpose in mind, the vibration measurements were concentrated on the central unit (monitored with sensors placed at the four corners of 1st, 2nd, 3rd, and 4th floors; two sensors were installed on the roof, and two in the underground basement). The two wings were also monitored, but less densely (the sensors were installed at the four corners of the 1st and 4th floors, and one sensor in the semi-basement). The spatial arrangement of the system of installed sensors is presented schematically in Fig. 3.3. The building was monitored for about 20 hours.

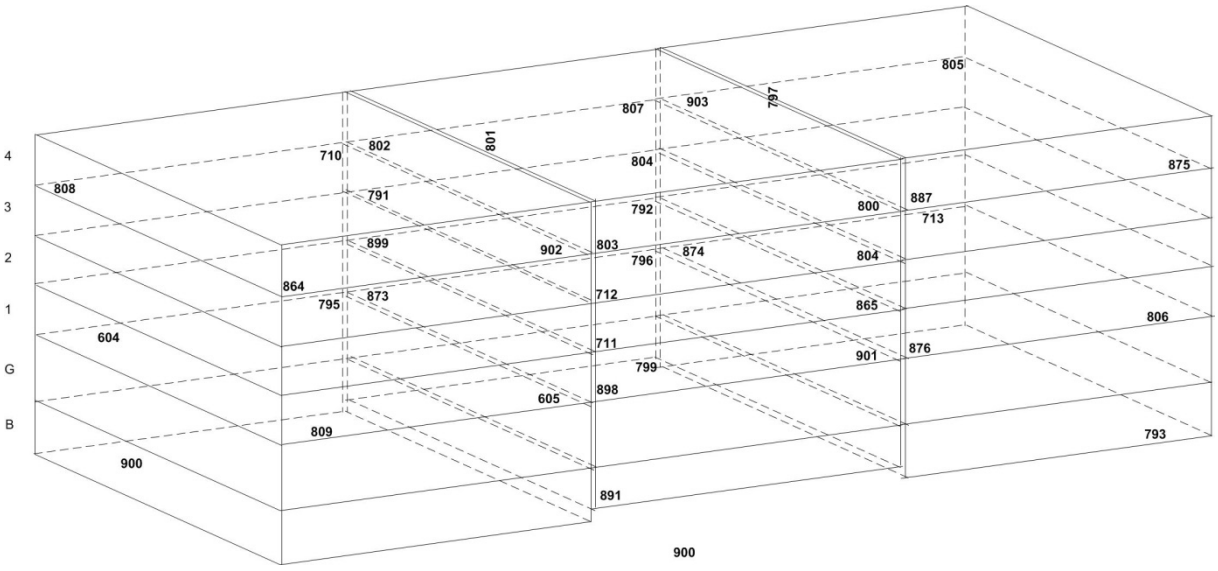

Figure 3.3: Schematic representation of the instrumentation layout in FB

3.2. Administration Building (AB)

The Administration building (AB) of AUTH was designed and constructed in the eighties/nineties. The façade of the building (a), the plan of the ground floor (b) and the plan of a typical floor (c) are shown in Fig. 3.4.

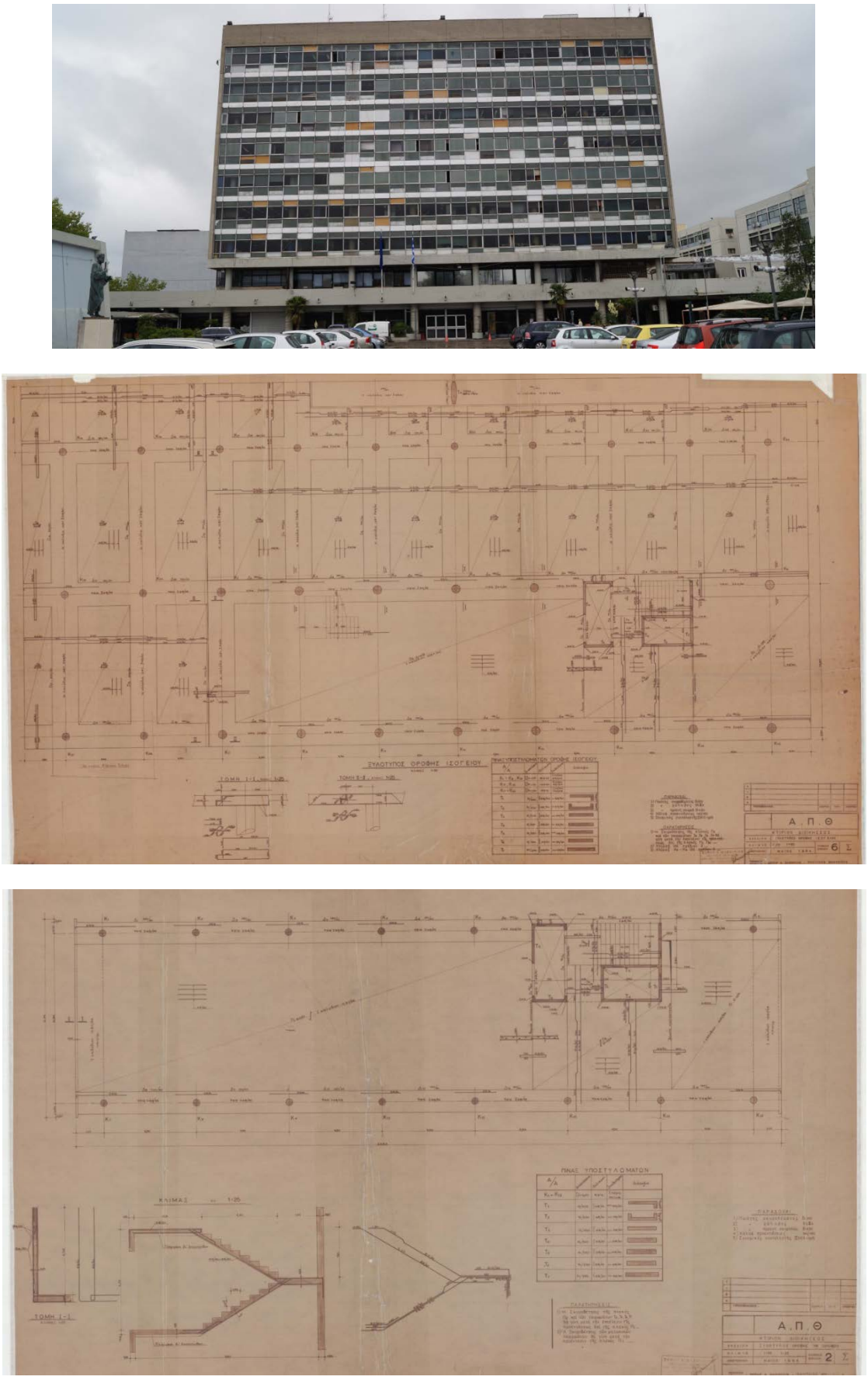

Figure 3.4: Main façade (a), the plan of the ground floor (b) and the plan of the typical upper floor (c) of the Administration building (AB)

This building is composed of 8 upper floors plus the ground floor and the basement. The structural system is represented by a grid of reinforced concrete columns and beams. The findings of in-situ structural survey are discussed below.

The sensors for the ambient vibration measurements were installed at the four corners of each floor (from the ground to the 8th), with two sensors installed in the basement. The scheme of the instrumentation layout is shown in Fig.3.5. The building was also monitored for about 20 hours.

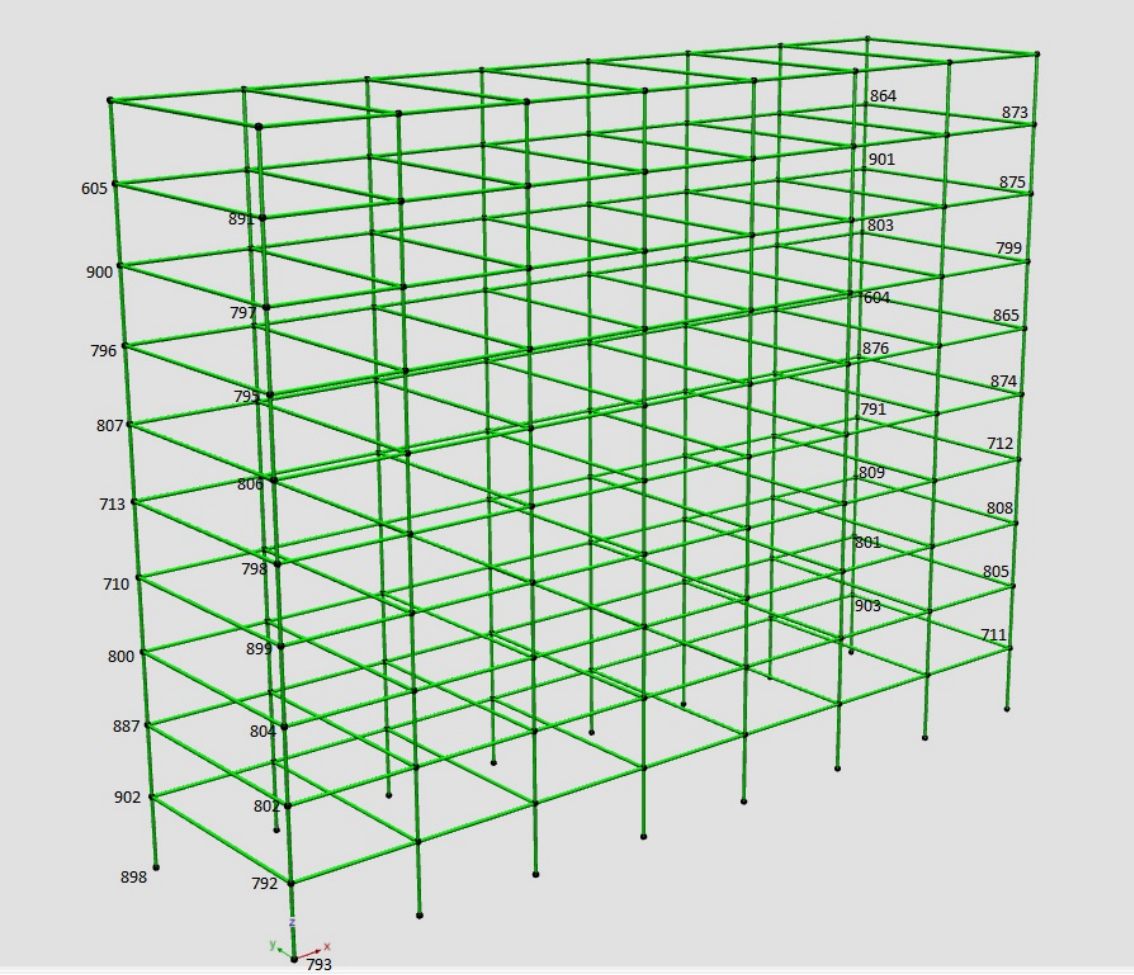

Figure 3.5: Schematic representation of the instrumentation layout in AB

3.3. In-situ structural survey and data collection

In-situ structural survey and inspections of the two buildings were performed in parallel with the ambient vibration measurements. The activities included collecting data about geometrical and physical parameters of the structural elements, which are required for the modeling and seismic analysis of the structures. The data collection procedure, which is a part of the approach under development, is especially important for the cases when the design drawings are not available or when the existing structures were modified in the process of the building exploitation. As it was mentioned above, the latter is exactly the case of the building of the Philosophical Faculty.

In particular, during the in-situ survey and inspection we have to collect information regarding: current physical condition of the structural elements and possible presence of damage or degradation; geometry (including overall structural geometry and member sizes, possible geometrical distortions or deficiencies, irregularities in plan and height); structural details (presence and amount of steel reinforcement in columns, beams and walls and depth of concrete cover); mechanical properties of construction materials (in particular, concrete strength and elasticity modulus, steel yield strength, ultimate strength and ultimate strain). As mentioned above, these are the main factors determining the knowledge level (KL) in accordance with the Eurocode 8.

If the original design documentation is available, in-situ inspection, first of all, should check correspondence between the available drawings and the actual state of the existing structure. If the original construction drawings are not available, the lacking information should be collected during the in-situ inspection or/and using the simulated design. The thoroughness and detail of the inspection and data collection procedure depend on the pursued knowledge level (considering and balancing, on the one hand, the acceptable accuracy and, on the other hand, the existing uncertainties).

During the measurement campaign in Thessaloniki, along with the use of available original design drawings provided by the AUTH partners, we conducted additional geometry measurements in both buildings under consideration. For these purposes we used conventional measure tapes, folding rulers and a laser distance meter HILTI PD 5 (Fig. 3.6).

Figure 3.6: Laser distance meter HILTI PD5

For investigating details of the existing concrete elements we used the HILTI PS 50 Multidetector, which “is designed to detect objects such as ferrous metals (rebars), non-ferrous metals (copper and aluminum), wood beams, plastic pipes and electric cables in dry materials” (HILTI PS 50, Bedienungsanleitung). In the process of the in-

situ inspection the device was used for scanning concrete members to detect the location of reinforcement bars and determine the depth of concrete cover (Fig. 3.7).

Figure 3.7: Detecting of ferrous metal in a concrete column with the use of HILTI PS 50 Multidetector

In the course of the structural survey in the Philosophical Faculty building (FB) considerable discrepancies with the original design documentation were detected. First of all, the existing building has one additional floor in comparison with the original drawings. In particular, the measured total height of the building (from the finished floor level to the roof) is about 5 m higher in comparison with the height value specified in the design drawings. Furthermore, sample measurements of the cross-sectional dimensions of structural elements (columns and beams) made in the course of in-situ inspection, showed considerable changes in comparison with the data from the available drawings. For example, in the drawings the cross-section of all the external raw columns of the ground floor (Fig.3.8) is indicated as 40 x 60 cm, while in the current state the existing columns are considerably thicker (the measured dimensions of the rectangle cross-sections of those columns range from 49 x 74 to 50 x 76 cm). Unfortunately, the scanning of the structures with multidetector (Fig. 3.7) did not allow to identify the exact reinforcement schemes of the considered structural cross-sections (the device showed presence of ferrous metal elements though at deeper layers than indicated in the drawings).

Figure 3.8: External RC columns of the Philosophical Faculty Building (FB)

Considering the available information, one may conclude that after completion of construction, the building was redesigned and structurally modified (one floor was added, in consequence of which the bearing structural elements were strengthened). In this situation, an extended/comprehensive in-situ inspection would be necessary to collect the information required for adequate structural modeling.

Obviously, such kind of structural modification would not only considerably change the vibration parameters of the building, but also influence its seismic vulnerability. Needless to say, any computational analyses solely based on the original design drawings of the building, neglecting the structural modifications made after the construction, would produce misleading results and, therefore, inadequate decisions. This fact emphasizes the crucial importance of in-situ inspections for assessment of actual structural vulnerability of existing buildings.

Similar engineering measurements were conducted also in the administrative building (AB). As mentioned above, the building has eight upper floors plus the ground floor and the basement. There were no visual discrepancies between the measured data and the values from available drawings found during the in-situ inspection.

The structural system is represented by a grid of reinforced concrete columns and beams. It is worth mentioning that all the supporting columns are of round cross-sectional shape, which is obviously not an optimum design solution from the earthquake engineering point of view.

It is important to note that there is an evident stiffness irregularity in plan, where (throughout the height of the building) instead of the columns, the supporting functions are carried by the walls of the elevator shaft (Fig.3.4). Besides, it is also worth mentioning that there is a horizontal extension of the structure at the level of the ground floor, which has two spans, while the upper floors represent a single-span structure in the transversal direction. Furthermore, the ground-floor extension in the longitudinal direction was not properly separated by the separation joints. This deficiency was, most probably, the cause of a cross-cutting crack in the concrete slab at the ground floor level, as it was found out during the in-situ inspection of the building (Fig.3.9).

Figure 3.9: Cross-cutting crack in the RC slab of the ground floor (AB). View from the front (a) and back (b) side of the building.

All the results of the measurements obtained from the in-situ inspections along with the data of vibration measurements (operational modal analysis) are used for structural modeling and seismic evaluation of the buildings.

3.4. Operational modal analysis

The recorded ambient vibrations for both buildings were processed by GFZ partners (as described in Section 1 of the case study) and provided in miniSEED format. Further processing and modal analyses were implemented with the help of MACEC 3.3 software (Reynders et al. 2014) using stochastic subspace identification approach (Reynders, 2012).

Several three-minute-long recordings (in the different day and night periods) were analyzed and compared. The calculations for all the analyzed recordings gave very similar output.

The three vibration modes obtained from the operational modal analysis for the building of the Philosophical Faculty are presented in Fig. 3.10. The obtained fundamental frequencies for two bending modes are equal to 1.60 Hz (in the lateral direction) and 1.72 Hz (in the longitudinal direction). The frequency corresponding to the third, torsional mode is 1.76 Hz. The torsional mode is, however, less relevant for the seismic vulnerability assessment due to the symmetry of the considered structure. In the further analyses we focus on the central unit and consider first of all the bending modes in the structural model described below.

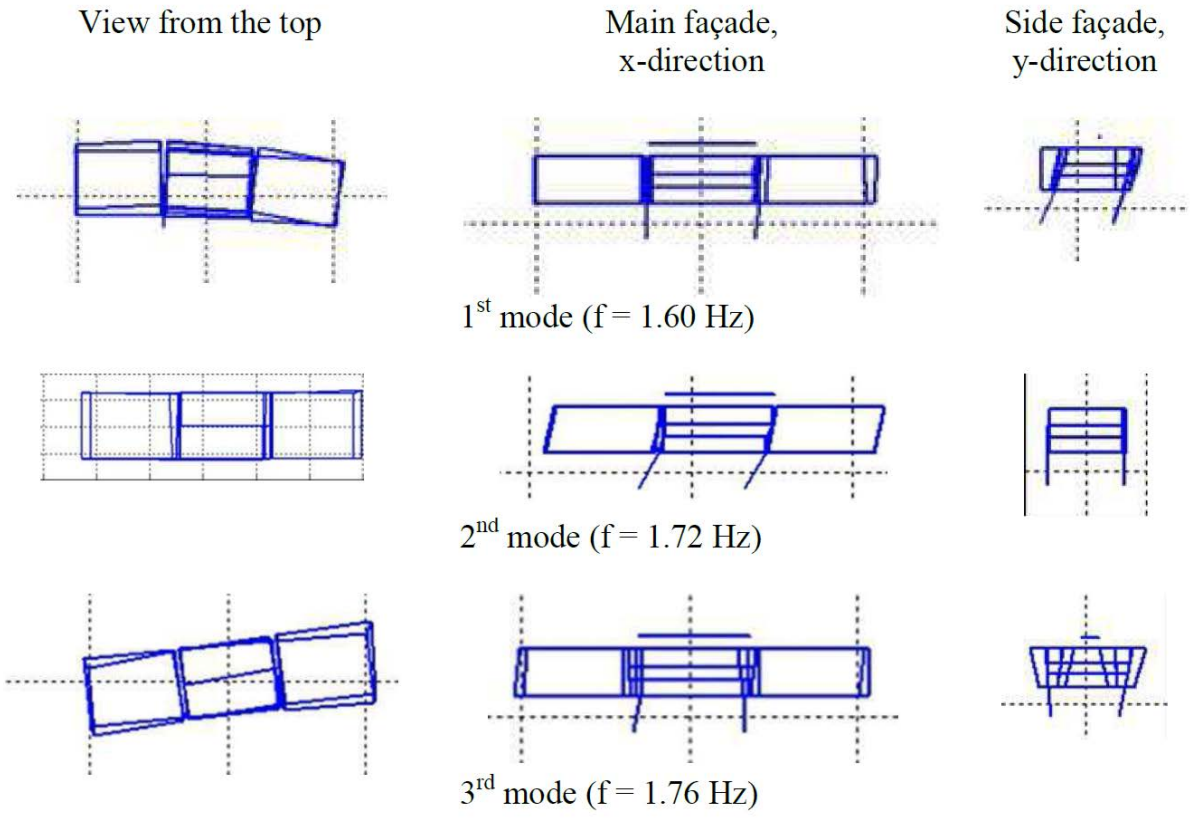

Figure 3.10: Results of operational modal analysis for the Philosophical building

The three modes for the Administration buildings obtained from the operational modal analysis are shown in Fig.3.11. The Administration building is taller and more flexible in comparison with the Philosophical building and correspondingly has longer periods of vibration (lower frequencies). The obtained frequency for the first mode is 1.17 Hz, for the second mode 1.25 Hz, and for the third mode 1.68 Hz. Important to note that due to the presence of the elevator shaft shifted to one side, the building has strong asymmetry in plan, which is also reflected in its vibrational performance (Fig.3.11).

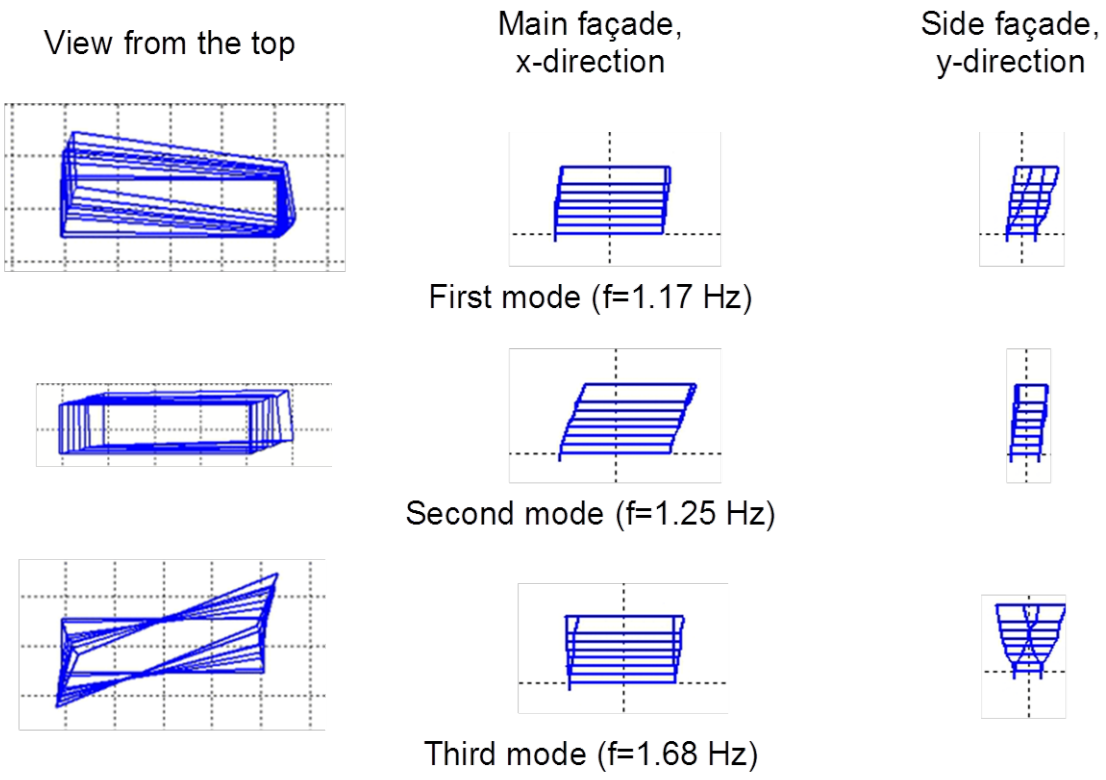

Figure 3.11: Results of operational modal analysis for the Administration building

3.5. Simplified integral structural model and seismic evaluation of the Philosophical building

Due to the strong asymmetry of the Administration building it was not considered for the simplified assessment; only the Philosophical building was analyzed with the use of the developed SISM approach. As mentioned above, only the central part of the building is considered for the structural modelling and analysis.

For constructing the building model we take into consideration that the structural system is presented by moment resisting frames, composed of reinforced-concrete columns and beams. The lateral-load resisting system is complemented with the reinforced-concrete elevator shaft located in the center of the building. There is also a system of masonry walls, defining the internal functional arrangement of the building. The walls do not belong to the support framework, however, they contribute to the stiffness and mass of the structure; therefore they have also been included to the structural model. The structural system is completed with reinforced concrete floor slabs, providing the spatial integrity of the building as a whole (Fig. 3.12). The modeled system is considered fixed at the ground level and, for the sake of simplification, we do not take into account possible influence of the underground part of the building and neglect possible ground-structure interaction effects.

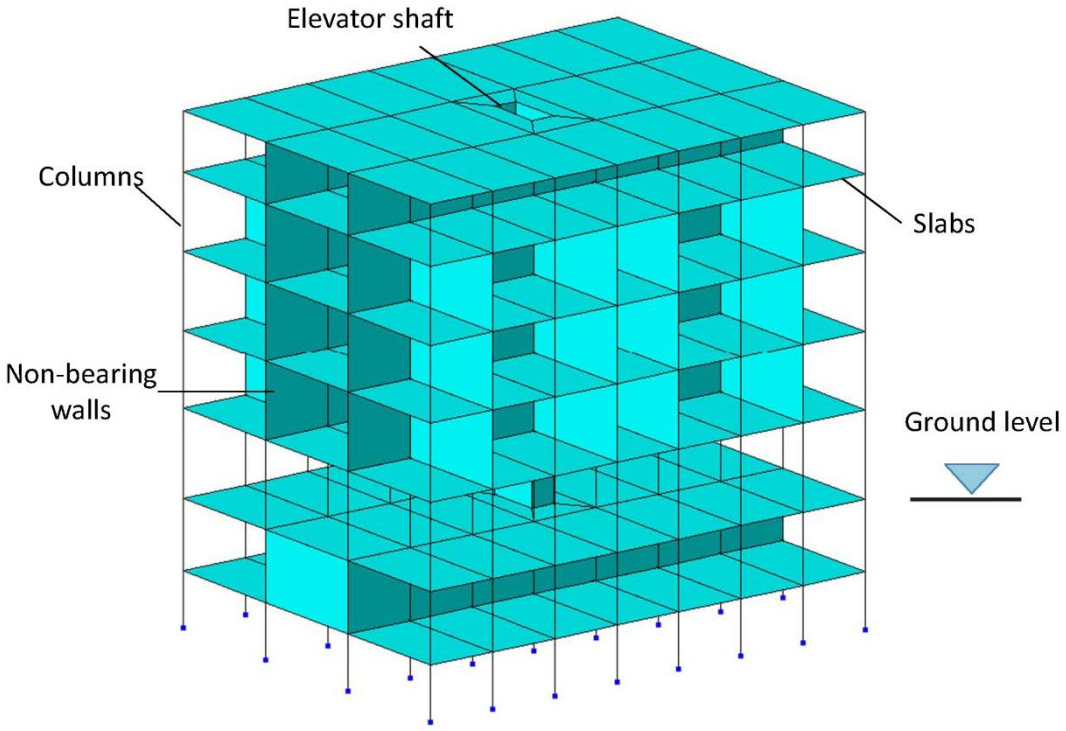

Figure 3.12: Structural model of the central unit of the building

On the basis of the collected geometry, material and structural data the SISM model for the building was constructed, considering two planar directions. The torsional stiffness and, correspondingly torsional mode of vibration, is not considered.

Two bending modes, calculated from the eigenvalue problem for K and M, are shown in Fig. 3.13. They match qualitatively well the measured bending modes of the building. The calculated natural frequencies (f_{c1}=1.59 Hz, f_{c2}=1.71 Hz) are very well comparable with the measured ones (f_{m1}=1.60 Hz, f_{m2}=1.72 Hz). The relative differences with respect to the measured frequencies are negligible in view of large uncertainties mentioned above and a quite simplified modeling procedure.

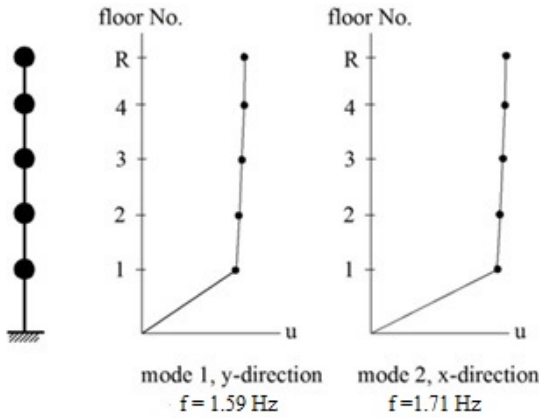

Figure 3.13: First bending modes of the SISM

According to Eurocode 8, the seismic base shear force F_b is determined using the following expression

$$F_b = S(T_1) * m * \lambda$$

where

$S(T_1)$ is the ordinate of the acceleration spectrum at the fundamental period of vibration of the building for lateral motion in the considered direction ($T_1 = 1 / f_1$);

m is the total mass of the building, above the foundation or above the top of a rigid basement;

λ is the correction factor, the value of which is equal to: λ = 0,85 if T1 < 2 TC and the building has more than two stories, or λ = 1,0 otherwise.

For calculation of seismic load we used the acceleration spectrum provided by AUTH-partners (Fig.3.14), from which the level of seismic acceleration corresponding to the vibration period of the building can be determined.

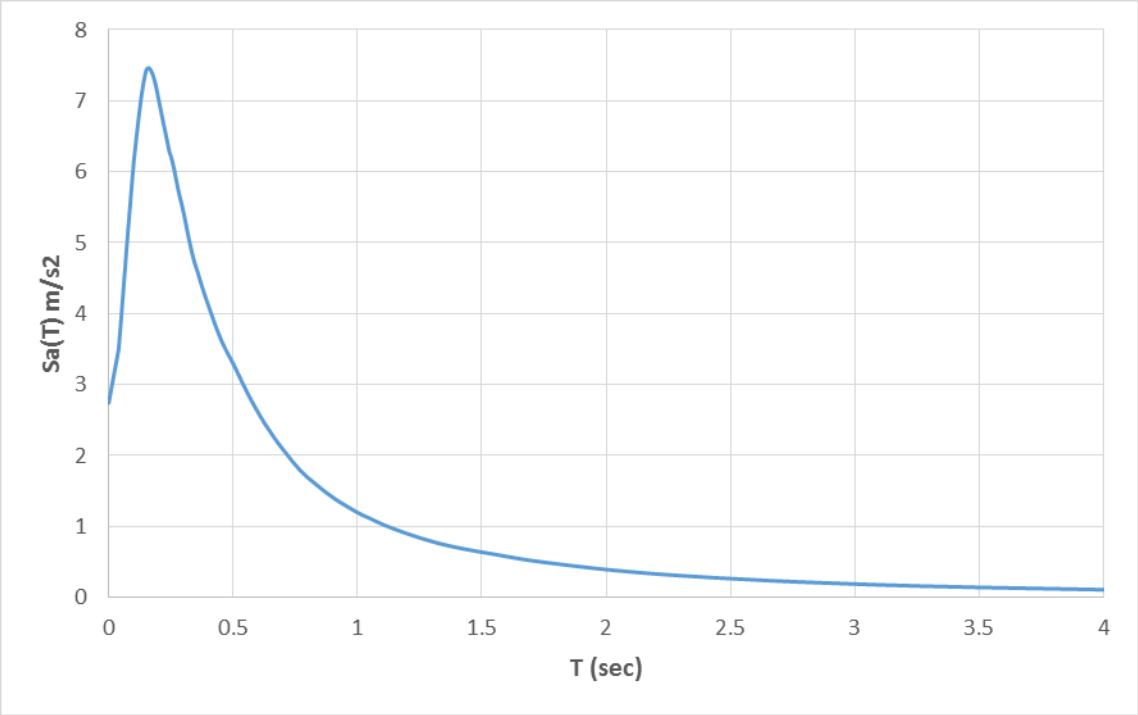

Figure 3.14: Acceleration spectrum for the investigated site

This input seismic data along with the collected information about the building were used for the structural analysis and seismic assessment of the building with the help of the SISM-tool.

In the considered case, the available and collected information corresponds to the knowledge level KL1. For this knowledge level for building assessment we used the developed SISM-based approach and the Excel tool (description of the developed method and the tool are given in DC1 and DC3). The numerical results obtained with

the use of the SISM-tool show that at the given level of seismic hazard (for the mean return period of 475 years) one may expect occurrence of the limit state 3 (failure of the structure) at the level of the ground floor, while the upper floors perform much better. In particular, the results obtained for the X-direction show that only the LS1 (cracks in concrete) is achieved in all upper floors, while for the Y-direction the LS2 (yielding in reinforcement bars) is achieved of the second and third floors and LS1 on the fourth and the fifth floors of the building (Fig 3.15).

Limit state assessment

X-direction

Story	EQ Force LS1 [MN]	EQ Force LS2 [MN]	EQ Force LS3 [MN]	LS1 Force [MN]	LS2 Force [MN]	LS3 Force [MN]
1	246.1182413	94.4290395	29.03190683	4.520715377	21.4232546	22.75822563
2	205.5056892	77.39480153	23.47226757	28.14041007	296.2669694	1074.037221
3	157.3586695	58.40913941	17.52149768	23.87799179	283.7937701	1293.642951
4	104.8435583	38.53019631	11.46952807	19.61557341	271.4026172	1592.061831
5	50.50540804	18.46710774	5.476084829	24.53039057	423.8126362	3270.811672

Y-direction

Story	EQ Force LS1 [MN]	EQ Force LS2 [MN]	EQ Force LS3 [MN]	LS1 Force [MN]	LS2 Force [MN]	LS3 Force [MN]
1	290.3190683	157.7165873	81.36970425	6.87046925	33.16692626	34.90576826
2	250.8568525	134.6503997	67.90313338	19.68146187	133.9094731	313.1754795
3	197.1905844	104.9808544	52.00672968	16.74463876	124.0534153	385.7307694
4	133.7174304	70.84212122	34.66057665	13.80781562	114.2411647	502.4295424
5	64.91948986	34.30243282	16.67741521	18.33726608	187.1751682	1280.781388

Figure 3.15: Results of building assessment with the use of the SISM-Tool

3.6. Conclusions

During the in-situ inspection in the Philosophical Faculty building considerable discrepancies with the original design documentation were detected. First of all, the existing building has one additional floor in comparison with the original design drawings. The measured total height of the building (from the finished floor level to the roof) is about 5 m higher in comparison with the height value specified in the design drawings. Furthermore, sample measurements of the cross-sectional dimensions of structural elements (columns and beams) made in the course of in-situ inspection, showed considerable changes in comparison with the data from the available drawings. For example, the cross-section of all the external raw columns of the ground floor in the drawings is indicated as 40 x 60 cm, while actually the existing columns are considerably thicker (the measured dimensions of the rectangle cross-sections of those columns range from 49 x 74 to 50 x 76 cm).

Considering the available information, one may conclude that after completion of construction, the building was redesigned and, consequently, structurally modified (one floor was added, in consequence of which the bearing structural elements were strengthened). In this situation, an extended in-situ inspection would be necessary to

collect the information required for the structural modeling of higher knowledge levels.

Obviously, such essential structural modification would not only considerably change the vibration parameters of the building, but also influence its seismic vulnerability and, therefore, any computational analyses solely based on the original design drawings of the building, neglecting the structural modifications made after the construction, would produce misleading results and, hence, inadequate decisions. This fact emphasizes the crucial importance of in-situ inspections for assessment of actual structural vulnerability of existing buildings.

The results of the operational modal analysis (Fig.3.10) show that the separation joints are only in part efficient and there is still certain coupling between the central and side units of the building at the level of the added floor (these effects, in particular, can be seen from consideration of the higher modes). Most probably, this can be the consequence of the structural modernization of the building, which is prompted also by the cracks found at the locations close to the separation joints. More detailed investigation of this structural imperfection would be required.

Having summarized the collected in-situ information and obtained numerical results one may conclude that the presence of the weak ground floor (soft-story) makes the building seismically vulnerable; therefore strengthening of the bearing structural elements would be recommended.

At the same time, one should keep in mind that in our simplified assessment only the central part of the building was considered, neglecting possible influence of the side units of the building on its performance as a whole. Furthermore, we have to take into account considerable uncertainty in the input parameters inasmuch as we had to use simulated design due to the lack of reliable information about actual parameters of the building. Nevertheless, our estimation obtained with the use of simplified approach reflects the in-situ findings; in particular, the presence of soft-story and the predicted damage mechanism in case of a strong earthquake seems to be plausible.

For the case of higher knowledge level (KL2), additional investigations should be conducted aimed at collecting more detailed information about parameters of the building and more sophisticated methods of analysis should be used (as described in Section 2 of the case study).

Cologne

1. Outline of the case study

The level of seismicity in Germany is, in general, comparatively low (in particular, in comparison with the other partner-countries of SIBYL, Greece and Italy). However the city of Cologne is located in the Lower Rhine Embayment, which is one of the most active seismic regions in western and central Europe (Rosenhauer and Ahorner, 1994). Strong earthquakes repeatedly occurred in the area in the past, e.g., Düren, 1756, Euskirchen, 1951, Roermond, 1992. According to the current estimates (Grünthal and Wahlström, 2006), for a non-exceedance probability of 90% in 50 years (a mean return period of 475 years) the level of seismic hazard for the city area is characterized by peak ground acceleration (PGA) about 0.1 g or by macroseismic intensity VI-VII in terms of the European Macroseismic Scale, EMS-98 (Grünthal, 1998). Recent seismological studies (e.g. Verbeeck et al., 2009, Vanneste et al. 2013) show that even stronger earthquakes cannot be ruled out in the area in the future. That is why assessment of seismic vulnerability of the existing built environment of such a large and densely-populated community as Cologne represents an important and challenging problem, which requires joint efforts and interaction of scientists, practitioners and policy-makers. It is worthwhile to note that, when TU-Berlin contacted the Cologne municipality with suggestion to conduct structural survey and measurements for several existing school buildings in the city, the response was very positive and concerned. With the support of the municipality we established direct contacts with seven schools of the city, whose administration also showed understanding of the problem and interest in the cooperation.

The list of the schools investigated within the SIBYL-program for the city of Cologne (as well as the schedule of conducted investigations) is presented in Table 1.1.

The program of engineering investigations for the school buildings included ambient vibration measurements (both outside the buildings for estimation of the seismic soil characteristics at site and inside the buildings for estimation of their vibrational parameters) and the in-situ inspection of the structures (i.e., collecting the data necessary for the structural analysis and vulnerability assessment).

At the stage of preparation it was planned that the total program of the investigations would confine within a time-frame of four hours for every school. Actually, as can be expected, the total duration of measurements can differ for different buildings depending on the amount and quality of a priori available information and on the complexity of the structural system of the investigated buildings. For some of the schools the structural drawings (plans and/or cross-sections) of the buildings were provided to the SIBYL research team beforehand. Though for some of the buildings no design documentation was available. Nevertheless, the SIBYL work team successfully met the allocated time-frame (Table 1.1).

The collected on-site information included the vibration recordings, both in the school yards (of about one hour duration) and inside the selected buildings (about half an hour) as well as the geometrical and structural characteristics of the buildings to be

used for the modeling. Furthermore, all the investigated buildings were described in terms of the GEM taxonomy (Brzev et al., 2012), which can also serve the purpose of the seismic vulnerability assessment.

Table 1.1: List of the selected schools in Cologne and the work schedule

NN	School Name	Address	Date & Time
1	Humboldt-Gymnasium	Kartäuserwall 40, 50676 Köln	Mo.30.11 8-12
2	Alfred-Müller-Armack Berufskolleg	Brüggener Str. 1, 50969 Köln	Di.01.12 12-16
3	Henry-Ford-Realschule	Karl-Marx-Allee 43, 50769 Köln	Mi.02.12 8-12
4	Berufskolleg Ehrenfeld	Weinsbergstraße 72, 50823 Köln	Mi.02.12 12-16
5	Otto-Lilienthal-Schule	Albert-Schweitzer-Straße 8, 51147 Köln	Do.03.12 8-12
6	Gymnasium Thusneldastraße	Thusneldastraße 17, 50679 Köln	Do.03.12 12-16
7	Gymnasium Kreuzgasse	Vogelsanger Str. 1, 50672 Köln	Fr.04.12 8-12

Keeping in mind the objectives of the Task C: ”Rapid and low cost in-situ building vulnerability assessment”, we engage easily-accessible methods and tools, combining analysis of available original design documentation and the simulated design with a limited/extended in-situ inspection including the visual survey and measurements of the existing structures and the methods of non-destructive in-situ testing.

We take into consideration that the end-users – Civil Protection (CP) authorities – can meet various situations in practice; therefore the operational framework should be flexible and afford a set of different approaches to solve the problems of

vulnerability analysis in different possible conditions, reflecting, in particular, different knowledge levels of Eurocode 8. Therefore, within the project we consider different possible approaches (corresponding to the different knowledge levels) for collecting data and for assessing the seismic vulnerability of existing buildings.

We assume that the choice of the appropriate approach should be done by the CP practitioners taking into account also the accuracy and completeness of the available information as well as the scale of the problem under consideration (e.g. a single structure or a group of buildings) as well as depending on their needs and available resources. More details can be found in DC1: Guidelines for the building assessment procedure and short-term monitoring.

2. Array measurements

The array measurements were done on the first day in a park on grass in front of the school of interest, but then because of the rainfall during these days, subsequent arrays were set up within the schools themselves (e.g., paved recreational areas) or on paved areas in front of the school (see Figure 2.1). The instruments consisted of 10 MP-WISE (Multi-Parameter WIreless Seismic array instruments (see Picozzi et al., 2010) connected to 4.5 Hz geophones, and a standard 17 Ah battery. The MP-WISE is an innovative system that allows several kinds of sensors to be combined with a computing system able to implement complex information integration and processing tasks at the node or sensor level and therefore suitable for a wide range of possible applications. The sampling rate was set to 400 samples per second (Nyquist at 200 Hz). Measurements were carried out usually for around 1 hour, after which some units were removed and installed within the buildings that were being inspected.

Figure 2.1: (left) A typical arrangement of a noise measurement array, where the instruments are set up on a paved area in front of a school. (right) The instrumentation employed.

The data are stored on the so-called CUBE[5] digitizer boards of the MP-WISE units, and can also be transmitted via WIFI to a laptop for real-time processing (see below). The data are converted in real-time to the miniSEED[6] format using the SeisComP3[7] cube_plugin. miniSEED is a subset of the SEED or Standard for the Exchange of Earthquake Data, while SeisComP3 is the latest version of the SeisComP suite of seismological software used for data acquisition, processing, distribution and interactive analysis that has been developed by the GEOFON[8] program at GFZ and gempa GmbH[9]. The data will be disseminated through the GFZ ftp site. The miniSEED files are day files following the SeisComP3 data structure and the three components (vertical, transverse and longitudinal) are split in separate files.

The extended spatial autocorrelation method (ESAC, e.g., Parolai et al., 2006) is applied to derive the dispersion curves for Rayleigh waves. From these curves, applying the method proposed by Albarello and Gargani (2010), the so-called Vs30 parameter was estimated at each location. Vs30 is the average shear wave velocity in the upper-most 30 m of the surface, and is a commonly used proxy that provides a measure of potential site amplification (Borcherdt, 1994). The obtained Vs30 values at each school are listed in Table 2.1. Albarello and Gargani (2010) estimated the uncertainties associated with these values to be of the order of 10%. The resulting values are consistent with those found in previous studies (e.g., Parolai et al., 2002). This processing can be undertaken in real time using the data transferred to a laptop which runs the required tool[10], also being developed within SIBYL.

Table 2.1: Vs30 values for the locations of the selected schools in Cologne.

School	Vs30 (m/sec)
Humboldt Gymnasium	286
Alfred-Mueller-Armack Berufskolleg	289
Henry-ford Realschule	307
Berufskolleg Ehrenfeld	371
Otto-Lilienthal Schule	312
Gymnasium Thusneldastrasse	293
Gymnasium Kreuzgasse	288

[5] The CUBE is a seismic recording unit developed by GFZ and is characterised by low-weight, and very low power consumption.
[6] https://ds.iris.edu/ds/nodes/dmc/data/formats/#miniseed
[7] https://www.seiscomp3.org/
[8] http://geofon.gfz-potsdam.de/
[9] http://www.gempa.de/
[10] http://www.sibyl-project.eu/tools/

3. Structural survey and measurements in the buildings

According to Eurocode 8 for assessing the earthquake resistance of existing structures, the input data can be collected from a variety of sources, including available documentation and design drawings, contemporary building codes and standards, field investigations and in situ or laboratory measurements and tests. If the original design documentation is available, in-situ inspection, first of all, should check correspondence between the available drawings and the actual state of the existing structure. If the original construction drawings are not available, the lacking information should be collected during the in-situ inspection or/and using the simulated design.

The structural survey and limited in-situ inspections of the school buildings in Cologne were performed in parallel with the ambient vibration measurements. The activities included, in particular, collecting data about geometrical dimensions and irregularities of the building and its structural elements.

Along with the use of the drawings (which were available only partly and not for all schools), we conducted additional geometry measurements in the school buildings. For these purposes we used a laser distance meter (HILTI PD 5) as well as conventional measure tapes and folding rulers (Fig. 3.1).

Figure 3.1: Measurements of structural elements of a building with a folding ruler

For investigating details of the structural elements we used the HILTI PS 50 Multidetector, which is designed to detect objects such as ferrous metals (rebars), non-ferrous metals (copper and aluminium), wood beams, plastic pipes and electric cables in dry materials. In the process of the in-situ inspection the device was used for scanning concrete members to detect the location of reinforcement bars and determine the depth of concrete cover. Unfortunately, it was not possible to obtain all details in the course of limited in-situ inspection. Therefore, the lacking information was updated using the simulated design.

4. Schools under investigation

4.1. Humboldt-Gymnasium

The Humboldt-Gymnasium is geographically located in the downtown of Cologne (Altstadt-Süd). The gymnasium was founded in 1873. Currently it has about 1200 school children. Last reconstruction, according to the information obtained from of the school administration, was in the fifties of the past century. Unfortunately, due to one of the recurrent flood disasters in the city the archives related to the construction of the gymnasium buildings were damaged and lost. Only some available paper drawings were provided by the administration. The main building, with the schoolrooms as well as the administration department of the gymnasium, was constructed in 1956. It consists of two structural units, which due to the presence of a separation joint can be considered independently. For the investigation we selected a four-story unit, which is shown in Fig.4.1.

Figure 4.1: Front (a) and back (b) façades of the building

The considered building unit has a complex structural system. The ground floor is presented by a grid of reinforced-concrete (RC) columns (6.6 m x 4.6 m) of a circular cross-section (diameter of 50 cm), which, being coupled with the RC floor (thickness of 32 cm), represent the moment frame system. The floors above are presented by infilled frames, where the bays between the rectangular columns (cross-section of 50 cm x 23 cm) along the main façade are infilled with masonry (thickness of 40 cm). The back façade wall of the upper floors is masonry and rests on the edge of the cantilever span over the ground floor (Fig.4.1, b). All interior walls are also masonry. The building roof is flat and is made (as all the inter-story slabs) of reinforced-concrete.

The measured dimensions of the considered building are as follows: the total length along the main façade 76 m (the building is divided by a separation joint into two parts of 38 m each); the width – 11.0 m; the total height above the ground level – 18 m. The building has a cellar of 3.0 m depth. The foundation system is unknown.

It should be noted that in case of a strong earthquake the presence of the vertical irregularity (the change in stiffness between the ground floor and the upper floors)

can potentially lead to so-called soft-story effects. Therefore, more detailed study is required for this case.

For the ambient vibration measurements we used six sensors: four sensors were installed on the flat roof of the building (two at the ends of the building and two in the middle on both sides of the separation joint); besides one sensor was installed on the ground level close to the separation joint and one more sensor was installed in the cellar close to the end of the building. The scheme of spatial arrangement of the sensors is presented in Fig. 4.2. The direction of all sensors coincided with the axis Y. Their coordinates are given in Table 4.1.

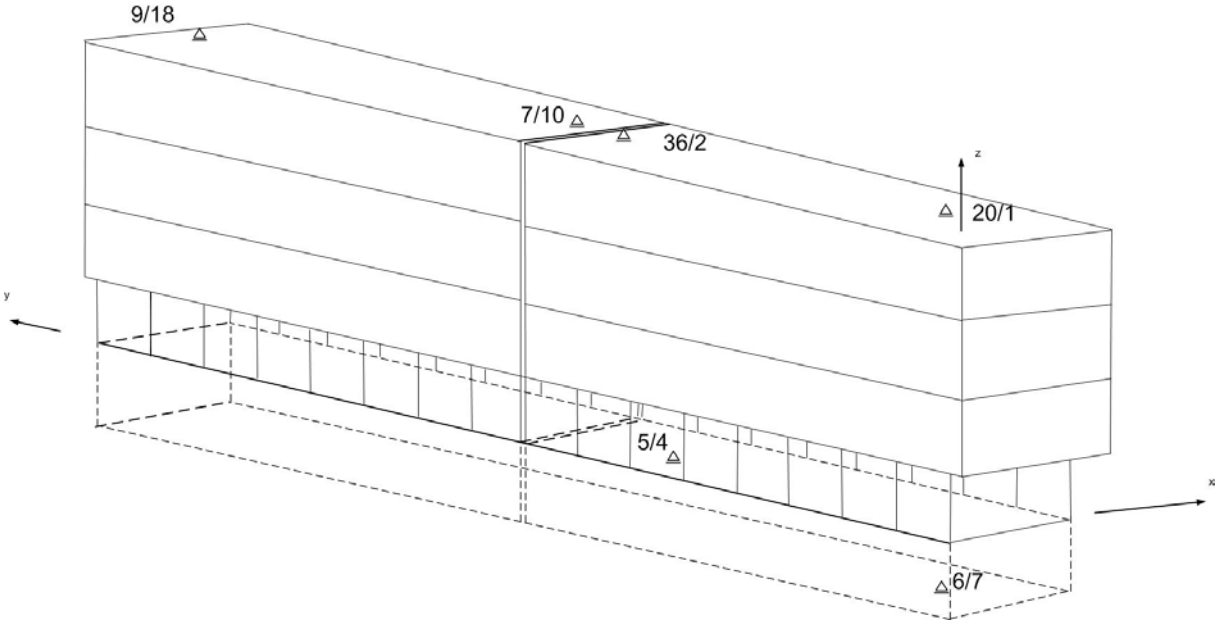

Figure 4.2: Scheme of spatial arrangement of sensors in the building of Humboldt-Gymnasium

Table 4.1: Coordinates of the sensors in the building of Humboldt-Gymnasium

NN	Sensor/Recorder	X (m)	Y (m)	Z (m)
1	6/7	41,0	1,1	-3,0
2	5/4	9,0	-5,5	0,0
3	9/8	-36,5	0,0	16,0
4	7/10	-2,5	0,0	16,0
5	36/2	3,0	0,0	16,0
6	20/1	25	0,0	16,0

4.2. Alfred-Müller-Armack Berufskolleg

The Alfred-Müller-Armack (AMA) Berufskolleg (vocational college) is located on the south of Cologne (in the district Zollstock). The total number of students is about 3000. The AMA College consists of a complex of buildings of different functional use. The section G of the college (selected for the investigation) was constructed in 2007. The design drawings (plans and cross sections) for this building were provided by the municipality of Cologne. The G-building has L-shape and consists of two independent units separated by a joint. Therefore, we considered only one part of the total G-building (Fig.4.3).

Figure 4.3: The building of Alfred-Müller-Armack Berufskolleg (G section)

The four-story building has overall dimensions of 75 m (length along the main façade), 18 m (width) and 18.5 m (height above ground). The lateral load-resisting system in both directions is represented by masonry shear walls. The floors and roof of the building are made of reinforced-concrete plates. The roof shape is pitched. The foundation system is unknown.

For the ambient noise measurements inside the building, four sensors were installed on the top floor in the central corridor close to the staircases (there are three staircases in the building, which are located at both ends and in the middle part). The fifth sensor was located outside on the ground in direct proximity to the building. The scheme of sensors is shown in Fig. 4.4. Their coordinates are presented in Table 4.2.

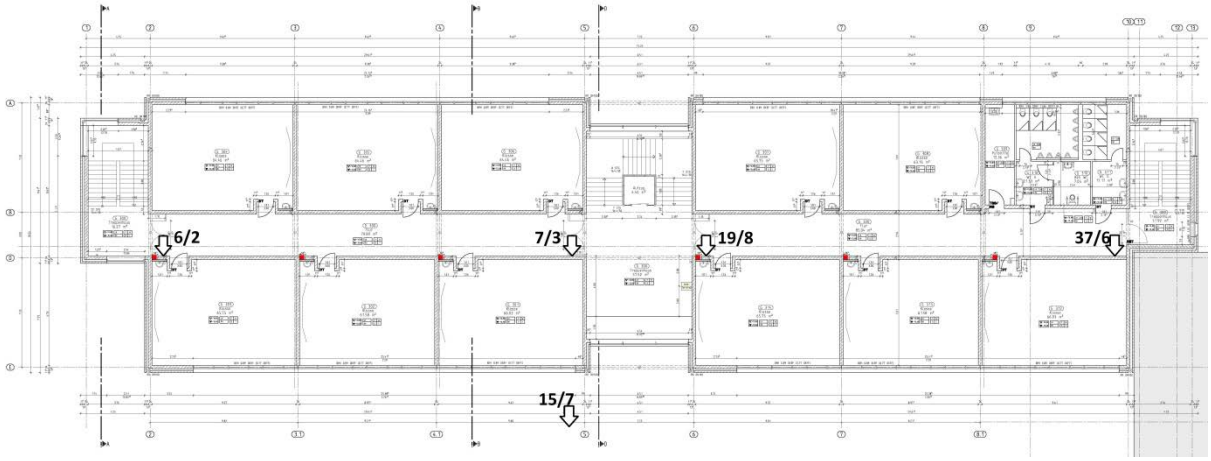

Figure 4.4: Scheme of spatial arrangement of sensors in the building of AMA-Berufskolleg

Table 4.2: Coordinates of the sensors in the building of AMA-Berufskolleg

NN	Sensor/Recorder	X (m)	Y (m)	Z (m)
1	6/2	-32,0	0,0	10,8
2	7/3	-4,0	0,0	10,8
3	19/8	4,0	0,0	10,8
4	37/6	32,0	0,0	10,8
5	15/7	-4,0	-10,0	0,0

4.3. Henry-Ford-Realschule

Figure 4.5: Henry-Ford-Realschule

The Henry-Ford-Realschule (secondary school) is located in the district Chorweiler (northern part of Cologne). With the current number of school children about 850 it is one of the largest secondary schools in the city. Approximated date of construction is 1965.

Some construction drawings for the school were provided by the city municipality. Additional information was collected on site.

The main building of the school (Fig.4.5) has rather complicated structure consisting of three units of different height, which are connected through a system of passages and separation joints. For the measurements we selected the central unit. The unit has an elongated rectangular shape with overall dimensions of 92 x 9 m. It has four floors above ground and a cellar. The height of the building above grade is about 15 m. The lateral load resistance of the one-bay structure is provided by a system of RC columns with masonry infill walls. The floors and roof are represented by reinforced concrete slabs.

The spatial arrangement of sensors installed in the building for vibration measurements is shown in Fig.4.6. Two sensors were installed on the basement level and three sensors – on the third floor. The coordinates of the sensors are shown in Table 4.3.

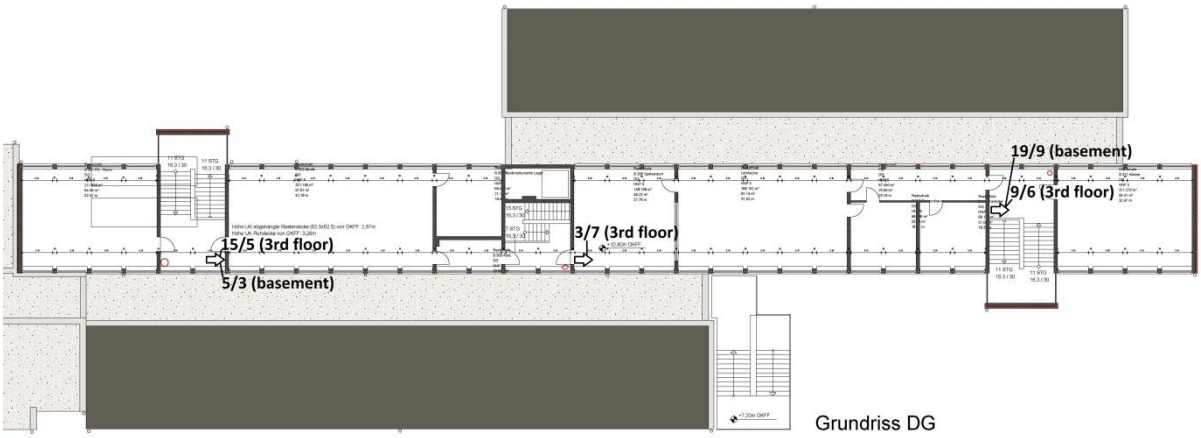

Figure 4.6: Scheme of spatial arrangement of sensors in the building of Henry-Ford-Realschule

Table 4.3: Coordinates of the sensors in the building of Henry-Ford-Realschule

NN	Sensor/Recorder	X (m)	Y (m)	Z (m)
1	5/3	-24,0	0,0	0,0
2	19/9	28,0	6,5	0,0
3	15/5	-24,0	0,0	13,8
4	3/7	0,0	0,0	13,8
5	9/6	28,0	6,5	13,8

4.4. Berufskolleg Ehrenfeld

Figure 4.7: The main building of Berufskolleg Ehrenfeld

The vocational college Ehrenfeld is located in the same-named district of Cologne (in the central part of the city). According to the information obtained from administration of the college the main building (which was selected for the investigation, Fig. 4.7) was constructed approximately in 1960. Only one paper drawing showing the technological plan of the ground floor of the building was available. Therefore, all information required for structural modeling and analyses was collected on site.

The overall dimensions of the buildings are about 61 x 18 m with the total height of about 11 m. There is a cellar of 3.3 m height. The lateral load resistance of the structure is provided by shear walls. The bearing walls are masonry with the thickness of 0.4 m. In the entrance vestibule instead of the shear walls there are two RC columns (of circular cross-section with diameter of 0.3 m), framing the staircase. All the floors (and the roof) are presented by reinforced concrete slabs (thickness of 0.2-0.25 m). The roof is flat.

For the vibration measurements four sensors were installed in the building, two of them on the second floor (at the ends of the building) and two – in the cellar (Fig.4.8). The coordinates of the sensors are presented in Table 4.4.

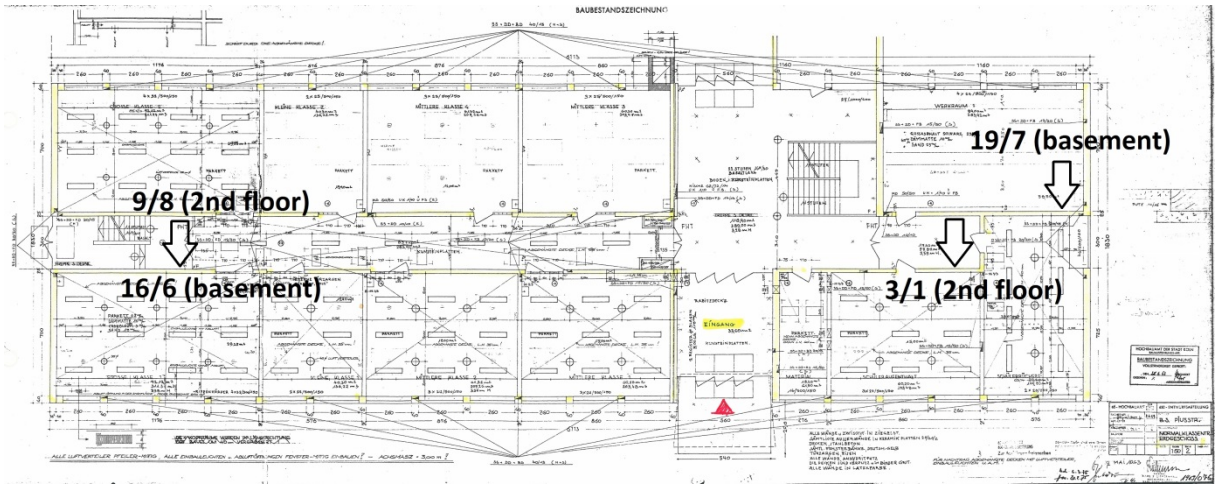

Figure 4.8: Scheme of spatial arrangement of sensors in the building of Berufskolleg Ehrenfeld

Table 4.4: Coordinates of the sensors in the building of Berufskolleg Ehrenfeld

NN	Sensor/Recorder	X (m)	Y (m)	Z (m)
1	16/6	-27,2	0,0	0,0
2	19/7	22,6	0,0	0,0
3	9/8	-27,2	0,0	10,6
4	3/1	17,6	0,0	10,6

4.5. Otto-Lilienthal-Schule

Figure 4.9: The building of Otto-Lilienthal-Schule

Otto-Lilienthal-Schule is a secondary school, which is geographically situated on the south of the city in the district Porz. The school was constructed in 1969. Some drawings of the school were provided by the city municipality in the electronic format.

The main building has three floors (Fig.4.9) with the overall dimensions of about 100 m x 19 m and the total height of 10.6 m above the ground level. Due to its elongated shape the building is divided by separation joints into three structural sections/units working independently. For the investigation we considered two sections, which have similar structural system, while the third section (a later addition to the main structure) has a considerable vertical irregularity (higher ground floor). The presence of such irregularity would require a special investigation, which is beyond the scope of the current study.

The lateral load-resisting system of the building is presented by RC columns and RC slabs. The most of columns are of rectangular cross-section (0.3 x 0.3 m), while in the entrance hall there are circular columns (diameter of 0.35 m). The roof is flat.

For the vibration measurements six sensors were installed in the building, two of them in the basement (close to the separation joint) and four on the roof of the building (two of the sensors were located close to the separation joint and the other two at the ends of the sections). Their spatial arrangement is shown in Fig.4.10, the coordinates – in Table 4.5.

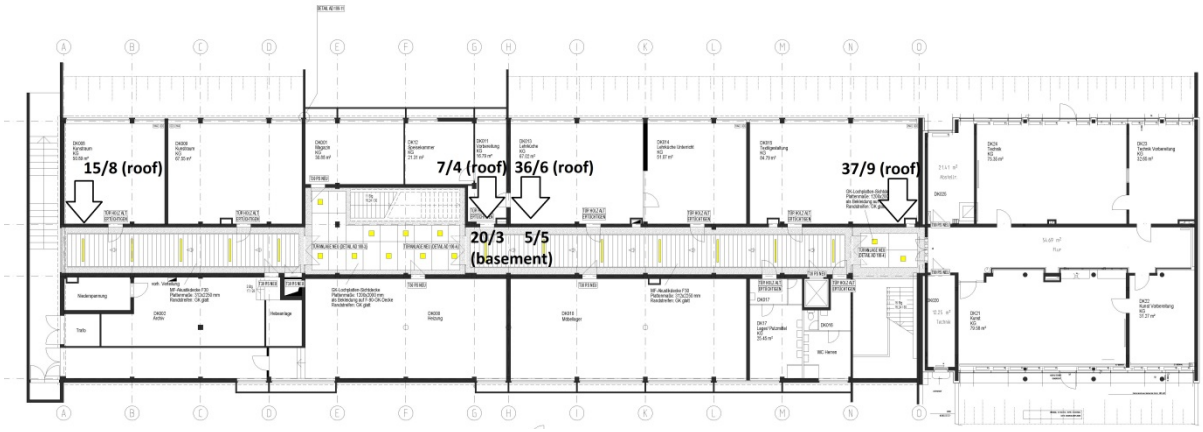

Figure 4.10: Scheme of spatial arrangement of sensors in the building of Otto-Lilienthal-Schule

Table 4.5: Coordinates of the sensors in the building of Otto-Lilienthal-Schule

NN	Sensor/Recorder	X (m)	Y (m)	Z (m)
1	20/3	-0,5	0,0	-3,5
2	5/5	0,5	0,0	-3,5
3	15/8	-28,3	0,0	11,0
4	7/4	-0,5	0,0	11,0
5	36/6	0,5	0,0	11,0
6	37/9	28,3	0,0	11,0

4.6. Gymnasium Thusneldastraße

Figure 4.11: The building of Gymnasium Thusneldastraße (section B)

The gymnasium is located in the central part of Cologne, in the district Deutz on the right side of the Rhine River. At present there are about 850 schoolchildren in the gymnasium. According to the administration of the gymnasium, it was constructed in the sixties of the last century. Some construction drawings were provided in the paper form. Additional information required for vulnerability analysis was collected on site.

The main building of the gymnasium consists of a complex of sections of different height, which are divided by separation joints into structural units. For the investigations we selected the section B, a four story unit shown in Fig. 4.11.

The selected section of the building has overall dimensions of about 60 x 10 m and it has rather complicated structural system. The lateral load resistance is provided by a combined contribution of a system of rectangular RC columns and masonry infill walls integrated with RC inter-story slabs. The total height of the building is about 14 m. The RC roof is flat.

For the vibration measurements three sensors were used, two of them were installed on the third floor, and one – in the cellar. The scheme of the sensor arrangement in the building is given in Fig.4.12 and their coordinates are shown in Table 4.6.

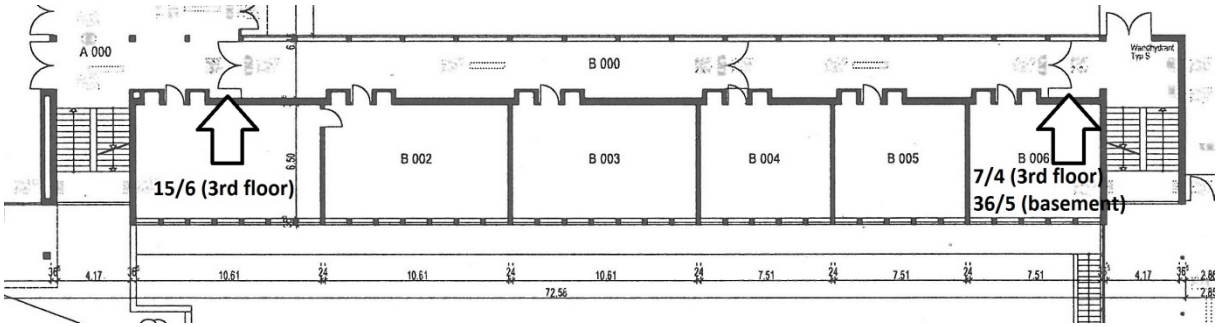

Figure 4.12: Scheme of spatial arrangement of sensors in the building of Gymnasium Thusneldastraße

Table 4.6: Coordinates of the sensors in the building of Gymnasium Thusneldastraße

NN	Sensor/Recorder	X (m)	Y (m)	Z (m)
1	36/5	24,0	0,0	-3,6
2	7/4	24,0	0,0	11,0
3	15/6	-24,0	0,0	11,0

4.7. Gymnasium Kreuzgasse

Figure 4.13: The building of Gymnasium Kreuzgasse

The gymnasium Kreuzgasse is located in the downtown (Altstadt-nord). At the present time there are about 1000 schoolchildren in the gymnasium. The year of construction is unknown. All information necessary for structural modelling and analysis was collected on site, because no construction drawings were available. The main façade of the investigated building is shown in Fig. 4.13.

The overall dimensions of the building are about 56 x 10 m. The total height above grade is about 18 m. The building has a complicated hybrid lateral load resisting system provided by a combination of RC columns and masonry shear walls. There is an obvious irregularity due to change in vertical structure; moreover, due to the gallery-type arrangement of the inner space (similar to the buildings of the Humboldt-Gymnasium and the Gymnasium Thusneldastraße) there is also irregularity in plan. The floors and roof of the building are made of reinforced concrete. The roof is flat.

For the noise vibration measurements six sensors were used, three of them were installed on the flat roof, two – on the 4th floor and one sensor was placed in the cellar. The scheme showing spatial arrangement of the sensors in the gymnasium building can be seen in Fig.4.14. Their coordinates are given in Table 4.7.

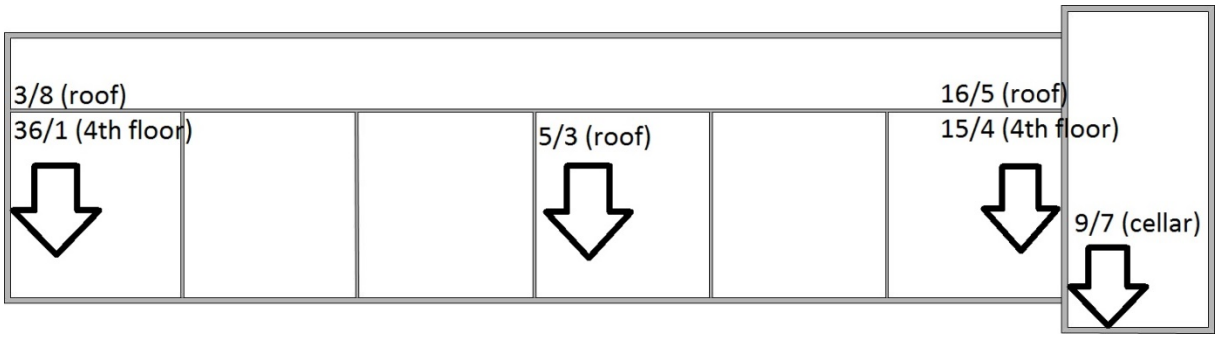

Figure 4.14: Scheme of spatial arrangement of sensors in the building of Gymnasium Kreuzgasse

Table 4.7: Coordinates of the sensors in the building of Gymnasium Kreuzgasse

NN	Sensor/Recorder	X (m)	Y (m)	Z (m)
1	9/7	28,0	-10,0	-6,2
2	15/4	26,0	0,0	13,7
3	36/7	-24,3	0,0	13,7
4	16/5	26,0	0,0	17,8
5	5/3	0,0	0,0	17,8
6	3/8	-24,3	0,0	17,8

5. Classification of the school buildings with the use of the GEM Building Taxonomy

The GEM Building Taxonomy, which is being developed in the frame of the GEM (Global Earthquake Model) project (http://www.globalquakemodel.org), intends to provide a common classification of building characteristics in an ordered system aiming at creating a unique description (code) for a single building or a building typology. For this purpose the current version of the GEM Building Taxonomy V2.0 (Brzev, 2012) uses 13 attributes, which are associated with specific building characteristics that can potentially affect their seismic performance, in particular: material and type of the lateral load-resisting system (in two principal horizontal directions of the building plan); height; date of construction or retrofit; occupancy; structural irregularity; building position within a block, shape of building plan; exterior walls; roof, floor, and foundation. A special Windows-based computer application

TaxT (Taxonomy Tester) is available (http://www.globalquakemodel.org), which enables a user to record information about a building (or a building typology) of interest using the above-listed attributes of the GEM Building Taxonomy. Having collected the information on-site, the user is able to create one-page report, which summarizes the building information, including a brief description and an image of the building, and moreover it generates a taxonomy string for a specific building (or a building typology). The collected information can be incorporated into a database for further vulnerability and risk analyses.

The GEM TaxT tool was used for the description of the investigated school buildings in Cologne. One page reports generated by the tool for the seven investigated schools are presented in Appendix. The summary of obtained results in terms of the GEM Building Taxonomy for all the schools is given in Table 5.1.

Table 5.1: Description of the school buildings in terms of GEM Building Taxonomy

NN	School name	Taxonomy string (code)
1	Humboldt-Gymnasium	DX /CR+CIP /LH /DY /CR+CIP /LH /HEX:4+HBEX:1 /YAPP:1956 /EDU+EDU2 /BP1 /PLFR /IRIR+IRVP:SOS+IRVS:CHV /EWMA/RSH1+RMTO+RC+RC1+RWCP /FC+FC1+FWCP /
2	Alfred-Müller-Armack Berufskolleg	DX /M99 /LWAL /DY /M99 /LWAL /HEX:4+HBEX: /YAPP:2007 /EDU+EDU2 /BP1 /PLFR /IRRE /EWMA /RSHO /FC+FWCP /
3	Henry-Ford-Realschule	DX /CR /LFINF /DY /CR /LFINF /HEX:4+HBEX:1 /YAPP:1965 /EDU+EDU2 /BP2 /PLFR /IRIR+IRVP:POP /EWMA /RSH2+RMTO+RC+RWCP /FC+FWCP /
4	Berufskolleg Ehrenfeld	DX /M99 /LWAL /DY /M99 /LWAL /HEX:3+HBEX:1 /YAPP:1960 /EDU+EDU2 /BPD /PLFR /IRIR+IRPP:TOR /EWMA /RSH1+RC+RWCP /FC+FWCP /
5	Otto-Lilienthal-Schule	DX /CR /LFINF /DY /CR /LFINF /HEX:3+HBEX:1 /YAPP:1969 /EDU+EDU2 /BP1 /PLFR /IRIR+IRVP:IRVO+IRVS:POP /EWMA /RSH1+RC+RWCP /FC+FWCP /FOSDL
6	Gymnasium Thusneldastraße	DX+PF /CR /LFINF /DY+OF /CR /LH /HEX:4+HBEX:1 /YAPP:1967 /EDU+EDU2 /BP1 /PLFR /IRIR+IRPP:IRHO+IRVP:POP /EWMA /RSH1+RC+RWCP /FC+FWCP /
7	Gymnasium Kreuzgasse	DX+PF /CR /LH /DY+OF /CR /LH /HEX:5+HBAPP:1 / /EDU+EDU2 /BP1 /PLFR /IRIR+IRPP:IRHO+IRVP:CHV /EWMA /RSH1+RMTO+RC+RWCP /FC+FWCP /

6. Vulnerability assessment based on the European Macroseismic Scale (EMS-98)

As a first approximation corresponding to the very limited knowledge level KL0 (see more details in DC1), we can estimate the seismic vulnerability of the school buildings on the base of the European Macroseismic Scale (EMS-98) (Grünthal, 1998). With the help of vulnerability table of EMS-98 (Fig. 6.1) and using the information collected during in-situ surveys, we can identify an appropriate vulnerability class (from A, the most vulnerable, to F, the less vulnerable in the range) for the investigated buildings.

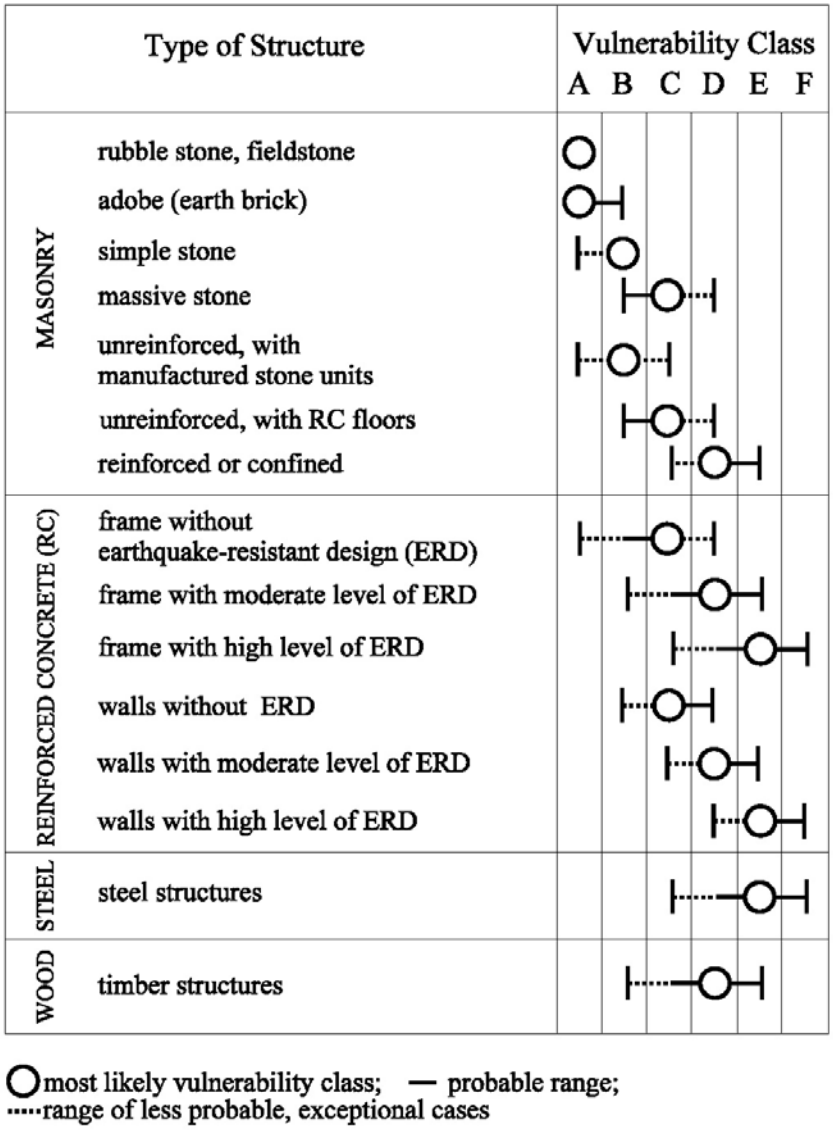

Figure 6.1: Vulnerability classification of the European Macroseismic Scale

The procedure of EMS-based vulnerability analysis starts with assigning an initial vulnerability class (shown by a circle in the table) in dependence on the material of bearing structures and the structural type of the building under consideration. After that, using the available/collected information about the building, one should analyze the presence of factors (strengths or weaknesses) that may affect its seismic

vulnerability, among which are, in particular, the quality of material, design and workmanship; regularity/irregularity of the structural system (both in physical and geometrical sense); state of preservation; possible interferences (re-planning or retrofitting) in the course of exploitation of the building, etc.

Taking into account all those factors the initial estimation can be refined (within the range shown by solid and dotted lines in the vulnerability table) and the appropriate vulnerability class should be assigned for the building. It is worth mentioning that vulnerability relationships (in the form of damage probability matrices, fragility curves, and vulnerability functions) are available for different vulnerability classes of EMS-98 (e.g. Lagomarsino & Giovinazzi, 2006, Tyagunov et al, 2006).

A set of six vulnerability functions (in terms of the mean damage ratio vs the level of seismic intensity) for the vulnerability classes of EMS-98 is shown in Fig. 6.2.

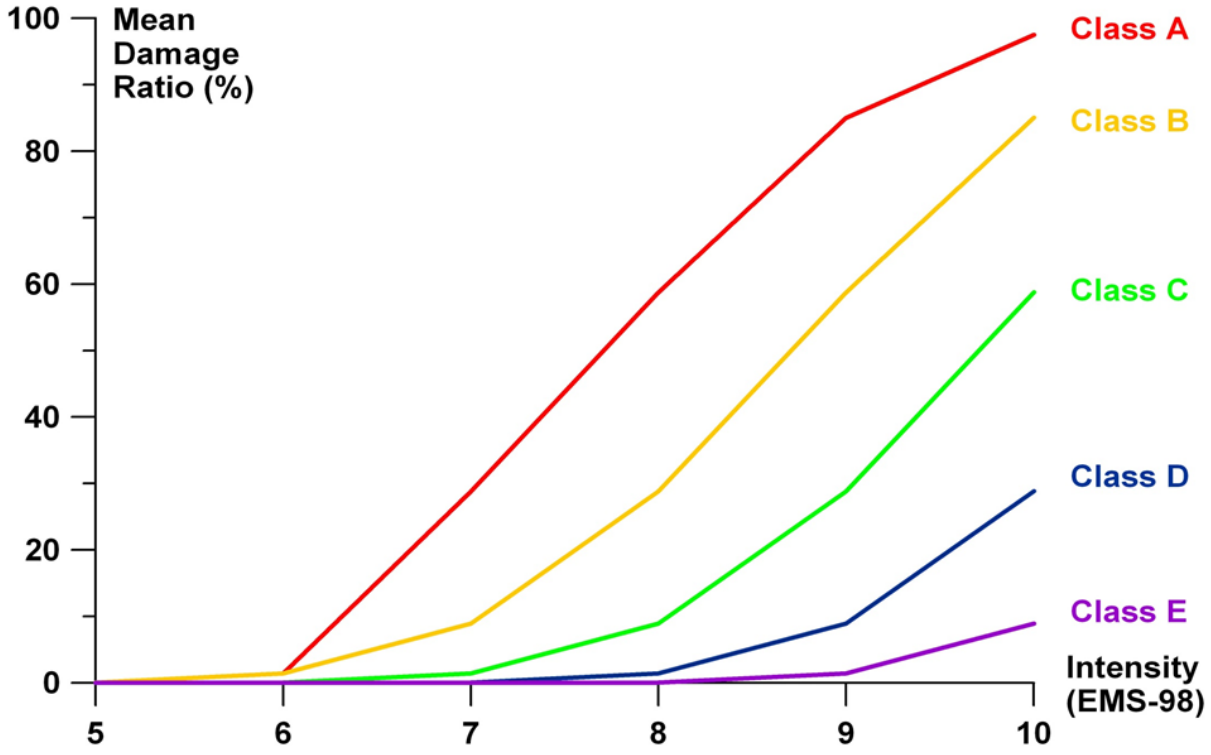

Figure 6.2: Vulnerability functions for different vulnerability classes of EMS-98

Using the procedure described above as well as the collected in-situ data we can estimate the seismic vulnerability for the school buildings in terms of the classification of EMS-98. Taking into consideration the available information, we conclude that the vulnerability class C can be assigned as the most probable for all the investigated buildings.

As indicated in Section 1 of the case study, the seismic hazard for the area of Cologne is estimated at the level of EMS intensity VI-VII for a non-exceedance probability of 90% in 50 years corresponding to the mean return period of 475 year (Grünthal, 2006).

In accordance with the definitions of intensity degrees (EMS-98) for the vulnerability class C in case of the level of ground shaking of intensity VI-VII the most probable damage grade is 1 or 2. The damage grades for reinforced concrete buildings are described in Table 6.1.

Table 6.1: Classification of damage to reinforced concrete buildings (EMS-98)

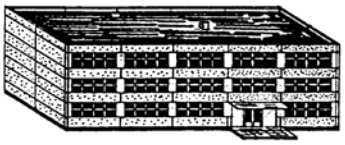	**Grade 1: Negligible to slight damage (no structural damage, slight non-structural damage)** Fine cracks in plaster over frame members or in walls at the base. Fine cracks in partitions and infills.
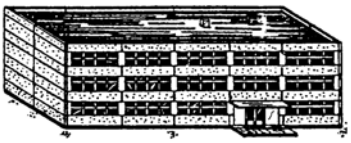	**Grade 2: Moderate damage (slight structural damage, moderate non-structural damage)** Cracks in columns and beams of frames and in structural walls. Cracks in partition and infill walls; fall of brittle cladding and plaster. Falling mortar from the joints of wall panels.
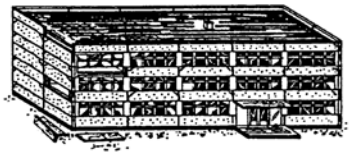	**Grade 3: Substantial to heavy damage (moderate structural damage, heavy non-structural damage)** Cracks in columns and beam column joints of frames at the base and at joints of coupled walls. Spalling of concrete cover, buckling of reinforced rods. Large cracks in partition and infill walls, failure of individual infill panels.
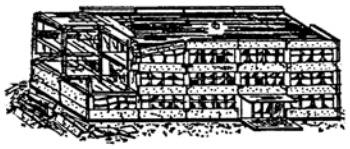	**Grade 4: Very heavy damage (heavy structural damage, very heavy non-structural damage)** Large cracks in structural elements with compression failure of concrete and fracture of rebars; bond failure of beam reinforced bars; tilting of columns. Collapse of a few columns or of a single upper floor.
	**Grade 5: Destruction (very heavy structural damage)** Collapse of ground floor or parts (e. g. wings) of buildings.

Therefore, considering the estimated seismic hazard level for Cologne in combination with the presented vulnerability functions (Fig. 6.2), one can conclude that the level of damage risk for the investigated school buildings is acceptable, while the structural damage for the buildings will most probably not exceed grade 2 (or the Limit State of Damage Limitation in terms of Eurocode 8) and the mean damage ratio (cost of repair over the construction cost) for the considered level of seismic hazard will not exceed 1%.

L’Aquila

1. In-situ data collection and operational modal analysis

The town of L'Aquila is situated in Central Italy, region Abruzzo, which has long known seismic history. The area was repeatedly struck by strong earthquakes, including the earthquake of April 6, 2009, which killed about three hundred people and caused extensive and severe damage to the building stock of the local community.

The building under study (which belongs to the commercial school - Instituto Tecnico Commerciale Luigi Rendina, Fig.1.1) was also damaged during the earthquake of 2009. Since that time the damaged building is closed by the local civil protection authorities.

(a)

(b)

Figure 1.1: Building of Instituto Tecnico Commerciale Luigi Rendina in L'Aquila (view from Google Maps (a) and the entrance board (b)

The SIBYL team had no preliminary information about the building, no construction drawings were available. Therefore, this was a typical situation when information necessary for structural modelling and assessment of the building was collected immediately on site within limited time frames (about two hours).

The year of construction is unknown; allegedly the building was constructed in the period of 1960s. The building of the school has a complicated configuration in plan (Fig.1.1, a), though due to the presence of separation joints it can be considered consisting of several units. In our study we considered only the central unit. On both ends of the central unit there are attached units of different height (which, probably, may cause effects of collision and pounding under strong ground motions).

The considered unit of the building has a cellar, 5 floors and duo-pitched roof. Overall dimensions in plan are 45.60 x 12.60 m; the total height of the building is 21.0 m.

The structural system of the building is represented by cast-in-place reinforced concrete frames of columns and beams, which can be seen at the level of the roof space (Fig.1.2).

Figure 1.2: Reinforced concrete frames of the building

The in-situ visual survey showed that the bearing reinforced concrete frames sustain the ground motions during the earthquake of 2009 quite well and seem to be in a good condition (only fine cracks were found in some of the reinforced concrete elements) and can serve their function; while, the infill walls, which are made of fragile hollow bricks, were severely damaged or even destroyed (Fig. 1.3) resulting from the earthquake of 2009.

Figure 1.3: Damage to the infill walls

The most of partition walls are very thin (as they are made of one layer of the hollow bricks). Some of internal walls (as well as the external walls) are made of two layers of the bricks with air space between them. These structures are very brittle, and their contribution to the stiffness and bearing capacity of the structural system in the current state can be neglected. Many external infill walls exhibit severe damage and are in fact separated from the reinforced concrete frame. Only a few infill walls were identified to contribute to the bearing system, as shown in Fig. 1.5.

It worth mentioning that at the level of the second story one can observe particularly more severe damage in comparison with the other stories. These effects (e.g., damage to the interiors or more extensive and deeper cracks in the walls, which can be seen both from outside and inside the building) can be explained, in our opinion, by collision of attached building units of smaller height during the seismic ground motions. These can be seen on both facades of the building as presented in Fig.1.4.

For the geometry measurements (including both overall dimensions of the building and member sizes) we used conventional measure tapes, folding rulers and a laser distance meter. The dimensions of the structural elements measured in the course of the in-situ survey and inspection are as follows: the columns have rectangular cross-section with sizes of 0.4 x 0.4 m; the bay-width in X-direction (along the building) 3.80 m, in Y-direction (across the building) 6.30 m. The measured height of one story is 3.30 m; slab thickness 0.30 m (Fig. 1.5,a).

For the sake of simplification of the structural model and the computational approach we simplify the geometry of the building, in particular, neglecting the presence of re-entrant corners in plan (Fig.1.5). Doing so, we neglect consideration of possible local damaging effects; however, this simplification allows simple and fast evaluation of

seismic performance of the building as a whole with the use of the developed SISM-tool.

(a)

(b)

Figure 1.4: Northern (a) and southern (b) facades of the damaged school building

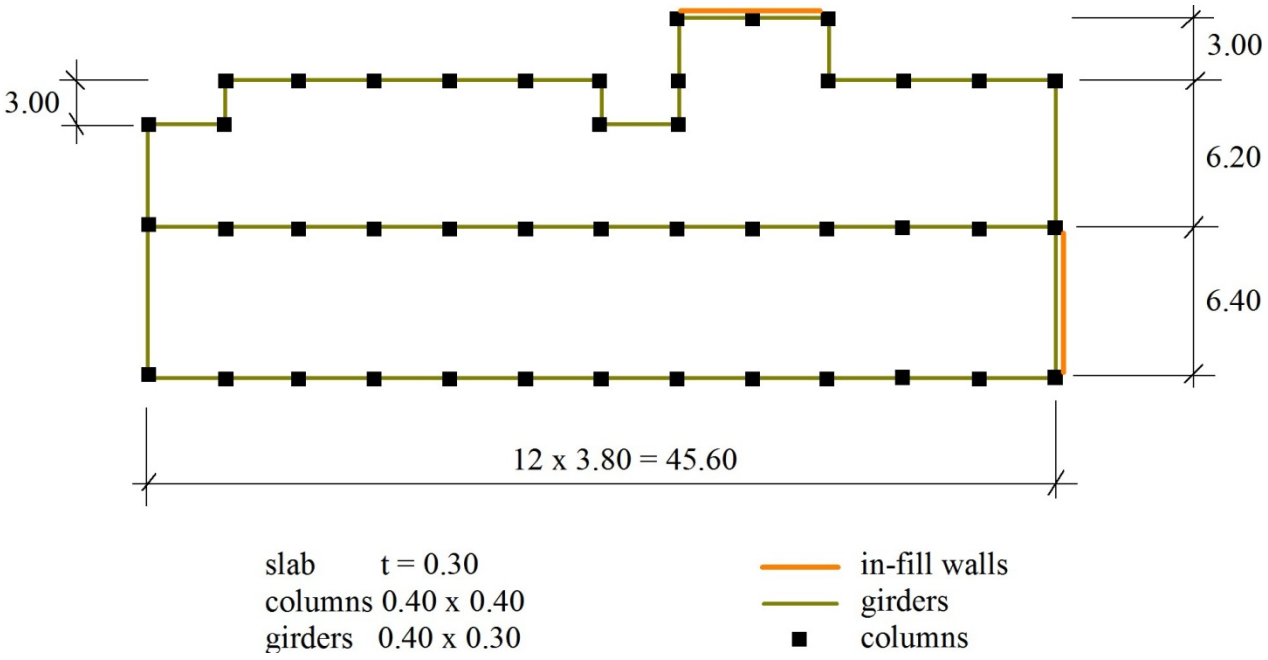

a) observed ground plan

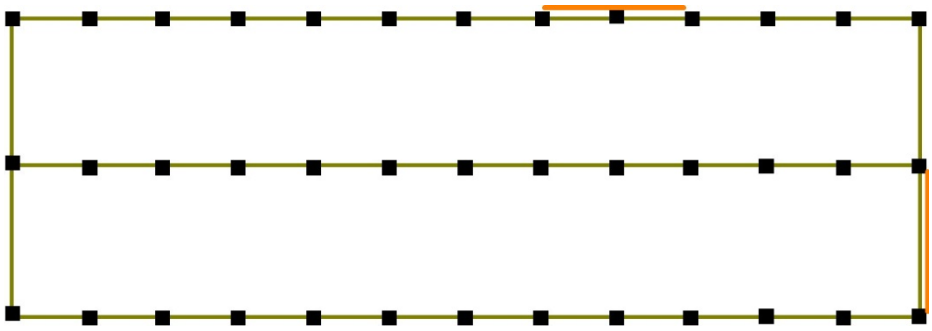

b) simplified ground plan

Figure 1.5. Main dimensions and structural elements of the school building in L'Aquila, as surveyed on site

For investigating details of the structural elements we used the HILTI PS 50 Multidetector for scanning the concrete members to detect the location of reinforcement bars and determine the depth of concrete cover. The investigations showed the presence of reinforcement in the structural members; however it was not possible to obtain all the details necessary for the structural modelling. Therefore, for lacking information we used simulated design as recommended by Eurocode 8 for the knowledge level KL1.

In parallel with the structural survey and inspection, the ambient measurements were conducted in the building. The vibration measurements were performed using CUBE digitizers connected to 4.5 Hz geophones, as shown in Fig.1.6.

Figure 1.6: Geophone and data logger

In total, ten sensors were installed in the building: three sensors at the levels of the second, third and fourth stories (two at the ends of the building and one in the middle part for each floor) and one sensor at the ground level. The total duration of the vibration measurements was 50 minutes.

The recorded ambient vibrations were processed by GFZ partners and provided in miniSEED format. Further processing and modal analysis were performed with the help of MACEC 3.3 software (Reynders et al. 2014) using stochastic subspace identification approach (Reynders, 2012).

The obtained results of the operational modal analysis in the form of stabilization diagram are presented in Fig. 1.7, where one can clearly see the stable modes at the frequencies of 1.65 Hz and 1.81 Hz, corresponding to two first bending modes, which are considered for further analyses. The first mode (f=1.65 Hz) corresponds to the bending vibration across the building, the second (f=1.81 Hz) – to the bending vibration along the building.

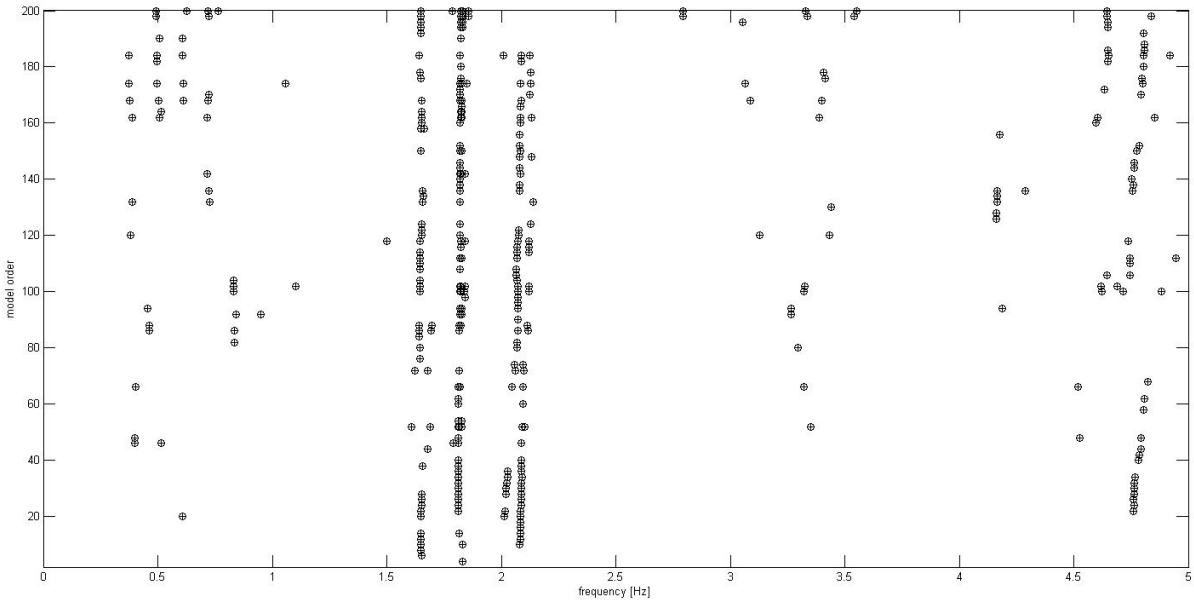

Figure 1.7: Stabilization diagram from MACEC.

2. Seismic evaluation of the school building

Further analysis and seismic evaluation of the building in the current, i.e. partly damaged state is implemented on the base of collected in-situ information (corresponding to the knowledge level KL1) with the use of the SISM-tool.

The material properties for reinforced concrete and masonry in the school building have been taken as typical values for civil structures in earthquake areas:

Reinforced concrete:

- compressive strength of concrete $f_c = 30\ MPa$;
- tensile strength of concrete $f_{ct} = 2.2\ MPa$
- E-modulus of concrete $E = 31900\ MPa$;
- E-modulus of rebars $E = 200000\ MPa$;
- Strength of rebars $f_y = 500\ MPa$
- Reinforcement ratio $\rho = 1.5\ \%.$

Masonry: E-modulus $E = 4000\ MPa$.

There are 13 columns in x-direction and 3 ones in y-direction with 39 columns in total in every story. Two in-fill walls are taken into account according to Fig. 1.5. The corresponding information is directly visible in the Excel sheet “Building” (Fig.2.1):

Number of Elements

Story	Number of columns	Number of shafts	Number of walls
1	39	0	2
2	39	0	2
3	39	0	2
4	39	0	2
5	39	0	2

Figure 2.1: Vertical structural components

The density of slabs is artificially increased from $2500\ kg/m^3$ to $4000\ kg/m^3$ $(40\ kN/m^3)$, i.e. by 60%, in order to account for the mass of all walls, windows and non-structural elements in each story. The mass of the 5th story is additionally increased by 12.5 % to $45\ kN/m^3$ due to the weight of the roof (Fig.2.2).

Masses and Weights

Story	Story Mass [kN/m]	Slab density [kN/m³]	Story Height [m]	Slab Thickness [m]	Weight [kN]
1	197.4	40	3.26	0.3	7479.024
2	197.4	40	3.26	0.3	7479.024
3	197.4	40	3.26	0.3	7479.024
4	197.4	40	3.26	0.3	7479.024
5	197.4	45	3.26	0.3	8048.712

Figure 2.2: Masses and weights of each story

The obtained eigenfrequencies for bending vibration modes in x- and y-direction match the measured ones very well, as can be seen in the right-hand part of the Excel screenshot in Fig. 2.3. Thus, the linear model of the building is considered as finalized. It is worth noting once more that it is a linear model for the current state of the building with damage that is mainly related to the infill walls. The majority of them are thus neglected in the model due to observed damage.

Building

Number of Stories	5	Length X [m]	45.6	E-Modulus [MN/m²]	31900	Poisson's ratio	0.2	E-Modulus, Walls [MN/m²]	Meas./Calc. Frequency, X [Hz]	1.81	1.90
Total Height	17.9	Length Y [m]	12.6	Siffness Ratio	2	Number of Column Types	1	4000	Meas./Calc. Frequency, Y [Hz]	1.65	1.67

Figure 2.3: Comparison of the measured and calculated eigenfrequencies

The seismic damage assessment starts with the calculation of the earthquake loading. In the particular case of L'Aquila, we can get not only the design seismic load (see Section 3 of the case study) but the actual load observed during the L'Aquila earthquake of 2009. Due to the records available for that earthquake and special investigations of Italian experts (Petti & Marino, 2009), we can use the response spectra marked in Fig. 2.5 by S_{ax} and S_{ay}. The other elastic spectra in Fig. 2.5 correspond to civil structures according to the Italian Code NTC2008.

Taking into account the measured and calculated eigenfrequencies of the school building and their corresponding vibration periods (as given in Fig. 2.4), we can estimate the spectral acceleration on site during the earthquake of 2009 and for the future potential earthquake. Currently, the bending eigenfrequencies are 1.81 Hz and 1,65 Hz. We can assume that those of the undamaged building in 2009 should be higher, for example between 2 Hz and 3 Hz.

In the SISM-tool we consider the actual state of the building as a "new" structure with the tuned linear model described above. Further, we can calculate the characteristic

stiffnesses of that structure and its corresponding eigenfrequencies for the three characteristic limit states (see Deliverable DC1 for explanations).

Calculated Frequencies [Hz]			Periods [s]	
Limit State	X	Y	X	Y
1	1.90	1.67	0.53	0.60
2	1.56	1.40	0.64	0.71
3	0.99	0.87	1.01	1.15

Fig. 2.4: Vibration frequencies and periods of the school building for three characteristic limit states (LS1: linear response until cracks; LS2: yielding; LS3: near collapse)

Since the vibration periods in x- and y-direction are close to each other (Fig. 2.4), we consider the same acceleration for both directions for the sake of simplicity. The corresponding spectral accelerations can be directly read from the diagram in Fig. 2.5 due to (Petti & Marino, 2009) as follows:

- Limit state 1: $T = 0.55\ s;\ S_a = 0.45g = 4.41\ m/s^2$ (red vertical arrow);
- Limit state 2: $T = 0.65\ s;\ S_a = 0.5g = 4.9\ m/s^2$ (blue vertical arrow);
- Limit state 3: $T = 1.0\ s;\ S_a = 0.35g = 3.43\ m/s^2$ (grey vertical arrow).

These values are used to calculate the total shear forces for each limit state, as given in Fig.2.6.

The results of the limit state assessment in Fig. 2.7 show that the school building in the current state would not be able to withstand a new earthquake with the same intensity as it was in 2009 (see red-marked cells for LS3 in the Excel sheet).

Without any information on the virgin state of the building before the earthquake of 2009, we cannot make any reliable statements on its seismic safety at that time. We can only state that the original building survived the L'Aquila earthquake 2009 with spectral acceleration of at least $0.5g$. At that, we observe severe damage to the infill walls and minor damage to the reinforced concrete frame, but no collapse.

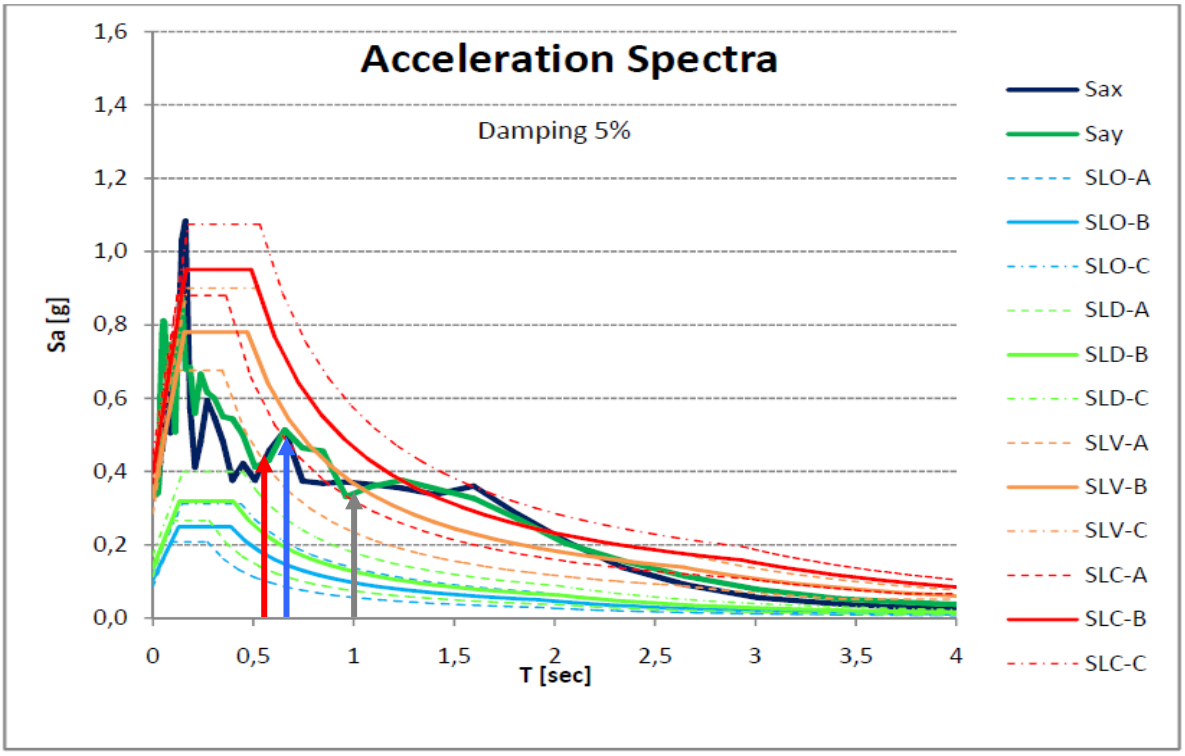

Figure 2.5: Response spectra for L'Aquila according to Petti & Marino (2009) with marked spectral accelerations for the school building (LS1: red arrow; LS2: blue arrow; LS3: grey arrow)

Base Shear Force

Lambda LS1 x	1	Spectral acceleration LS1 x	4.41	Shear Force F_{tot} LS1 x [MN]	167.425
Lambda LS1 y	1	Spectral acceleration LS1 y	4.41	Shear Force F_{tot} LS1 y [MN]	167.425
Lambda LS2 x	1	Spectral acceleration LS2 x	4.9	Shear Force F_{tot} LS2 x [MN]	186.028
Lambda LS2 y	1	Spectral acceleration LS2 y	4.9	Shear Force F_{tot} LS2 y [MN]	186.028
Lambda LS3 x	1	Spectral acceleration LS3 x	3.43	Shear Force F_{tot} LS3 x [MN]	130.219
Lambda LS3 y	1	Spectral acceleration LS3 y	3.43	Shear Force F_{tot} LS3 y [MN]	130.219
Weight [MN]	37.964808				

Figure 2.6: Spectral accelerations and total shear forces for the school building according to the L'Aquila earthquake 2009

Limit state assessment

X-direction

Story	EQ Force LS1 [MN]	EQ Force LS2 [MN]	EQ Force LS3 [MN]	LS1 Force [MN]	LS2 Force [MN]	LS3 Force [MN]
1	167.425	186.028	130.219	3.676	20.760	51.013
2	154.167	172.285	120.525	3.144	19.055	53.719
3	128.717	145.145	101.367	2.612	17.326	57.096
4	93.118	106.066	73.871	2.080	15.570	61.208
5	50.241	57.723	40.077	1.549	13.779	66.100

Y-direction

Story	EQ Force LS1 [MN]	EQ Force LS2 [MN]	EQ Force LS3 [MN]	LS1 Force [MN]	LS2 Force [MN]	LS3 Force [MN]
1	167.425	186.028	130.219	3.557	19.581	41.516
2	154.167	172.182	120.665	3.043	17.799	43.002
3	128.717	144.938	101.665	2.528	15.999	44.977
4	93.118	105.831	74.228	2.013	14.179	47.489
5	50.241	57.564	40.331	1.499	12.334	50.572

Fig.2.7: Limit state assessment of the school building under earthquake load according to records of 2009.

The damaged school stays closed since 2009 due to its unsafe condition. Local civil protection authorities tend to demolish the building and to build a new one. It is not possible to evaluate the seismic safety of the building without the information about the original (undamaged) state of the building and without detailed information about the current state of the structural elements survived the strong earthquake. We have to make additional assumptions about the material properties of the structures to estimate the current seismic safety of the building using the SISM approach.

First of all, we need the site-specific seismic hazard estimation, which is given by the AMRA contribution in Section 3 of this case study. We recall here Fig. 3.4 and take the spectral acceleration of the earthquake with return period of 200 years according to three limit states (three different principal frequencies).

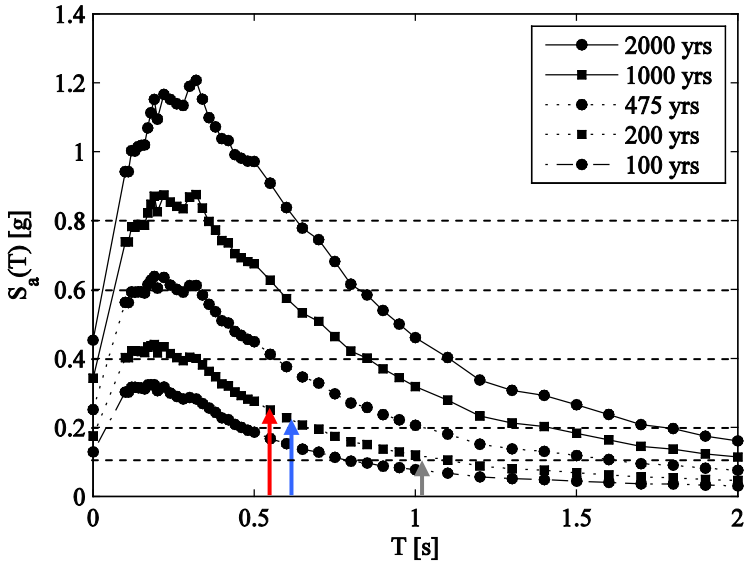

Figure 2.8: Uniform hazard spectra for L'Aquila for different return periods with marked spectral accelerations for the school building (LS1: red arrow; LS2: blue arrow; LS3: grey arrow)

We get the following accelerations:

- Limit state 1: $T = 0.55\ s;\ S_a = 0.25g = 2.45\ m/s^2$ (red vertical arrow);
- Limit state 2: $T = 0.65\ s;\ S_a = 0.22g = 2.16\ m/s^2$ (blue vertical arrow);
- Limit state 3: $T = 1.0\ s;\ S_a = 0.1g = 0.98\ m/s^2$ (grey vertical arrow).

That leads to the base shear forces given in Fig. 2.9.

Base Shear Force

Lambda LS1 x	1	Spectral acceleration LS1 x	2.45	Shear Force F_{tot} LS1 x [MN]	93.014
Lambda LS1 y	1	Spectral acceleration LS1 y	2.16	Shear Force F_{tot} LS1 y [MN]	82.004
Lambda LS2 x	1	Spectral acceleration LS2 x	2.16	Shear Force F_{tot} LS2 x [MN]	82.004
Lambda LS2 y	1	Spectral acceleration LS2 y	2	Shear Force F_{tot} LS2 y [MN]	75.930
Lambda LS3 x	1	Spectral acceleration LS3 x	0.98	Shear Force F_{tot} LS3 x [MN]	37.206
Lambda LS3 y	1	Spectral acceleration LS3 y	0.98	Shear Force F_{tot} LS3 y [MN]	37.206
Weight [MN]	37.964808				

Fig.2.9: Spectral accelerations and total shear forces under earthquake with return period of 200 years

The corresponding limit state assessment in Fig. 2.10 shows that the building would experience severe damage (LS1 and LS2 would be reached in all stories). At the same time, the limit state LS3 (near collapse) would be almost reached in y-direction in the first story.

Limit state assessment

X-direction

Story	EQ Force LS1 [MN]	EQ Force LS2 [MN]	EQ Force LS3 [MN]	LS1 Force [MN]	LS2 Force [MN]	LS3 Force [MN]
1	93.014	82.004	37.206	3.676	20.760	51.013
2	85.649	75.946	34.436	3.144	19.055	53.719
3	71.509	63.982	28.962	2.612	17.326	57.096
4	51.732	46.755	21.106	2.080	15.570	61.208
5	27.911	25.445	11.450	1.549	13.779	66.100

Y-direction

Story	EQ Force LS1 [MN]	EQ Force LS2 [MN]	EQ Force LS3 [MN]	LS1 Force [MN]	LS2 Force [MN]	LS3 Force [MN]
1	82.004	75.930	37.206	3.557	19.581	41.516
2	75.511	70.279	34.476	3.043	17.799	43.002
3	63.045	59.159	29.047	2.528	15.999	44.977
4	45.609	43.196	21.208	2.013	14.179	47.489
5	24.608	23.496	11.523	1.499	12.334	50.572

Fig.2.10: Limit state assessment of the school building under earthquake with return period of 200 years

Conclusions:

The building under study was damaged during the L'Aquila earthquake of 2009. The in-situ visual survey and limited inspection showed that the reinforced concrete frame sustained the earthquake quite well, while the infill walls were severely damaged or even destroyed.

Without any information on the virgin state of the building before the earthquake of 2009, it is impossible to make any reliable estimates of its seismic safety at that time. We can only state that the original building survived the L'Aquila earthquake with spectral acceleration of at least $0.5g$. The earthquake loads could be, probably, even higher than the estimated loads, if we take into account the fact that the original (undamaged) building would have higher stiffness and, therefore, the eigenfrequencies than it exhibits in a partly damaged state in 2016.

It is not possible to evaluate the seismic safety of the building without detailed information about the current state of the structural elements survived the strong earthquake. We had to make additional assumptions about the material properties of the structures to estimate the safety of the building using the SISM approach. It has been shown that the school building in the current state will not withstand a new earthquake with the same intensity as 2009. It is able to sustain relatively weaker ground motions (corresponding to an earthquake with a return period of 200 years) without collapse; however, its current seismic safety is evidently insufficient for a school building.

3. Seismic hazard assessment for L'Aquila

This section provides results of the probabilistic seismic hazard analysis (PSHA) (i.e., Cornell, 1968; McGuire, 2004) for the "Instituto Tecnico Commerciale Luigi Rendina" site, L'Aquila (long. 13.415, lat. 42.356). Analyses are performed by REgionAl, Site-SpEcific and Scenario-based Seismic hazard analysis (REASSESS) software (Iervolino et al., 2016), relative to rock soil conditions (soil category A, according to NTC08 (2008) and EC8 (CEN, 2004).

According to Stucchi et al. (2011), which forms the basis of the current official seismic hazard map of Italy, the source model (called ZS9; Meletti et al., 2008) for the country is made of 36 seismic zones; Figure 3.1.

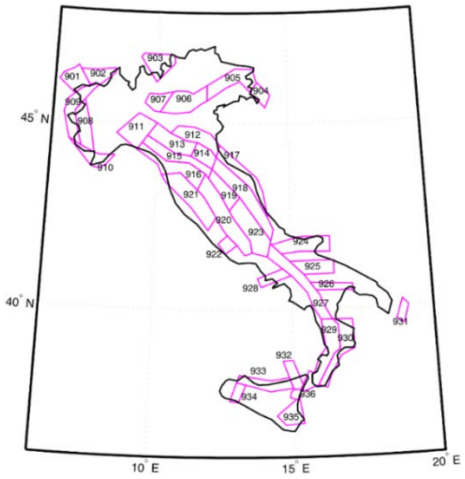

Figure 3.1: Italian seismic sources zones

The site of interest and the surrounding seismic sources are plotted in Figure 3.2.

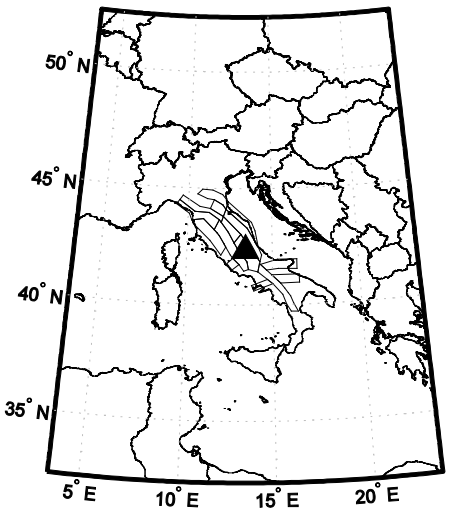

Figure 3.2: L'Aquila site and seismic sources.

The Italian seismic hazard model accounts for some epistemic uncertainties (e.g., different estimated rates and maximum magnitudes and multiple ground motions prediction equations, GMPEs) by adopting a logic tree approach. Figure 3.3 shows its structure. Input parameters adopted for hazard computation are those for the branch 921 (i.e., historical completeness, A-R rates, and Ambraseys et al., 1996) which is, according to Stucchi et al., 2011, the one better at approximating the median result of the whole logic tree.

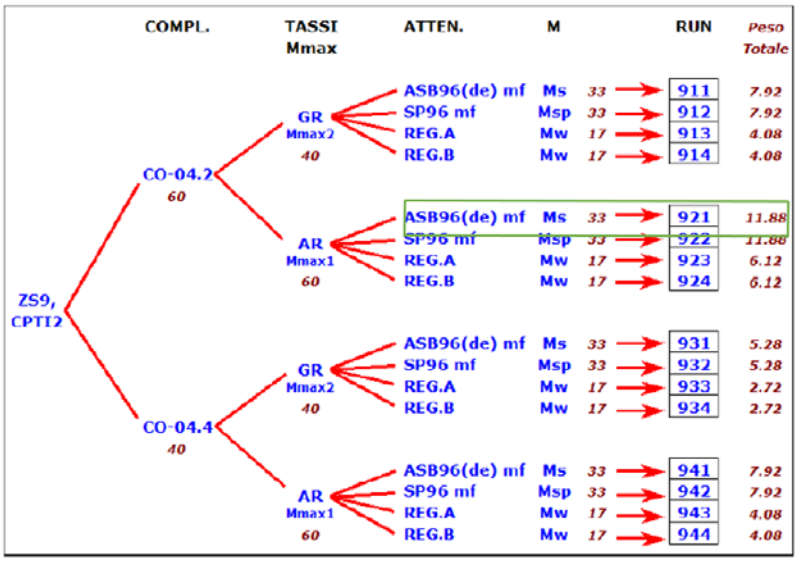

Figure 3.3: ZS9 logic tree (adapted from Gruppo di Lavoro; 2004). Note the branch 921 which was the one used for the hazard calculations.

Fig 3.4 presents plots of the uniform hazard spectra for different return periods (specifically for 100, 200, 475, 1000 and 2000 years).

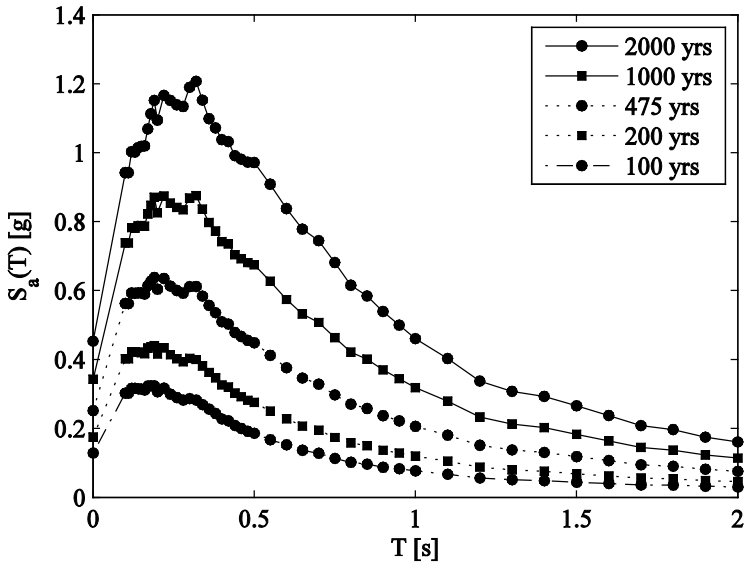

Figure 3.4: Uniform hazard spectra for different return periods.

Fig.3.5 shows the elastic design spectra according to the Italian Building Code (NTC 08, 2008) for soil classes A and B. These spectra were performed by REXEL (Iervolino et al, 2009) for a return period of 712 years, which is in accordance with the indications of NTC 08 for school buildings.

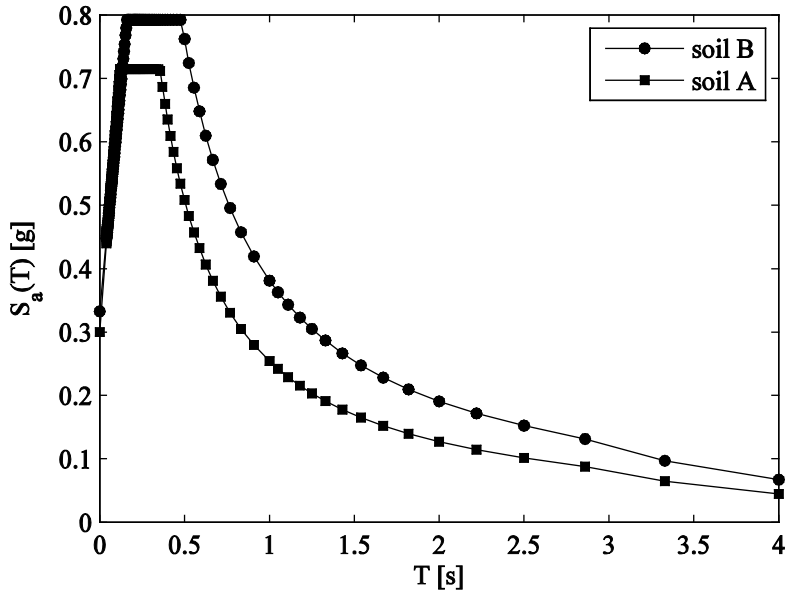

Figure 3.5: Italian building code spectra, Tr 712.

References

Akkar S, Bommer JJ (2010) Empirical equations for the prediction of PGA, PGV and spectral accelerations in Europe, the Mediterranean and the Middle East. Seismol Res Lett 81:195–206

Akkar S, Sandıkkaya MA, Bommer JJ (2014) Empirical ground-motion models for point- and extended source crustal earthquake scenarios in Europe and the Middle East. Bull EarthqEng 12:359–387. doi:10. 1007/s10518-013-9461-4.

Allemang R.J., Brown D.L. (1982), “A correlation coefficient for modal vector analysis”, In Proceedings of the 1st international modal analysis conference, vol. 1, pp. 110-116, SEM, Orlando.

Ambraseys, N. N., K. A. Simpson, and J. J. Bommer (1996). Prediction of horizontal response spectra in Europe, Earthquake Engineering and Structural Dynamics 25, 371–400.

Bommer J.J., Acevedo A. B. (2004). The use of real accelerograms as input to dynamic analysis, ; 8(1):43-91. DOI: 10.1080/13632460409350521

Brzev, S., Scawthorn. C., Charleson, A.W., Jaiswal, K. Interim Overview of GEM Building Taxonomy V2.0, GEM Foundation, 2012.

Cauzzi, C**.**, Faccioli, E., Vanini, M., & Bianchini, A. (2015). Updated predictive equations for broadband (0.01–10 s) horizontal response spectra and peak ground motions, based on a global dataset of digital acceleration records**.** Bulletin of Earthquake Engineering, 13/6: 1587–612. DOI: 10.1007/s10518-014-9685-y

CEN (2004), “Eurocode 8: Design of structures for earthquake resistance - Part 1: general rules, seismic actions and rules for buildings”, EN 1998-1:2004, European Committee for Standardization, Brussels.

Computers and Structures Inc (2004). SAP 2000-Structural Analysis Programm: Linear and Nonlinear Static and Design of Three dimensional structures. Berkley, California, USA.

Cornell, C.A. (1968). Engineering seismic risk analysis, Bulletin of the Seismological Society of America 58, 1583-1606.

Danciu L, Tselentis G-A (2007) Engineering ground-motion parameters attenuation relationships for Greece. Bull SeismolSoc Am 97:162–183

DIN 4149:2005-04 Bauten in deutschen Erdbebengebieten - Lastannahmen, Bemessung und Ausführung üblicher Hochbauten, 2005.

Eurocode 8 (2004). Design of structures for earthquake resistance. part 1: General rules, seismic actions and rules for buildings, EN 1998-1, European Committee for Standardization (CEN), http://www.cen.eu/cenorm/homepage.htm.

Eurocode 8 – Design of structures for earthquake resistance – Part3: Assessment and retrofitting of buildings. EN 1998-3: 2005

Fajfar P. (2000), “A Nonlinear Analysis Method for Performance-Based Seismic Design”, Earthquake Spectra, vol. 16, no. 3, pp. 573-592.

Google Maps (2016): https://www.google.de/maps/@42.3532948,13.3901523,127a,20y,

193.7h,38.1t/data=!3m1!1e3. (26.12.2016)

Gruppo di Lavoro MPS (2004). Redazione della mappa di pericolosità sismica prevista dall'Ordinanza PCM del 20 marzo 2003 n. 3274, All. 1. Rapporto conclusivo per il Dipartimento della Protezione Civile, aprile 2004, Istituto Nazionale di Geofisica e Vulcanologia (INGV), Milano-Roma, Italy, available at http://zonesismiche.mi.ingv.it/, 163 pp. (in Italian).

Grünthal, G.: European Macroseismic Scale 1998, Cahiers du Centre Europeen de Geodynamique et de Seismologie, Vol. 15, Conseil de l'Europe, Luxembourg, 99, 1998.

Grünthal, G. and Wahlström, R.: New Generation of Probabilistic Seismic Hazard Assessment for the Area Cologne/Aachen Considering the Uncertainties of the Input Data, Nat. Hazards, 38, 159–176, 2006.

HILTI PS 50. Bedienungsanleitung. (https://www.hilti.de/downloads)

Iervolino, I., E. Chioccarelli, and P. Cito (2016). REASSESS V1.0: a computationally-efficient software for probabilistic seismic hazard analysis. Proc. of VII European Congress on Computational Methods in Applied Sciences and Engineering, ECCOMAS, Crete Island, Greece, 5–10 June.

Iervolino I., C. Galasso, E. Cosenza (2009) "REXEL: computer aided record selection for code based seismic structural analysis." Bulletin of Earthquake Engineering, No. 8 pp 339-362. DOI 10.1007/s10518-009-9146-1.

Kappos A.J., Panagiotopoulos C., Panagopoulos G., Panagopoulos E.l. (2003), "WP4-Reinforced concrete buildings (Level I and II analysis)", RISK-UE: An advanced approach to earthquake risk scenarios with applications to different European towns.

Kappos A.J., Panagopoulos G., Panagiotopoulos C., Penelis G. (2006), "A hybrid method for the vulnerability assessment of R/C and URM buildings" Bulletin of Earthquake Engineering, vol. 4, no. 4, pp. 391-413.

Karapetrou S, Manakou M, Bindi D, Petrovic B, Pitilakis K (2016) ''Time-building specific'' seismic vulnerability assessment of a hospital RC building using field monitoring data. Eng Struct 112:114–132

Krawinkler H., Seneviratna, G.D.P.K. (1998), "Pros and Cons of a pushover analysis of seismic performance evaluation", Engineering Structures, vol. 20, no. 4-6, pp. 452-464.

Kwon O.S., Elnashai A.S. (2007), "Probabilistic seismic assessment of structure, foundation and soil interacting systems", NSEL Report NSEL-004, Department of Civil and Environmental Engineering, University of Illinois, Urbana-Champaign, IL.

Lagomarsino, S., Giovinazzi, S.: Macroseismic and mechanical models for the vulnerability and damage assessment of current buildings. Bulletin of Earthquake Engineering, Volume 4, Issue 4 , 415-443, 2006.

Mander J.B., Priestley M.J.N., Park R. (1988). "Theoretical stress-strain model for confined concrete". Journal of Structural Engineering 114(8), 1804-1826.

McGuire, R.K. (2004). Seismic hazard and risk analysis, Oakland, CA, USA: Earthquake engineering research institute.

Meletti, C., F. Galadini, G. Valensise, M. Stucchi, R. Basili, S. Barba, G. Vannucci, and E. Boschi (2008). A seismic source zone model for the seismic hazard assessment of the Italian territory, Tectonophysics 450, 85-108.

Mottershead J.E., Friswell M.I. (1993), “Model Updating in Structural Dynamics: A Survey”, Journal of Sound and Vibration, vol. 167.

Mouroux P., Bertrand E., Bour M., Le Brun B., Depinois S., Masure P. (2004), “The European RISK-UE project: an advanced approach to earthquake risk scenarios”, Proceedings of the 13th World Conference on Earthquake Engineering, Vancouver, BC, Canada, paper 3329 (CD-Rom).

National Institute of Building Sciences NIBS (2004), “Direct physical damage – General building stock”, HAZUS-MH Technical manual, Chapter 5. Federal Emergency Management Agency, Washington, D.C.

Norme Tecniche per le Costruzioni (NTC) (2008). Norme Tecniche per le Costruzioni, Decree of the Minister of the Infrastructures, 14 January 2008, Italian Official Gazette n. 29 of 4 February 2008.

Papazachos B., Mountrakis D., Psilovikos A., Leventakis G. (1979), “Surface fault traces and fault plane solutions of the May-June 1978 shocks in the Thessaloniki area, North Greece”, Tectonophysics, vol. 53, pp. 171 – 183.

Peeters B., De Roeck, G., Andersen, P. (1999), “Stochastic system identification: uncertainty of the estimated modal parameters”, Proceedings of IMAC 17, Kissimmee, FL, USA. pp. 231-237.

Petti L., Marino I. (2009), Preliminary comparison between response spectra evaluated at close source for L’Aquila earthquake and elastic demand spectra according to new seismic Italian code (v.1.00), available at http://www.reluis.it

Pitilakis, Kyriazis (2015). "Earthquake Risk Assessment: Certitudes, Fallacies, Uncertainties and the Quest for Soundness." Perspectives on European Earthquake Engineering and Seismology. Springer International Publishing, pp. 59-95.

Pitilakis K., Crowley H., Kaynia A. (Eds.). (2014), “SYNER-G: Typology Definition and Fragility Functions for Physical Elements at Seismic Risk. Buildings, Lifelines, Transportation Networks and Critical Facilities”, Series title: Geotechnical, Geological and Earthquake Engineering, series vol. 27. DOI: 10.1007/978-94-007-7872-6

Pitilakis K., Riga E., Anastasiadis A., 2013, “New code site classification, amplification factors and normalized response spectra based on a worldwide ground-motion database”, Bulletin of Earthquake Engineering, 11, 4, 925-966, DOI: 10.1007/s10518-013-9440-9.

Reynders E. (2012), “System Identification Methods for (Operational) Modal Analysis: Review and Comparison”, Archives of Computational Methods in Engineering”, vol. 19, pp. 51-124.

Reynders E., Schevenels M., De Roeck G. (2011), “MACEC 3.2: A Matlab toolbox for experimental and operational modal analysis-User's manual”, Katholieke Universiteit, Leuven.

Reynders E., Schevenels M., De Roeck G. (2014): MACEC 3.3: A MATLAB toolbox for experimental and operational modal analysis. User's Manual, Report BWM-2014-06, Department of Civil Engineering, KU Leuven.

Rosenhauer, W. and Ahorner, L. Seismic hazard assessment for the Lower Rhine Embayment before and after the 1992 Roermond earthquake, Geol. Mijnbouw, 73, 415–424, 1994.

Royal Decree on the Seismic Code for Building Structures (1959) Government's Gazette, Issue A, No. 36, February 19, 1959, Greece (in Greek)

Scodeggio A., Monteiro R., Daccaro F., Crowley H., Pinho R. (2012), "Finite Element Model Updating of Buildings using Dynamic Identification Measurements", Proceedings of 15WCEE, Lisboa.

SeismoSoft, SeismoStruct (2016). A computer program for static and dynamic nonlinear analysis of framed structures. Available from URL: www.seismosoft.com.

Selva J., Argyroudis S., Pitilakis K. (2013), "Impact on loss/risk assessments of inter-model variability in vulnerability analysis", Natural Hazards, vol. 67, no. 2, pp. 723–746. doi:10.1007/s11069-013-0616-z

Soufleris C., Jackson J.A., King G.C.P., Spencer C.P., Scholz C.H. (1982), "The 1978 earthquake sequence near Thessaloniki (northern Greece)", Geophysical Journal of the Royal Astonomical Society, vol. 68, pp. 429 – 458.

Stucchi, M., C. Meletti, V. Montaldo, H. Crowley, G. M. Calvi, and E. Boschi (2011). Seismic hazard assessment (2003–2009) for the Italian building code, Bulletin of the Seismological Society of America 101, 1885-1911.

Tsionis G., Papailia A., Fardis M.N. (2011), "Analytical Fragility Functions for Reinforced Concrete Buildings and Buildings Aggregates of Euro-Mediterranean Regions – UPAT methodology", Internal Report, Syner-G Project 2009/2012.

Tyagunov, S., Grünthal, G., Wahlström, R., Stempniewski, L., and Zschau, J.: Building stock vulnerability modeling for earthquake damage and loss assessment, First European Conference on Earthquake Engineering and Seismology, Geneva, Switzerland, 2006.

Vamvatsikos D., Cornell C.A. (2002), "Incremental dynamic analysis", Earthquake Engineering and Structural Dynamics, vol. 31, no. 3, pp. 491-514.

Vamvatsikos D., Cornell C.A. (2004), "Applied incremental dynamic analysis", Earthquake Spectra, vol. 20, no. 2, pp. 523–553.

Vanneste, K., Camelbeeck, T., and Verbeeck, K.: A Model of Composite Seismic Sources for the Lower Rhine Graben, Northwest Europe, Bull. Seismol. Soc. Am., 103, 984–1007, 2013.

Verbeeck, K., Vanneste, K., and Camelbeeck, T.: Seismotectonic zones for probabilistic seismic-hazard assessment in Belgium, NIROND TR-2008-31 E ONDRAF/NIRAS Technical Report 47, 2009

Wen Y.K., Song S.H. (2002), "Structural reliability/redundancy under earthquakes", Journal of Structural Engineering ASCE, vol. 129, pp. 56–67.